**US Army Corps
of Engineers**
Waterways Experiment
Station

AD-A280 960

Geomorphic and Sedimentation Investigation of the 15 June 1991 Eruption of Mount Pinatubo, The Philippines

by Monte L. Pearson

Karl W. Eriksen
U.S. Army Engineer District, Portland

DTIC
ELECTE
JUN 2 3 1994
S
G
D

94-19766

94 6 28 120

Geomorphic and Sedimentation Investigation of the 15 June 1991 Eruption of Mount Pinatubo, The Philippines

by Monte L. Pearson

U.S. Army Corps of Engineers
Waterways Experiment Station
3909 Halls Ferry Road
Vicksburg, MS   39180-6199

Karl W. Eriksen

U.S. Army Engineer District, Portland
Hydraulics and Hydrology Branch
333 S.W. First
Portland, OR   97204

Accesion For		
NTIS CRA&I		☒
DTIC TAB		☐
Unannounced		☐
Justification		
By		
Distribution /		
Availability Codes		
Dist	Avail and / or Special	
A-1		

Final report

**US Army Corps
of Engineers**
Waterways Experiment
Station

Preface

The U.S. Army Corps of Engineers Portland District, was authorized by the Economy Act (31 U.S.C. 1535) and Section 632 of the Foreign Assistance ACT (22 U.S.C. 2357), the United States Agency for International Development (USAID) requested the Department of the Army, acting through the U.S. Army Corps of Engineers (USACE) to prepare a comprehensive Recovery Action Plan (RAP) for Mount Pinatubo, the subsequent hyurologic events. The RAP is being prepared in accordance with a Participating Agency Service Agreement (PASA) signed on 18 June 1992 between USAID/Philippines and the Department of the Army.

This investigation was begun and the report was prepared by MAJ Monte L. Pearson, PhD, U.S. Army Engineer Waterways Experiment Station (WES) and Mr. Karl W. Eriksen, U.S. Army Corps of Engineers Portland District from June 1992 to March 1994. Data were collected and analysis was conducted by the authors. Five trips were made to the study site, Mount Pinatubo, The Philippines, during the study period.

This report was initially published as an Appendix B: Sedimentation Analysis to the report entitled "Mount Pinatubo Recovery Action Plan, Long-Term Report," published in March 1994 by the U.S. Army Corps of Engineers Portland District, and submitted to the Department of State in March 1994.

This investigation was performed under the direct supervision of Messrs. Ron Mason, Chief, River and Coastal Engineering Branch, and Mike Roll, Program Manager, U.S. Army Corps of Engineers Portland District, and Jerry Cornell, Project Manager, U.S. Army Engineer Division, Pacific Ocean; and Drs. W. F. Marcuson III, Director, and Paul F. Hadala, Assistant Director, Geotechnical Laboratory, WES.

At the time of publication of this report, Director of WES was Dr. Robert W. Whalin. Commander was COL Bruce K. Howard, EN. Commander of the U.S. Army Engineer District, Portland, was COL Charles Hines, EN.

GEOMORPHIC AND SEDIMENTATION INVESTIGATION
OF THE 15 JUNE 1991 ERUPTION
OF MOUNT PINATUBO, THE PHILIPPINES

TABLE OF CONTENTS

LIST OF TABLES

LIST OF FIGURES

MOUNT PINATUBO
RECOVERY ACTION PLAN
LONG TERM REPORT

TECHNICAL APPENDIX B
SEDIMENTATION ANALYSIS

1. INTRODUCTION

A catastrophic eruption of Mount Pinatubo occurred between June 12 and 15. 1991. By the afternoon of June 15, 1991, when the initial eruption phase terminated, about 5.6 billion cubic meters (m^3) of medium- to fine-grained pyroclastic-flow material had been deposited in the upper watershed areas around Mount Pinatubo. Another 1 cubic kilometer (km^3) of ash covered the landscape to a radius of more than 40 km around the mountain (Pierson et al., 1992).

Rainfall-runoff has rapidly eroded eruption material, causing lahars that have flooded low-lying areas. Flooding and sedimentation from Mount Pinatubo lahars have displaced tens of thousands of people from their homes, destroyed bridges and crops, and decreased the amount of land available to agriculture in the lower basin. Several barangays and town centers were flooded and buried by sediment deposits of up to 3 meters deep. Hundreds of people have died as a result of the eruption and its aftermath.

In October 1993, heavy rainfall and rapid erosion caused about 21 km^3 of the Sacobia River basin to be diverted into the Pasig River basin. This large increase in Pasig River drainage area is very likely to cause a tremendous increase in sediment yield in 1994 and beyond. The full impact of this basin change has not been evaluated for this report, but it is judged to present an extreme hazard to communities along the Pasig-Potrero River and also to endanger surrounding areas. Sediment yields and lahars in the Pasig River in 1994, are expected to be similar to those experienced in the Sacobia River in 1991 or 1992. Pasig-Potrero River sediment deposition of 50 to 100 million m^3 is considered possible in 1994.

1.1 Purpose

The purpose of this analysis is to assess the future sedimentation hazards due to continuing erosion of the 1991 pyroclastic deposits around Mount Pinatubo. A sediment yield forecast is presented for each basin containing large amounts of pyroclastic material. The areas most likely to experience sediment deposition were also identified. That information is used throughout this report to determine future damages, plan and design sediment control measures, and to assess the potential benefits (economic and physical) for those control measures.

1.2 Study Area

Mount Pinatubo is located in the Zambales Mountain Range on the west coast of Central Luzon in the Philippines, approximately 100 km northwest of Manila. Eight major river basins -- the Gumain-Porac, Pasig-Potrero, Abacan, Sacobia, O'Donnell, Bucao, Maloma, and Santo Tomas-Marella -- form the drainage basins around the mountain. Before the 1991 eruption, Mount Pinatubo stood 1,745 meters above the sea level. The eruption reduced the peak elevation to some 1,520 meters and caused major perturbations in five of the eight affected basins, filling them with volcanic material (see Figure B-1).

The principal drainages on the east side of Mount Pinatubo include the Gumain-Porac, Pasig-Potrero, Abacan, Sacobia and O'Donnell basins. The O'Donnell River joins the Bulsa River to form the Tarlac River, which flows north to the Agno River and thence to the Lingayen Gulf (see Appendix A). The Gumain-Porac, Pasig-Potrero, Abacan and Sacobia Rivers drain the remaining eastern section, flowing south into Manila Bay through the Pampanga delta along with the Pampanga River.

The principal west-side drainages include the Bucao, Maloma and Santo Tomas basins. The Bucao is the largest of these watershed systems, draining approximately 656 km² of the northwestern sector and ultimately flowing to the South China Sea. Headwaters of the Maloma and Santo Tomas-Marella systems originate on the southwestern sector and also drain to the South China Sea (see Figure B-1).

1.3 1991 Eruption of Mount Pinatubo

Starting in April 1991, a series of minor volcanic eruptions occurred on Mount Pinatubo. The culminating phase began on June 12, climaxing sometime after 1400 hours on June 15 with a violent eruption phase (Pierson et al., 1992) -- a classic, catastrophic chamber explosion which ejected pyroclastic-flow material and ash into the atmosphere and deposited it in a radial pattern onto the mountain flanks and watersheds.

The eruption left thick accumulations of pyroclastic-flow material in most of the volcano's upper basins. The Gumain-Porac River system, the southernmost of the east-side river complexes, received no measurable pyroclastic-flow deposits, but its upper basins were thickly blanketed by airfall ash. On the west side, the Maloma River headwaters and the upper reaches of the Santo Tomas and Balin-Buquero Rivers, which originate approximately 7 km southwest of the caldera, received only minimal initial pyroclastic-flow deposits, but both basins were blanketed by airfall ash.

During the eruption, pyroclastic flows, fast-moving mixtures of gas and tephra particles, flowed down the flanks of the volcano, tending to follow existing stream valleys, particularly on the east side. These deposits ranged in thickness from a few meters to as much as 200 meters in the deeper valley reaches of the upper and middle basins. In addition, airfall

ash accumulated in thicknesses ranging from more than 50 cm near the crater to just a trace at distances of 30 km from the mountain. Some rock fragments (lithics) from the former crater and crater walls are also present in deposits, generally within 3 to 5 km of the new crater. Initial pyroclastic flows were extremely hot; by 1992, deposits were maintaining temperatures in the 300° Celsius range, and were expected to hold temperature values for a number of years (R. Hoblitt, U.S. Geological Survey, oral communications, 1991 and 1992). The 1991 tephra (pyroclastic flow) deposits are geologically similar to deposits observed elsewhere from other recent plinian eruptions, resulting from gas-charged, highly silicic magmas moving upward in the cone and venting through the existing crater. The tephra produced from this magma type is lightweight and rich in pumice.

1.4 Regional Geology

The two main physiography provinces within the study area are the Zambales Mountain Range and the Central Luzon basin.

Mount Pinatubo is located in Central Luzon on the eastern edge of the Zambales Mountain Range, an area of orogenic uplift extending from the western coastline to the east central lowlands. Superimposed on this uplift region is a volcanic arc composed of Pliocene to Quaternary composite volcanoes, of which Mount Pinatubo is the highest and youngest. This volcanic arc is trending north-south parallel to and probably associated with the offshore Manila Trench, a subduction zone in the South China Sea that dips eastwardly towards Luzon. The Zambales Range is underlain by dense ultramafic rocks known as the Zambales Ophiolite Complex (Delfin, 1984). These ophiolites consist of predominantly peridotite-basalt rock suites rich in serpentine, chlorite, epidote and other low-grade metamorphic minerals. Minor sedimentary units also exist within the stratigraphic column.

East of Mount Pinatubo lies a sediment-filled depression 80 km wide known as the Central Luzon basin (Delfin, 1984; see Figure B-1), bounded on the west by the Zambales Range and on the east by the Southern Sierra Madre Range, and extending from Manila in the south to the Lingayen Gulf in the north. The oldest sequence of sedimentary units on the western flank of this basin, adjacent to the foothills of the Zambales Range, consists of essentially flat-lying, undeformed late Eocene rocks that directly overlie the Zambales Ophiolite Complex. Most of the sediments filling the Central Luzon basin are volcanically-derived alluvial materials composed mainly of loosely compacted gravels and sands.

1.4.1 <u>Historic Eruption Deposits</u>. Mount Pinatubo is a composite andesitic volcano. The present-day hornblende-dacite dome is constructed upon older sedimentary and ultramafic strata. Underlying older volcanic rocks consist mostly of andesitic agglomerates, tuff breccias and tuffaceous sandstones interspersed with andesitic or basaltic flow rocks. These strata are much older than the pyroclastic-flow deposits that covered the mountain's flanks at the time of the 1991 eruption.

Mount Pinatubo's flanks are draped by massive pyroclastic deposits from a number of past eruptive events, each of which produced significant volumes of unconsolidated volcanic debris. At least two prior eruption episodes have been documented from existing pyroclastic-flow deposits (Delfin, 1984). The youngest is estimated to be 600 years old and Carbon 14 dating on woody material found within the deposits have identified older eruptive phases at 2,600 to 8,000 years before the present (Pierson et al., 1992). Fluvial erosion has highly dissected these older pyroclastic deposits. Fluvial processes transported the volcanic material from the upper basins onto the lower-gradient alluvial-fan complex surrounding the mountain. Pre-eruption channels were broad braided systems transporting high volumes of sediment (JICA, 1978) from the eastern fan apex more than 30 km to the distal reaches coalescing from the Pampanga River delta landward of Manila Bay. West side channels were also transporting large volumes of sediment prior to 1991 (Alejandrino et al, personal communications, 1993).

1.4.2 <u>1991 Eruption Deposits</u>. The 1991 pyroclastic flow deposits are massive poorly sorted units, tens of meters thick and generally very non-cohesive. Stratification is common within these thick units. Initial pyroclastic-flow deposits were emplaced as a series of flow events. Stratification differences resulted from various crater explosions at different locations around the mountain and in each upper basin.

Numerous samples of the 1991 pyroclastic-flow deposits and 1991-1992 lahar deposits were taken in several of the basins during the 1992 rainy season and 1992-1993 dry season as part of this study, and were analyzed for gradation and bulk density. Gradation testing showed the pyroclastic deposits to be typically composed of about 75 percent sand sizes with 10 to 15 percent silty fines and 10 to 15 percent coarse sizes (greater than about 5 mm). Bulk densities ranged from about 1.8 to 2.6 kg/m^3 with an average of about 2.3 kg/m^3. Visual observations in the field show the older pyroclastic and lahar deposits to be similar to the 1991 deposits, but more consolidated with age and burial. Greater consolidation thus increases resistance to erosion. Weathering also forms clay minerals that increase the cohesive strength of the sediment and its resistence to erosion. The 600-year old deposits appear nearly identical to the 1991 pyroclastic-flow deposits, generally discernible only by the well-developed vegetation on the top surface. Still older, more weathered and more dense pyroclastic deposits were also observed, presumably representing the eruptive episode of about 2,000 years ago. These deposits are noticeably more resistant to lateral erosion than the younger deposits due to their greater consolidation. Since the lahar deposits are derived from the pyroclastic deposits, they have similar characteristics except that the coarser

fragments tend to be segregated at the tops of individual flow sheets or separated from the main deposit because of their low density; thus in general the coarse fraction is significantly smaller in the lahar deposits. Gradation tests in samples of the lahar deposits generally showed a composition of about 95 percent sand size or finer.

1.4.3 Current Volcanic Hazards. Mount Pinatubo has settled into a period of reduced eruptive activity following the major eruption of June 1991. This pattern is similar to the historical pattern of similar volcanoes. Current activity at the mountain consists mostly of periods of dome growth accompanied by occasional small-scale explosive events. Earthquake activity fluctuates, with many phases of low-frequency tremors. While the mountain is still active, another very large eruptive event is not probable during the next few years. Meanwhile, significant hazards from the 1991 eruption still exist for those living and working near the volcano. The lahar hazard is still very high, especially during the monsoon season, and will continue to be a significant hazard for many years to come. Occasional ashfalls may yet occur in conjunction with secondary eruptions and/or phreatic explosions, decreasing in frequency and magnitude with time. There has been a marked reduction in the reported number of explosive events from 1991 to 1993.

Secondary pyroclastic-flow events represent a continuing and significant hazard, particularly during the rainy season. The random occurrence and size of secondary pyroclastic flow materials make sediment yield and impact predictions extremely difficult, but these will nevertheless be discussed in the basin analysis. Phreatic explosions appear linked to secondary pyroclastic-flow events (exactly how is unknown at this time) but in themselves are not a major factor in sediment production. They are spectacular, resembling small volcanic eruptions, but in the outyears they will be a non-factor.

1.5   Regional Climate

Mount Pinatubo is located approximately 15°N latitude on the west coastal area of Central Luzon. A tropical climate dominates during the Northeast Monsoon season (November through May). The Southwest Monsoon season dominates during the summer months (June-October). This seasonal airflow reversal results in a two-season condition. The Southwest Monsoon generates typhoons (high winds and heavy rain) and associated severe weather conditions. Eighty percent of the region's rain falls from June through September. This wet season coincides with the time of year when intense tropical storms are spawned in the lower latitudes of the Pacific Ocean and pass close to the Philippine Islands. Data available from the Philippine Atmospheric, Geophysical, and Astronomical Services Administration (PAGASA) indicate that between 1948 and 1991, a yearly average of 16 tropical cyclones (tropical depressions, tropical storms or typhoons) affect weather conditions in the region (Northwest Hydraulic Consultants Inc., 1993). Intense localized rainfall is associated with the major cells, which produce severe and intense storms over a small geographical area.

On average, the east side of the volcano receives less rainfall than the west side. Near Mount Pinatubo, the annual rainfall varies from a low of about 1,700 mm at Clark Air Base,

Pampanga, on the east, to more than 3,700 mm at Iba, Zambales, on the west. Additional climatological data are provided in Appendix A.

1.6   Regional Topography

1.6.1 <u>Upper Basins/Headwaters</u>. Prior to the initial phase of volcanic activity in April 1991, Mount Pinatubo stood some 1,745 meters above sea level. The upper basin slopes had a dense drainage network with channels incision from 100 to 150 meters deep. Crater wall slopes ranged from 20° to 65° (Pierson et al., 1992), with channel gradients of up to 400 m/km. Streams flowed through steep, narrow valleys with channel slopes of 0.02 to 0.10 m/m. This upper basin area was densely covered by shrubs and tall grass before the eruption phase. Eight major watersheds drained these slopes through the transition reach, before exiting onto the alluvial fan and flowing to the delta or sea.

1.6.2 <u>Transition Reach</u>. This reach includes areas within the older pyroclastic deposits and the upper parts of the alluvial fans. Pre-eruption channels incision ranged from 60 to 100 meters upstream end, to only a few meters at the downstream end. Channel gradients through this area flatten to about 0.01 to 0.02 m/m at the fan apex (about 200 meters elevation above sea level) with a corresponding increase in vegetation density and diversity. Crops include sugar cane, cassava, and maize. On the west side, the Bucao and Santo Tomas transition reaches are characterized by a mid- to upper-slope channel complex, controlled by the north-south trending mountain range.

1.6.3 <u>Lower Alluvial-Fan Complex</u>. A broad alluvial-fan complex surrounds Mount Pinatubo (see Figure B-1), with the highest degree of geomorphic development and complexity in the eastern sector. The highest population density and agricultural diversity are also on the east side. The Gumain-Porac Rivers drain an area south of the mountain, flowing across the southeastern portions of the alluvial-fan complex. The east-central and northeastern sectors of this fan complex are dissected by the Pasig-Potrero, Abacan, and Sacobia Rivers. The northernmost portion is affected by the O'Donnell River. Channels are confined by natural banks of not more than a few meters, except where the streams have been channelized. Channel gradients range from near 0.02 m/m in the upper reaches to as little as 0.0001 m/km to 0.0002 m/m in the delta. Channels are broad braided systems covering large geographical areas and transporting fine sediment to the delta.

Geomorphically, the west side alluvial fans can be divided into the similar physiographic sections, but different geologic events have created a different landscape. The north-south trending, westernmost mountains of the Zambales Range separate the upper fan from the smaller lowland area. This lowland alluvial-fan complex is best described as a coastal fan complex.

2. SEDIMENTATION ANALYSES AND METHODOLOGIES

The sedimentation analysis for Mount Pinatubo use, methods developed by the Corps of Engineers during its work on the Mount St. Helens recovery program (Corps, 1984 and 1985). The analysis involves three main components: 1) definition of the geomorphic processes active within the basins, 2) a sediment yield forecast, and 3) a sediment deposition forecast. Each component involves a combination of photogrametric analysis, field investigations, literature reviews, and consultation with other engineers and scientists. This section outlines the methods used. The general results of these analyses are discussed in Chapter 3, and basin specific results are presented in their respective chapters.

2.1 Geomorphic Analysis

The geomorphic analysis involved identifying the physical processes actively reshaping the pyroclastic deposits, and determining the importance of each one to long-term sediment production. Aerial photographs, both vertical and oblique, taken of the pyroclastic deposits in 1991, 1992, and 1993 were studied to identify active geomorphic processes. The processes identified were phreatic explosions, secondary pyroclastic flows, lake formation and failure, and rill, gully and channel erosion.

 2.1.1 Photogrametric Analysis. The photographs and field observations indicated that channel erosion, lake formation and failure, and secondary pyroclastic flows were the major factors in sediment production. A topographic analysis was conducted to determine the magnitude of each process and the volume of the pyroclastic deposits. Pre-eruption topography was obtained from 1:50,000 scale, 20-meter contour maps prepared by the Defense Mapping Agency, Washington, D.C. Post-eruption topography was produced from November 1992 aerial photography supplied by USAID-Manila. The volume of 1991 pyroclastic deposits was measured by comparing the pre-eruption topography to the immediate post-eruption surface. On the east side, pre- and post-eruption valley cross sections were produced and the pyroclastic volumes computed using the double end-area method. On the west side, digital terrain models (DTMs) were prepared for the Santo Tomas and Bucao basins. The pre- and post-eruption DTMs were then merged in a Unix-based computer workstation and the pyroclastic deposit volumes were computed. Channel dimensions and erosion volumes were obtained from post-eruption cross sections. Volumes for some of the secondary pyroclastic flows were also computed.

 2.1.2 Field Investigations. Field visits were made to each basin to verify the process conclusions and define smaller scale features. Both visual methods and geo-positioning systems were used to locate field sites. Spot measurements were made of active channels, channel slopes, and terrace formations. Soil samples were taken and material types in and adjacent to the channels were noted. Soil temperatures were observed but not measured. During the field visits, specific investigations included channel descriptions, comparative differences in surface and channel conditions between the initial pyroclastic deposits and the

secondary pyroclastic flow areas, flow and deposition characteristics of secondary pyroclastic flows, and the formation and failure of lakes.

2.1.3 Literature Review. The geomorphic processes at Mount Pinatubo were compared to those at other volcanoes and to other research results available in the literature. The rapid channel evolution at Mount Pinatubo was compared to that at two other volcanoes, Mount St. Helens (Meyer and Dodge, 1988) and Mount Mayon (Rodolfo and Arguden, 1991) to help identify limiting factors. The conclusions of the Mount Pinatubo studies were compared to the results of laboratory experiments on channel evolution, presented by Schumm, et al (1987). Although the secondary pyroclastic flows occurring at Mount Pinatubo were not found elsewhere, work on coal spoils in Canada (Sasitharanand et al., 1992) provided some information. The conclusions of the geomorphic analysis were also discussed with representatives of the U.S. Geological Survey (USGS), Philippine Institute of Volcanology and Seismology (PHIVOLCS), and outside consultants.

2.2 Sediment Transport Analysis

2.2.1 Objectives. The overall objective of the sediment transport analysis was to develop an understanding of the processes sufficient to forecast future hazards. Standard methods of analysis, such as streamflow and sediment transport measurements and computer modeling were generally not used in this study. The extreme sediment transport concentrations in the lahars precluded the direct application of sediment transport models and the limited scope of this study did not allow for data collection. However, the magnitude and mechanics of the sedimentation problems allowed for a more generalized approach based on consultation with other experts, limited field investigations and aerial photography.

2.2.2 Transport Processes. The significant transport processes were initially described by PHIVOLCS and USGS personnel, and other observers, who were on site during the 1991 rainy season (Punongbayan et al., 1991; Janda et al., 1991; and Umbal et al., 1991). They described mudflows causing several meters of channel aggradation in a single day. During the initial phase of the study, the sediment transport processes were defined as muddy water, hyperconcentrated flow, and mudflows.

During subsequent field visits, muddy water and hyperconcentrated flow conditions were observed in several rivers, but fate did not allow direct observation of mudflow conditions. Discharge and sediment transport measurements could not be made because of the diffic t river conditions and limited study scope. Additional observations of transport processe: were provided by PHIVOLCS (Daag and Tungol, personal communication, 1992), Zambales Lahar Scientific Monitoring Group (ZLSMG) (Rodolfo and Umbal, personal communication, 1993), Dolan (personal communication, 1993), and others throughout the study. A limited amount of sediment transport concentration data for muddy water conditions was obtained from the Philippines' Bureau of Research and Standards (unpublished). Mudflow concentration data for three events in 1992 were provided by ZLSMG (Rodolfo, written communication, 1993).

Sediment transport calculations were made for some basins to estimate long-term potential erosion/deposition conditions downstream of the hyperconcentrated flow and mudflow zones. On the basis of experience at Mount St. Helens (Eriksen, 1989), Yang's sediment transport equation was used for these calculations.

2.2.3 **Sediment Deposition**. During initial field trips in September 1991 and February 1992, muddy water, hyperconcentrated flow, and mudflow deposits were identified. On subsequent visits, deposits from each of the three sediment transport processes were examined in the field. During field visits, deposition areas were photographed and deposit depths were estimated. Field data and aerial photographs were used to map the extent of the different deposits. In November 1992, a field trip was made for the express purpose of examining August and September 1992 mudflow deposits in the Pasig-Potrero and Sacobia-Bamban rivers.

2.3 Sediment Forecasts

After an understanding of the active processes was developed, the next step was to prepare a sediment yield forecast. The key elements in the forecast are the sediment available for rapid erosion, the initial rate of erosion, and the predicted rate of decline in sediment yields.

2.3.1 **Sediment Available**. The geomorphic analysis determined that the extremely high sediment yields were the result of rapid channel erosion (many times higher than pre-eruption levels, with transport occurring as hyperconcentrated flow or mudflows) and that these high yields would continue until the main channels reached a "stable" cross-sectional geometry. Judgments were made about the dimensions that each main channel would have when it reached a "stable" condition, based on the geomorphic analysis, pre-eruption channel dimensions, hydrology, and local geologic conditions. The "stable" channel dimensions were plotted on 1992 channel cross sections and the sediment available for rapid erosion was the material remaining within the boundaries of the "stable" main channels.

To forecast the potential sediment yield from secondary pyroclastic flows, sites with topographic and geologic characteristics similar to previous secondary pyroclastic flows sites were identified and potential volumes computed. Where appropriate, the volumes were then added to the sediment available from the main channels to arrive at the total sediment available for rapid erosion.

2.3.2 **Initial Erosion Rate**. The next step in developing the sediment yield forecast was to determine what the initial average annual sediment yield would be for the first year. This was done by multiplying the average annual storm runoff by an average sediment transport concentration. The storm runoff volume was approximated by the volume of the upper 10 percent time period of the flow-duration curve for each of the pyroclastic drainages (computed during the hydrologic analysis described in Appendix A). An average sediment transport concentration during storm runoff had to be estimated from field observations and discussions with USGS, PHIVOLCS, and ZLSMG personnel, as no suitable data were

available. A sediment transport concentration range of 25 to 30 percent by volume was considered representative of the average storm runoff concentration. While concentrations have been higher, this figure near the middle of the hyperconcentrated flow range, seems to reflect an overall average.

2.3.3 <u>Sediment Yield Forecast</u>. Using the initial average annual yield as a starting point, the total sediment available was then distributed over time to generate the sediment forecasts. Annual sediment yields for each succeeding year were generally proportioned downward according to the ratio between the amount of available sediment remaining and the initial sediment available.

2.3.4 <u>Sediment Deposition Forecast</u>. Sediment deposition investigations also utilized field visits, aerial photography, and discussions with PHIVOLCS, ZLSMG, and USGS staff. In addition, there were discussions with DPWH staff and a limited number of river cross sections surveyed by PHIVOLCS.

Sediment deposition was found to be governed by the transport mechanism (muddy water, hyperconcentrated flow or mudflow) and the local topography. The type and location of deposition caused by each transport mechanism was identified in the field. Topographic maps were used to delineate areas threatened by each process. For purposes of economic analysis, the potential deposition reaches were divided into inner and outer zones, and probabilities of being impacted were assigned.

2.3.5 <u>Storm Event Sediment Yields</u>. Sediment yields were computed for large, infrequent storm events for use in designing sediment control measures. Sediment volumes and water-plus-sediment peak discharges were estimated at each sediment control measure site. The upstream basin area and clear water flows at each site were obtained from the hydrologic analysis presented in Appendix A. Calculations were made using the peak discharge and the highest 3-day volume for the 2-, 10-, 50-, 100-, and 500-year storm events in each basin.

Sediment concentration data do not exist for large storm discharges on any of the impacted rivers. Therefore the sediment concentrations were assigned on the basis of watershed conditions and the type of sediment transport mechanism expected at each design site. In the rivers with pyroclastic deposits, at sites where mudflows were expected, a concentration of 67 percent by volume was assigned to the peak discharge

and peak day volume, and a concentration of 40 percent by volume was assigned to the next highest 2-day volumes. At sites downstream of the mudflow zones, a concentration of 40 percent by volume was assigned to discharges for the peak and the three highest days. A concentration of 10 percent by volume was assigned to discharges from basins having no pyroclastic deposits.

This method provides for very large sediment yields during infrequent storm events. As time passes, the same geomorphic processes that reduce annual sediment yields will also work to lower the sediment transport concentrations during storm events. The concentrations used provide appropriately high volumes for design of control measures.

2.4 Sediment Distribution Model

2.4.1 General. A sediment distribution model was developed for each basin to provide input to the economic analysis. The model simulated erosion of the pyroclastic material by storm events and routed the sediment downstream until it was deposited or discharged by the rivers. The model uses Monte Carlo simulation involving numerous iterations to incorporate some of the natural variations and knowledge uncertainties of the sedimentation processes.

2.4.2 Sediment Yields. Sediment yield functions were developed to account for the sediment available and potential erosion rates described above. The rainfall/runoff function provided for a normal distribution of annual storm events, centered around the storm runoff analysis described in section 2.3.2. Secondary pyroclastic flows were assigned probabilities of occurrence and potential volumes that could be added to the sediment available for erosion. Sediment concentrations were a function of runoff and sediment availability, with the first year's sediment transport concentration averaging approximately 25 to 30 percent by volume. The maximum sediment concentration for any storm event was limited to 60 percent by volume.

2.4.3 Sediment Distribution. Sediment yields were distributed throughout the river basins as functions of sediment transport concentration, flow depth, bank height remaining, levee conditions, and topography. Deposition in the channel was controlled directly by the inflowing concentration, but overbank distribution also involved probability functions for levee failure and flow paths. The probability of a hazard zone being impacted was based on the results of the analysis described in section 2.3.4.

2.4.4 <u>Model Limitations and Results</u>. As noted above, this model is a simulation model, the sediment forecasts from the model, approximately imitate the sediment forecasts presented in this report. The Monte Carlo simulation provides a statistical representation of the possible natural variations in sediment yields that are useful in assessing the potential damages or economic benefits. The internal formulation of the model is not physically based, so the model can not be used as an analytical tool. The results from the model provides at least some indication of the variations that can be expected in the sediment yields and distribution. Those variations are reflected in the economic analysis presented in Appendix C which can be obtained from the U.S. Army Engineer District, Portland, or the Department of State.

3. GEOMORPHIC DEVELOPMENT AND SEDIMENT TRANSPORT

3.1 General

The 1991 eruption left 5.6 billion m³ of pyroclastic flow deposits in the upper watershed around Mount Pinatubo. The deep river valleys near the mountain were filled with up to 200 m of deposits. Since their emplacement, these pyroclastic deposits have experienced rapid geomorphic changes. The formation and subsequent erosion of channels in the deposits have caused many lahars that have done extensive damages in the populated areas lower in the basins. Secondary pyroclastic flows and phreatic explosions have reshaped the deposits, but their impacts have generally been limited to upper basins.

3.2 Pyroclastic-flow Deposits

3.2.1 Emplacement. Pyroclastic flows are formed from the combination of hot volcanic clasts, lithic rock fragments, and gases traveling down the volcano's flanks at gravity-induced velocities of 10 to 300 meters per second (Carey, 1991). Under the influence of gravity pyroclastic flows produce thick and geographically widespread deposits. Most of the pyroclastic-flow material from the initial (June 15) eruption was emplaced between 5 km and 15 km from the new crater (see Figure B-2). Only a thin veneer of new material was retained on the upper 3 to 5 km of the crater's flanks.

Incised valleys in Mount Pinatubo's upper basin areas appear to have had a direct influence on flow and depositional patterns. The high velocity pyroclastic flows appear to have crossed the high, flat plateaus and accumulated in the deep valleys. Only a thin deposit of pyroclastic and airfall ash materials remained on the plateau surfaces. Deposits in the upper valleys surrounding Mount Pinatubo range from 200 meters thick in the proximal area to 50 meters thick at the distal areas. Those deposits tend to be massive poorly sorted units, tens of meters thick and generally very non-cohesive. Stratification is common because the material was emplaced by a series of flow events. Stratification differences resulted from differing material exploded from the crater and varying geographical locations.

Topographical lows in the crater rim sector may have influenced the pyroclastic flow vectors. Prior to the eruption, a large, deep low existed in the northwest side of Mount Pinatubo. Nearly half of the total accumulation of pyroclastic flow deposits are located in this sector. During the eruption, smaller topographical lows formed in the rim at the heads of the other basins containing large pyroclastic deposits.

3.2.2 <u>Pyroclastic Deposit Geotechnical Characteristics</u>. Recent pyroclastic and lahar deposits consist predominantly of sand-sized particles which are angular and composed primarily of quartz, volcanic glass, feldspar, and other high-silica minerals consistent with a dacitic magma source. The pyroclastic deposits are 10 to 15 percent pumice, ranging from fine gravel to boulder sizes, and 10 to 15 percent non-plastic fine material. The deposits are unconsolidated and massive. The older pyroclastic deposits are similar except that they are somewhat weathered and appear to be well consolidated with a higher clay component.

Material deposited on the flanks of the volcano consists of ash, rockfall and pyroclastic material from secondary crater eruptions occurring after June 15, 1991. Deposits of lithic cobbles and boulders can also be found in these areas.

3.2.3 <u>Secondary Pyroclastic Flows</u>. Secondary pyroclastic flows are mass movements of material that have occurred after emplacement of the primary pyroclastic deposits. Figure B-3 shows the general location in the basins of these major mass movements. Two features common to most, but not all, secondary pyroclastic flows are; failure scarps at points of contact between pre-eruption valley walls or channel surfaces and the initial pyroclastic flow deposit, and deeply eroded channels across the toe.

The triggering mechanisms and flow mechanics of secondary pyroclastic flows are still poorly understood. They evidently tend to occur during the rainy season. Perhaps infiltration of rainwater adds enough weight to the deposits that the shear strength of the soil is exceeded. Liquefaction might also be a triggering mechanism, even though the material has a low water content. The investigations of Sasitharanand et al. (1992) into catastrophic flows of well-drained coal spoils in Canada indicate that as little as 10 percent water by volume may be enough to induce flow. Phreatic explosions are another possible triggering mechanism.

Secondary pyroclastic flows can carry large volumes of material many kilometers downstream. Work by Francis and Baker (1977) suggests that large-volume pyroclastic flows are far more mobile than other particulate gravity flows, with deposits abundant in ash or pumice showing the most pronounced mobility. Mount Pinatubo's pyroclastic-flow deposit contain both pumice and fine-grained airfall ash. Once flow is initiated, some type of bulking and increased fluidization seems to occur, the resulting flows appear to range in concentration from debris flows to mudflows to muddy water flows (see Figure B-4). Down-slope travel distances vary, depending on channel configuration and geometry. Down-slope movement of these flows at Mount Pinatubo has been measured at up to 8 km.

Secondary pyroclastic flows can fill downstream channel reaches, increasing the amount of sediment available for future erosion. They may also cause channel blockages, creating in-channel and/or tributary lake formation. Sediment may be temporarily stored, with subsequent lake breaching producing mudflows.

Analysis indicates that once movement has occurred, the scarp and failure surfaces are less susceptible to fluvial erosional processes, perhaps as a result of increased porosity and permeability. Field observations show a lag type of pumice gravel deposit present on these failure surfaces. A few mass movement areas have undergone some fluvial erosion and channelization, however, analysis indicates that erosion was initiated up slope and migrated across the failure surface.

The potential magnitude and temporal and spatial distribution of secondary pyroclastic-flow events are unknown at present.
The potential for activity remains high in the near future. Such events can produce catastrophic basin modifications that may either increase or decrease the amount of sediment available for erosion. This risk and uncertainty impacts both the short and long term sediment budget.

3.2.4 <u>Phreatic Explosions</u>. While rapid erosion launched the development of new drainage networks, dynamic phreatic explosions also occurred in the deposit, producing ashfall and actively increasing the erodibility of the initial deposit. Such explosions influence channel formation but are not by themselves major sediment producers. Craters from the explosions filled with water to form ponds and lakes. Overtopping of these and other depressions in the pyroclastic-flow deposit also aided the redevelopment of channel networks. Water accumulation in these depressions may have increased phreatic explosion activity.

Phreatic explosions occur mainly during the rainy season when infiltration increases the amount of available moisture coming into contact with hot primary pyroclastic-flow deposits. The process of flash-to-steam upon contact between water and hot volcanic sediment is one of the driving factors. In addition, the action of streamflows undercutting banks in the pyroclastic deposit resulted in bank failure, causing phreatic explosions from contact of channel water with hot pyroclastic sediment.

Spatial and/or temporal predictability of future explosions is currently not possible. These events may continue for several (up to 10) more years, especially in the basins containing the greatest thicknesses of initial pyroclastic-flow deposits, but their frequency should drop off over time as the deposits cool and channel stability increases.

3.3 Drainage Development and Erosion Processes

3.3.1 <u>General</u>. The pyroclastic flow deposits were initially featureless, domed (high-centered) plains following longitudinal axes down the valleys. Initial drainage development occurred very shortly after pyroclastic flow emplacement. The non-cohesive nature of the deposit and other geomorphic processes acting on the material combined rapidly to form a new and highly complex drainage network. A major tropical storm that was battering Central Luzon on June 15, 1991, also helped re-establish drainage networks within a few days. The deposit geometry aided in channel network redevelopment, with small rills and gullies forming along the center and draining into larger channels along the valley margins.

3.3.2 **Rills and Gullies**. Rill and gully erosion was the first step in re-establishing the drainage network on the pyroclastic deposits. It was also an important erosion process on the ash covered mountains around Mount Pinatubo.

Rill and gully formation on the pyroclastic surfaces was very rapid in 1991, creating intricate drainage patterns. These small channels were only a few meters wide and deep, but because they were so numerous they produced significant quantities of sediment in 1991. They also provided a highly efficient drainage system for the pyroclastic deposits main channels. Analysis of the 1992 and 1993 rills and gullies found that they had not grown significantly larger than they were in 1991. Rills and gullies are not expected to be important sources of sediment in the future.

Rain events after June 1991 eroded airfall ash from the mountain slopes and deposited it in many river channels. Most of the airfall ash was removed from the mountain slopes during the first rainy season (1991), resulting in large sediment yields to the rivers. The Gumain, Porac, and Maloma rivers, which had no major pyroclastic deposits within their headwaters, were impacted by this erosion and deposition of airfall ash in the lowland channels. These streams are still heavily laden with ash.

3.3.3 **Channel Development**. Initial drainage development occurred once the pyroclastic flow deposit was in place. The non-cohesive nature of the deposit combined with high rainfall to rapidly form a new and highly complex drainage pattern. The main channels developed predominantly by headcutting and incision of gullies and small channels. As small channels merged, the in-channel discharges increased and the erosion potential also increased. Channel development processes were similar to those identified at Mount St. Helens by Pearson (1986).

The dome-shaped geometry of the initial pyroclastic-flow deposit helped direct channel development toward the margins of the deposits (Tom Pierson, USGS, personal communication, August 1992). The channels along the deposit margins received additional runoff from the adjacent mountains, further increasing their erosion potential. Even during the first year, many of these channels incised 20 to 40 meters into the pyroclastic deposit. Bank collapses temporarily blocked some channels, causing mudflow or hyperconcentrated flow surges when the blockage was overtopped and eroded. Additional mudflows were created by the violent mixing of hot bank material into rapidly flowing discharges. Channel widening due to bank erosion was the dominant sediment source in 1992 and 1993.

The post-eruption stream profiles are elevated above the pre-eruption channels, but show the same general slopes of 4 to 5 percent. The hinge points, the locations at which channel slopes increase, were moved downstream by the pyroclastic deposits. The resulting slope relations would suggest stream energy may not have increased. The post-eruption channel lengths have increased an average of 2 km. Without an increase in hydrology or stream energy, the river systems have about the same potential transport limits as they did prior to

the eruption. Sediment bulking of the flows to hyperconcentrated or mudflow conditions appears to be limited to bank failure mechanisms.

An unusual factor that contributed to channel formation was the overtopping of ponds and lakes formed in craters from phreatic explosions. Analysis of aerial photographs taken in October-November 1991 by the GOP indicates that phreatic explosions occur primarily at points of contact between pyroclastic-flow deposits and pre-eruption valley side slopes. The contact of hot sediment and cold groundwater from the hillsides is one explanation for phreatic explosions along the deposit margins. The potential magnitude and distribution of sediment generated for transport by this geomorphic process is unknown, but its importance is decreasing with time.

3.3.4 Lake Formation and Blockage Failure. Lake formation and failure has been an important sediment producing process in some basins. Its importance has been dependent on a number of geomorphic factors including, pre-eruption basin geology, topography, hydrology, and the initial pyroclastic-flow deposit. Those factors and the resulting sediment impacts have been quite variable from basin to basin. Lake failures have been most serious in the Pasig-Potrero and Santo Tomas basins.

Lake breakouts were a significant mode of large lahar generation in the Pasig-Potrero basin during the first two years following the eruption. A side drainage of the Pasig basin was blocked by secondary pyroclastic flows during both 1991 and 1992, and a lake developed behind the blockage. Both blockages were overtopped and eroded, causing large lahar flows that damaged areas on the lower alluvial fan. The potential for future lake formation has been reduced, because the tributary has filled with sediment and the occurrence of the secondary pyroclastic flows has reduced the potential for more such events.

Mudflow events in the Marella River blocked the Mapanuepe River, also forming a lake. This lake underwent a series of blockages, failures, and mudflows in 1991 and 1992. Construction of an outlet to control lake water level prevented any lake failures in 1993. Nevertheless, there is still some threat of future lake breakouts.

Blockages have formed lakes in other basins without causing serious lahar problems. An unnamed lake formed in the Sacobia basin, just upstream of the Gates of the Abacan, and drained in August 1991 without generating a noticeable lahar (Scott, K. M., USGS, oral communication, 1992). A second lake in the Sacobia basin formed on the Marimla River upstream of Bamban. This lake was formed by mudflows on the Sacobia-Bamban River, blocking the valley. This lake has overtopped the blockage, but the blockage has not failed. Several small lakes have also been observed in the Bucao River basin.

3.4 Transport Processes

3.4.1 General. The term "lahar" refers to any rapidly flowing mixture of volcanic material and water. The terms "muddy water," "hyperconcentrated flow," and "mudflow"

are used in this report to refer to lahars of increasingly higher sediment transport concentrations. Figure B-5 gives a visual comparison of relative erosion and deposition factors for these various sediment transport mechanisms, showing how sedimentation impacts vary in magnitude and location with the different mechanisms. Each type of lahar presents a different hazard to areas downstream of Mount Pinatubo.

3.4.2 Muddy Water. Muddy water refers to sediment transport concentrations of less than 20 percent by volume, which are typical of storm runoff concentrations observed around the world. However, at Mount Pinatubo such flows occur during minor rainfall events and also under base flow conditions. Suspended sediment samples collected from impacted streams during base flow conditions before and after the 1991 eruption (Bureau of Research and Standards, unpublished) indicate a post-eruption increase of 10 to 100 times the pre-eruption base flow sediment transport levels. Post-eruption concentrations on impacted streams range from near 100 parts per million (ppm) to over 10,000 ppm. The sediment entrainment process for muddy water flows appears to be common bed and bank erosion.

Muddy water flows have caused both erosion and deposition damages, carrying and depositing sediment as far as Manila Bay and the South China Sea. They have also caused infilling of the lower reaches of the Abacan, Gumain, Pasac, Maloma, Olongapo, and Tanguay Rivers, and have caused major damage in the form of toe erosion to levees on the Abacan, Bamban, Gumain, and Santo Tomas Rivers.

3.4.3 Hyperconcentrated Flow. Hyperconcentrated flows generally have sediment transport concentrations between 20 and 50 percent by volume (Julien and Lan, 1989). The action of these flows is similar to that of muddy water flows, but they can transport very large sediment volumes in a short time. The sediment entrainment process seems to require some extraordinary mechanism to raise concentrations above the muddy water range. At Mount Pinatubo, it appears that this mechanism is the collapse of high, hot pyroclastic banks into the rapidly moving storm runoff in confined channels. Once entrained, the concentrations tend to remain high until the flow loses energy down in the valley.

Observations of storm events on the Sacobia River by Daag and Tungol (personal communication, 1992) and Dolan (personal communication, 1993) and on the Marella River by Rodolfo and Umbal (personal communication, 1993) indicate that discharges undergo transition from muddy water to hyperconcentrated flow and then may alternate between hyperconcentrated flow and mudflow before receding back to muddy water base flow conditions. The only hyperconcentrated or mudflow sediment transport concentration data available for analysis (Rodolfo and Umbal, written communication,

1993) support these observations. These data show sediment transport concentrations on the Marella River rising from around 10 percent by volume to nearly 86 percent by volume during a storm on June 27, 1992. They also show a series of measurements taken on July 11, 1992 that fluctuate between 30 and 60 percent by volume. Discharge measurements for

those sediment transport concentrations are not available, nor have discharges for any other storm event been measured due to the difficult river conditions. The high sediment load, rapidly shifting channels, and high water temperatures during hyperconcentrated flows or mudflows make measurements very difficult.

Because hyperconcentrated flows behave like muddy water, they can cause flooding and sediment deposition over broad areas of the lower valleys. The most damaging hyperconcentrated flow events have been on the Sacobia and Abacan Rivers in August 1991, and on the Pasig-Potrero River in September 1991 and October 1993. In each of these events, hyperconcentrated flows breached levees and caused widespread damage. Sediment layers deposited in overbank areas by hyperconcentrated flow events were typically less than one meter deep, with nearly flat surfaces. Soil samples from the deposits showed them to be similar in composition to the pyroclastic deposits, with little variation across the floodplain.

3.4.4 Mudflow. Mudflows have sediment transport concentrations of over 50 percent by volume and are commonly said to resemble rapidly moving wet concrete. Like hyperconcentrated flows, mudflows are formed by the collapse of high, hot pyroclastic banks into rapidly moving storm runoff in confined channels. Mudflows (also called "debris flows" in some technical literature) are non-Newtonian fluids that have shear strength (Julien and Lan, 1989). Mudflows continue to move as long as the shear stress exceeds the shear strength. At Mount Pinatubo, mudflows in confined channels have traveled through channel reaches with slopes of only 0.015 m/m.

Mudflows are also capable of building natural levees along their flow margins that serve to keep the flow confined. Mudflow levees have been observed to have surface slopes perpendicular to the main flow path of approximately 2 to 4 percent. Some very large Mount Pinatubo mudflows, confined by their own levees to widths of 200 to 700 meters, have traveled several kilometers across valley reaches with slopes approaching 0.006 m/m.

As noted in the hyperconcentrated flow section above, there is a scarcity of available measured data for Mount Pinatubo mudflows.

Mudflows present a unique hazard, not only because they move very large volumes of sediment very quickly, but also because their depositional characteristics are different from those of muddy water or hyperconcentrated flows. Mudflow deposition can occur on slopes of between 0.006 and 0.02 m/m. Most of the mudflow deposition around Mount Pinatubo has occurred in the transition channel reaches between the base of the pyroclastic deposits and the gently sloping valley floors. Typical of these reaches are the Marella River upstream of Mapanuepe Lake and the Sacobia River near Clark Air Base.
Mudflow deposition seems to occur in two main ways, either as shallow outwash or as massive units. Shallow outwash deposits occur when the mudflow exceeds channel capacity and fluid spills out onto the overbanks and dewaters. It appears that the transition channels have aggraded through this process and that the mudflow levees are also built this way.

Most mudflow deposition seems to occur in massive units. It appears that as the front of a mudflow is stopped, either by loss of energy or by an obstruction, the entire flow for a kilometer or more upstream may also stop. The patterns of abandon flow paths observed in deposition zones after large mudflows suggest that as the flow stops, a number of reactions can follow: breaches can occur in the natural levees allowing the mudflow to continue on another path, subsequent flows can be diverted near the upstream end of the deposit, or subsequent flows can flow up and over the earlier deposit.

Single mudflow events around Mount Pinatubo have created in-channel deposits up to 7 meters thick. This process has filled several river channels, enabling later flows to spill onto the overbanks. These overbank deposits are in the general range of 1 to 2 meters deep, rarely exceeding 3 meters at the deepest.

The mudflow deposits are similar to the pyroclastic source deposits, but contain a smaller percentage of coarse pumice fragments and may also contain other debris such as wood. The mudflow deposits tend to have a massive (1 to 3 meters) thick bedding structure and some upward sorting by particle size.

3.5 Sediment Forecasts

3.5.1 General. Three types of sediment forecasts are presented in this study. The first is the 10-year forecast of annual sediment yields and deposition patterns. The second is a more generalized long-term forecast of sediment yields and related sediment problems, covering the 25 year project life. The third is a forecast of sediment yields during infrequent storm events that was used to determine storage requirements for sediment control measures.

3.5.2 10-Year Forecasts. Ten-year forecasts were made for basins that contain significant volumes of pyroclastic deposits. These included the Pasig-Potrero, Sacobia-Bamban, O'Donnell, Bucao, and Santo Tomas basins. It was found that a rapid decline in erosion rates could be expected during the next five years in all basins. This expectation is based on the comparison of erosion rates and channel dimensions found at other volcanoes.

At Mount St. Helens (USACE, 1984), sediment yields were very high during the first year as the streams reestablished drainage networks. Stream gradients stabilized greatly after the first year and channel widening became the dominant sediment-producing process. As the channel widths increased, the collapse of high banks directly into flowing water became less ... and sediment yields declined. At Mount St. Helens, annual sediment yields had ... d by 75 percent within five years and have remained around that level (USACE, ... Cross sections of mudflow-producing channels at Mount Mayon presented by ...dolfo and Arguden (1991) show a similar trend of channel widening with only minor ...cision after the first year. These field observations are supported by the experimental results of Schumm et al. (1987). The experimental channels responded very quickly to changes in elevation when a narrow channel was incised to reestablish a more stable

gradient. The incision period was then followed by a prolonged period of channel widening and high sediment yields. As the widening slowed, sediment yields declined proportionally.

Since the channel gradients appear to have been reestablished in the first year or two, the width of the "stable" channel then determined the amount of sediment available for future rapid erosion. The maximum amount of channel widening that could occur before the channels became "stable" was set at 300 meters -- approximately the maximum width obtained by channels at Mount St. Helens. In most cases, channel widths at Mount Pinatubo were less than this maximum value, being limited by local features such as pre-eruption geology, runoff volumes, or the widths of pre-eruption channels in older pyroclastic deposits. In some basins an additional volume was included to account for the likely occurrence of secondary pyroclastic flows.

The first-year sediment yield for each basin was determined by multiplying the average annual storm runoff by an assumed sediment concentration (see Section 2.3.2). Subsequent annual yields were roughly proportioned according to the ratio between the initial sediment available and the sediment available at the end of each year. The resulting sediment forecasts tend to decline according to trends predicted by Pierson et al. (1992). Figure B-6 shows the declining trend of an idealized annual sediment yield forecast. Specific basin forecasts are presented in following sections of this Appendix.

These sediment yield forecasts reflect average annual conditions. Variations in sediment yields can be expected due to above- or below- average rainfall, the presence or lack of secondary pyroclastic flows, or major changes in channel alignments. Sediment yields in any one year may therefore be above or below the forecast yield, but the overall trend should follow the forecast.

3.5.3 <u>Long-term Forecast</u>. The long-term forecasts are the conditions expected after channel conditions become significantly more stable. Annual yields during this time are governed by water availability and normal muddy water sediment transport. Before the eruption, all the impacted rivers were broad, braided channels with sandy bed material. The long-term sediment yields and related problems are expected to be very similar to pre-eruption conditions. Specific basin conditions are discussed in following sections of this Appendix.

3.5.4 <u>Storm Event Sediment Yields</u>. The sediment yield during large, infrequent storms, such as typhoons, must also be considered in determining the overall hazard and in designing control measures. An event of the magnitude of a 100-year or larger flood may be capable of producing more sediment than several years of near-average flows. Without specific data, the sediment volumes that are forecast for large storm events can only be considered gross estimates (see Section 2.3.5). Storm event yields are likely to decline for the same reasons as annual yields, but no attempt has been made to account for that likely reduction. Specific volume estimates for storm events in each basin are given in Appendix E. Figure B-7 shows the effect that a large sediment yield from a single large storm occurring in 2010 could have on the declining annual sediment yield trend.

These types of events are not directly incorporated into the annual sediment yield forecast because they are rare occurrences. The sediment volumes for 100-year flood events were included in the designs of the sediment control measures.

4. PASIG-POTRERO RIVER BASIN ANALYSIS

The Pasig-Potrero basin is an area of 77 km² originating on the eastern flank of Mount Pinatubo, draining the center section through a deeply incised reach, and exiting the valley onto the alluvial fan-complex above Mancatian. The headwater area is drained by four streams, the Bucbuc, Yangca, Timbu, and Papatac Rivers, which combine to form the Pasig-Potrero River. The upper basin area is about 14 km long with an area of approximately 10 km². The uppermost headwaters originate 13 km from the crater.

The following basin analysis is limited to basin conditions prior to October 1993. A natural diversion of the Sacobia River headwaters into the upper reaches of the Pasig-Potrero River basin occurred during October 1993. This increase in drainage area will greatly increase the flow in the pyroclastic deposit main channel and correspondingly increase sediment yields. The increase in sediment yields has not been fully analyzed or included in this report, but is expected to be very large, perhaps as much as 50 to 100 million m³ in 1994 above the amounts forecast in the report. The new basin conditions are judged to present an extreme threat to communities along the Pasig-Potrero River.

Initial basin analysis between August 1991 to December 1992 indicated that the massive volume of volcanic material deposited in the upper basin presents a number of flooding and sedimentation hazards to the upper and lower alluvial-fan complex. Large-scale secondary pyroclastic flows, lake blockage failures, and rainfall/runoff processes could generate large volumes of sediment, overwhelming the channel system, breaching levees, and impacting large regions of the alluvial-fan complex. The area from Mancatian to Potrero and Bacolor could receive the greatest impact. Sedimentation and shallow flooding would be the dominant processes. Sedimentation within the channel system could also cause levee failures and out-of-channel impacts (USACE, 1993).

Sediment discharged from the Pasig-Potrero upper basin will cause deposition in the Guagua and Cama Chiles Rivers. High sediment yield rates to the lower alluvial-fan complex could cause ponding and increase the potential for severe poolage flooding around Bacolor, San Fernando, Minalin, and Santo Tomas (see Figure B-1).

4.1 Sedimentation History

4.1.1 <u>Pyroclastic Deposits</u>. On June 15, 1991, pyroclastic avalanches flowed down the eastern slope from the exploding crater of Mount Pinatubo, traveling at high speeds under the influence of gravity and following pre-eruption topography, and deposited 302 million m³ of pyroclastic-flow material in the upper basin. The highly incised pre-eruption channel geometry influenced the pyroclastic-flow depositional pattern. A plateau 1.5 km wide and 4 km long, 11 km from the newly formed caldera, separates the upper Pasig-Potrero and Sacobia River basins. During the initial pyroclastic-flow emplacement, material flowed across this plateau and cascaded into the deep Pasig-Potrero basin (see Figure B-8). A

change in momentum occurred and deposition was initiated, partially filling drainage channels carved into older pyroclastic deposits from previous eruptions, the most recent dating back approximately 600 years. Maximum thickness of the new deposits ranges from about 150 meters in the middle to upper reaches to 30 meters in the upper basin 13 km from the crater.

The pre-eruption stream channel cuts through pyroclastic deposits in the upper reaches of the basin, and through sediment and alluvial deposits in the upper alluvial-fan reaches. The sedimentary deposits in the upper reaches are underlain at variable depths by bedrock consisting of andesite, basalt (dikes as well as flow units), agglomerates, conglomerates, tuff breccias and tuffaceous sandstones. The lower reaches consist of a broad alluvial-fan complex which has been under formation for at least 600 years, as sediments from higher in the basin have been mobilized by erosional processes and redeposited downstream.

The drainage boundaries and areas used for the hydrologic analysis of the Pasig-Potrero River basin are shown in Appendix A of this document. Figure B-8 shows the upstream half of the drainage areas while Figure B-9 shows the downstream drainage area and hazard zones. The lower basin was divided into mudflow and flooding zones for sediment impact analysis. Immediately north of Bucbuc Creek, pyroclastic deposits covered and obliterated the pre-eruption drainage network. Following the eruption, a new drainage network quickly formed. Approximately 1.5 km² of the pre-eruption Bucbuc Creek drainage now contributes flow to Timbu Creek.

4.1.2 1991-1993 Erosion and Deposition. Sediment yields in the Pasig-Potrero basin have been dominated by a few large events. These include lake failures in 1991 and 1992, and intense tropical storms in 1992 and 1993. Typhoon Kadiang, in October 1993, not only produced a very high sediment yield, it also triggered the diversion of over 20 km² of the Sacobia River drainage area into the Pasig-Potrero basin. The full impacts of this diversion have not yet been determined.

The pre-eruption channel geometry at the confluence of Papatac and Yangca Creeks favors rapid sediment accumulation due to a natural constriction and a reduction in slope. The rapid narrowing of the pre-eruption channel caused the June 1991 pyroclastic flow to deposit approximately 5 million m³ of material in the confluence area. The blockage measured 100 to over 400 meters in width. During the first rainy season the blockage functioned as a dam and grew to an approximate volume of 10 million m³ before its failure on September 7, 1991. The failure rapidly eroded the entire 10 million m³ of sediment, causing it to cascaded onto the alluvial-fan complex (USACE, Portland District, June 1993). An additional 10 to 15 milion m³ of material was eroded from the Pasig River as this flood moved downstream. The Potrero River levees were breached near Potrero and there was flooding in Potrero, Santa Barbara, Bacolor, and Gaugau. The type and location of the sediment deposits suggest this flood was a hyperconcentrated flow.

A second blockage formed in early August 1992 as the result of a large secondary pyroclastic flow above Yangca Creek on Papatac Creek (Figure B-8). This blockage was larger than the first, with a maximum elevation of 380 meters along the eastern edge. More than 20 million m³ of material filled the confluence area and Papatac Creek as far downstream as its confluence with Timbu Creek. During a tropical storm on August 29-30, 1992, the blockage was overtopped, but this time it eroded at a slower rate. The August 29-30 storm and another on September 3-4, 1992 combined to deliver 10 million m³ of sediment to the lower Pasig-Potrero River basin. Both these events were mudflows and they deposited 7 to 10 km upstream of the 1991 event. Deposition filled the channel at Mancatian and for 4 km downstream. Mudflow deposits in the overbank areas were 1 to 2 m deep around Mitla and about 1/2 m near Balas.

Typhoon Rubing on August 17, 1993, caused a mudflow and 3 to 5 million m³ of deposition around Mancatian. The deposits filled the channel for about 1 km upstream of Mancatian and damaged the northern portion of the barangay. Flooding occurred in Santa Rita, where lahar flowed through an uncompleted portion of the levee. On October 4, 1993, typhoon Kadiang caused hyperconcentrated flows and mudflows that delivered another 20 to 25 million m³ of material to the lower alluvial fan. Most of this sediment was deposited in the southern overbank from Mancatian to Gaugau. Santa Rita was heavily damaged by the 1993 lahars.

Analysis of channel cross sections taken from aerial photographs indicate that main channel erosion also has been a large source of sediment. From June 1991 to November 1992, main channel erosion was 23 million m³, with an unmeasured additional amount in 1993. Figures B-10 and B-11, show the v-shaped main channel geometry that existed in November 1992. An unknown volume was also eroded from tributaries and rill and gully systems on the pyroclastic-flow deposit. The main channel developed along the base of Mount Dorst. The new channel appears to be locked against the valley wall. New craters or sinks formed from phreatic explosions are modifying the drainage system, temporarily trapping volumes of sediment within the basin and reducing initial sediment yields.

Downstream from the pyroclastic deposit the channels have undergone a complex response to the increased sediment loads. The beds of Papatac and Timbu creeks, and the Pasig River were eroded 5 to 10 m in 1991, as far downstream as Mancatian. Papatac Creek's bed was raised by the secondary pyroclastic flow in early August 1992, only to be eroded again in late August 1992, when the lake overtopped the blockage. From the Mancatian to the confluence with the Guagua River, sediment deposition raised the channel bottom elevation of the Pasig-Potrero River by 2 to 4 meters. The Manibaug Pasig Creek still enters the Pasig-Potrero River, but downstream of this confluence other pre-eruption tributaries are now lower than the river and consequently are no longer contributing flow. Loss of tributary flow has reduced the drainage area of the Pasig-Potrero River approximately 78 km² at the confluence with the Guagua River.

4.2 Sediment Forecast

4.2.1 Sediment Producing Events. Sediment production from the upper basin is expected to remain high. Main channel erosional processes are expected to dominate future sediment yields. Pyroclastic-flow deposits from about 4 km of the main channel above Yangca Creek (see Figure B-8) will provide most of this sediment. As shown on Figure B-10, channel geometry is still V-shaped along the base of Mount Dorst. Inflowing clean water appears to have stabilized the channel location. Bank failures from phreatic explosions will continue to occur. Large secondary pyroclastic flow events in 1991 and 1992 have also increased the stability of this channel reach. Channel reaches below Yangca Creek appear to fluctuate within 5 to 10 meters plus or minus pre-eruption elevations. From this area down to Mancatian, channel geometry is trapezoidal and 50 or more meters wide (Figure B-11).

Lake blockage failures like those of 1991 and 1992 appear unlikely under current basin conditions. The lake area is mostly filled with sediment, reducing the water storage potential of the site. Nevertheless, another large secondary pyroclastic flow event in the upper basin could result in another lake blockage formation and possible failure. The risk of another large secondary pyroclastic flow cannot be confidently determined, but given the basin geometry, additional events seem likely in the next 5 to 10 years. The magnitude and frequency of secondary pyroclastic flows appear to be diminishing over time.

Hyperconcentrated flows and mudflows can be expected to dominate sediment transport from the upper basin to the upper alluvial-fan area and lower. Main channel processes will provide the sediment to generate these flow conditions. Bank collapses along the deep v-shaped channels will be a major source. Secondary pyroclastic flows may deposit material in the channel, increasing the supply of material available for future erosion. Drainage density may be near maximum state and sediment yields from the tributary channels should decline.

4.2.2 10-Year Sediment Forecast. The 10-year sediment forecast for the Pasig-Potrero basin is based upon examination of aerial photographs, maps, photogrammetric cross sections, PHIVOLCS channel cross sections, and DPWH channel cross sections as well as interviews and reports of PHIVOLCS and DPWH staff and field investigations. As shown on Figure B-12, sediment yields are forecast to decline from 17 million m³/year in the first year, to about 3 million m³/year in five years. The declining sediment yield is linked to channel location within the basin and the "stable" channel configuration. The pyroclastic deposit will be a major sediment source for the next 20 years.

Sediment available for rapid erosion along the channel ranges from 27 to 33 million m³. For the sediment yield forecast an average of 30 million m³ was used. This forecast is for a relatively short time (10 years). The potential exists for a number of secondary pyroclastic flows to develop in the upper basin during this period and flow onto the middle and distal sections of the alluvial-fan complex in the lower valley. Sizing of these potential secondary pyroclastic flows is based on analysis of flows occurring in 1991 and early 1992, which suggests that secondary pyroclastic-flow sediment yield will be 17 million m³ for the first three years. These potential events are not calculated into the 10-year sediment forecast, but due to their random nature are simply added on.

The forecast distribution of sediments over the 10-year period is shown in Table B-1. Hazard zones are outlined in Figure B-9. Nearly half of the deposition is forecast for the first five years. In-channel (including the area inside the 1993 levee between Mancatian and Santa Rita) deposition accounts for 27 million m³, whereas deposition in the right overbank area is expected to be 7.5 million m³. Mudflow and hyperconcentrated flows will deliver the bulk of the sediment to the lower alluvial-fan complex.

Analysis indicates that the right overbank inner sections have the highest probability of sediment deposition and flooding. Overbank sedimentation and flooding is expected to be frequent but shallow and widespread within these zones. Because sediment has already filled stream channels, even some leveed reaches, overbank areas can be flooded several times each year. Sediment deposition depths are anticipated to average less than 1 meter per event, but accumulations of up to 2 meters could occur. Mudflows could produce overbank deposits of up to 3 m over a limited area.

Overbank impacts could occur in the Potrero area (see Figure B-9 and Table B-1), but the depth should be less than 0.5 meters. In the Porac and Mancatian zones, out-of-channel deposition could be linked to in-channel sedimentation. Localized deposition could induce major levee breaches and increased overbank sediment and flood impacts. In-channel point deposition is not possible to predict.

The sediment yield curve shown in Figure B-12 represents a forecast of average annual conditions. Variations in sediment yields can be expected due to above- or below-average rainfall, the occurrence or lack of secondary pyroclastic flows, lake failures, or major changes in channel alignments. Therefore, sediment yields in any one year may be higher or lower than the forecast yields, but annual yields are expected to follow the forecast trend.

TABLE B-1 *Annual Pasig-Potrero River sediment deposition in million m³*

YEAR & REACH IDENTIFICATION	FLOODING AND DEPOSITION ZONES				
	LEFT OVERBANK			RIGHT OVERBANK	
	OUTER	INNER	CHANNEL	INNER	OUTER
1993					
Pasig	-	0.5	4.0	0.5	-
Mancatian	-	0.5	4.5	0.5	-
Potrero	-	-	3.0	2.0	-
Bacolor	-	-	0.5	-	-
1994					
Pasig	-	0.5	2.0	0.5	-
Mancatian	-	0.5	1.5	0.5	-
Potrero	-	-	0.5	1.5	-
Bacolor	-	-	0.5	-	-
1995					
Pasig	-	-	2.0	-	-
Mancatian	-	0.5	1.5	0.5	-
Potrero	-	-	1.5	4.5	-
Bacolor	-	-	0.5	-	-
1996					
Pasig	-	-	0.0	-	-
Mancatian	-	-	1.0	-	-
Potrero	-	-	2.0	0.5	-
Bacolor	-	-	0.5	-	-
1997-1998					
Pasig	-	-	0.0	-	-
Mancatian	-	-	1.0	-	-
Potrero	-	-	1.0	0.5	-
Bacolor	-	-	0.5	-	-
1999-2000					
Pasig	-	-	0.0	-	-
Mancatian	-	-	0.5	-	-
Potrero	-	-	1.0	-	-
Bacolor	-	-	0.5	-	-
2001-2002					
Pasig	-	-	0.0	-	-
Mancatian	-	-	0.0	-	-
Potrero	-	-	0.5	-	-
Bacolor	-	-	0.5	-	-

4.2.3 Long-term Sediment Forecast. The long-term sediment forecast projects 50 years into the future, based on the major assumption that no further major volcanic action occurs. Over the next 50 years, erosion could total 77 million m³. The analysis indicates that sediment yields initially will be high, but they are expected to return to the pre-eruption range (Figure B-12).

Analysis of pre-eruption aerial photographs (1974) shows a wide and highly braided channel. Sediment transport appears to have been high and the river may have been transport-limited rather than sediment-supply-limited. These active channel data and the JICA (1978) report provide supporting documentation that the Pasig-Potrero River basin had high sediment transport volumes and massive seasonal floods before 1991. Unstable channel conditions and bed aggradation will continue indefinitely.

Future sediment problems in the Pasig-Potrero River system will also depend on the size, location, and timing of secondary pyroclastic flows. These flows could create lakes on Yangca Creek that could be capable of producing sediment yields of 10 million m³ in a single year. The timing of these events cannot be predicted and they will remain a risk for many years. Secondary pyroclastic flows could create smaller lakes in Bucbuc and Timbu Creeks, but they would probably be too small to produce sediment yields comparable to the Yangca Creek lake.

In the future, the Pasig-Potrero River is likely to undergo periods of erosion and deposition as water and sediment discharge rates change. Sediment transport calculations show the sediment transport potential decreasing in the downstream direction during storm events. Thus, when runoff from heavy rainfall on the pyroclastic deposits moves large amounts of sediment into the Pasig River, deposition is likely. However, when the inflowing sediment load is small, the sandy river bed is likely to erode. The long-term trend will be one of deposition and redevelopment of the historic alluvial fan. The stream may eventually come out-of-bank and migrate to other drainages unless controlled in its present location. Flooding will be a frequent occurrence until the stream channel is stabilized.

The future impact of lake failures (if lakes form) appears to depend on the relative amounts of water and sediment. Evidence suggests that the 1991 lake failure had more water than sediment in the upper reaches of the Papatac, resulting in scour throughout the Pasig River, while the 1992 lake failure may have had more sediment available in Papatac Creek than it could transport, producing deposition in the Pasig River. The potential impact of lake failures will thus change over time as lakes form and fail. If the Pasig River channel completely fills with sediment, the entire alluvial-fan area from Angeles City to Floridablanca could be threatened by potential lake-failure lahars.

Future sediment conditions along the Potrero River will be dominated by the occurrence or lack of lake failures in the headwaters. Rainfall/runoff processes, including monsoons and typhoons, are likely to produce less than 2 million m' per year of sediment inflow, resulting in sediment inflow similar to the pre-eruption conditions described by Japan International Cooperation Agency (JICA 1978). The river's ability to transport sediments through the reach was decreased when it perched in 1991 and local inflows were blocked. Lake failures have the potential to produce sediment yields of 10 to 20 million m' in a matter of hours. These events will almost certainly be depositional in this reach of the river. The location of deposition can range over the entire reach. As sediment accumulates in the channel, the potential will increase for the river to breach the levees and migrate across the alluvial fan.

Sediment from the Pasig-Potrero River system will slowly but steadily accumulate in delta channels. The severity of Delta flooding will depend on the extent to which deposition restricts the flow to Pampanga Bay. Lake failures may cause small surges of sediment to reach the delta channels, but this does not appear to be a serious problem for the future. Lake failures may cause additional deposition in the Bacolor and Guagua areas. However, raising the San Fernando-Olongapo Highway decreased that probability for Bacolor.

5. SACOBIA-BAMBAN RIVER BASIN ANALYSIS

The Sacobia basin is an area of 146 km² extending northeasterly from the upper flanks of Mount Pinatubo to the alluvial fan complex of the Central Luzon Basin (see Figure B-1). The basin headwater area consists of narrow steep parallel valleys on the mountain's flank. The Bamban drainage includes three other tributaries, the Sapang-Cauayan, Marimla, and Malago Rivers, but the subject of this study is the Sacobia-Bamban River. Only the upper Sacobia River basin was filled with pyroclastic-flow deposit as a result of the 1991 eruption. Approximately 25 km downstream from the crater this stream becomes the Bamban River. Appendix A (Hydrology and Hydraulics) provides a detailed basin discussion.

The following basin analysis is limited to basin conditions prior to October 1993. A natural diversion of the Sacobia headwaters into the upper reaches of the Pasig-Potrero River basin occurred during October 1993. This reduction in drainage area will significantly reduce sediment yields in the Sacobia-Bamban River. However, the full impact of this basin change has not been analyzed and is not accounted for in this report.

5.1 Sedimentation History

5.1.1 Pyroclastic Deposits. When the initial eruption phase terminated on June 15, 1991, 602 million m³ of pyroclastic-flow material was emplaced in the upper Sacobia River basin. Most of the deposit was in the deep river valley within 5 to 15 km from the caldera, at depths ranging up to 160 meters (see Figures B-13, B-14, B-15, and B-16). These deposits filled the pre-eruption valley with unstable and non-cohesive volcanic material. The upper basin was also covered with 5 to 50 cm of ash. During the initial emplacement, secondary pyroclastic flows were generated which aided sediment redistribution and channel redevelopment. The deposit's non-cohesive nature combined with high rainfall rapidly formed a new drainage network.

5.1.2 1991-1993 Erosion and Deposition. Erosion was very high during 1991, and declined during each of the next two years. Analysis of channel cross sections taken from aerial photographs show erosion of the channels in the pyroclastic deposit, from June 1991 to November 1992 totaling 138 million m³. No measurement was made for the 1993 erosion volume. During the 1991 rainy season, an unknown volume of airfall ash was eroded from the mountain and valley slopes and deposited along the edges of the pyroclastic flow deposit and in downstream channels on the alluvial fan.

During June and July 1991, much of the Sacobia River discharge was diverted into the Abacan River at the Gates of the Abacan, about 3 km upstream of Clark Air Base. On July 25, 1991 (Pierson and Scott, USGS, personnel communication, July 1992), headward erosion on the main stem of the Sacobia recaptured the upper Sacobia River basin at the Gates of the Abacan blockage and stopped flow to the Abacan River. Subsequent reduction of drainage

area, discharge, and sediment supply in the Abacan River decreased impact in the new Abacan River area of the lower alluvial-fan complex.

Sediment data show that 68 million m³ and 48 million m³ of material was deposited in the Sacobia system during 1991 and 1992, accounting for a total of 116 million m³ out of the 138 million m³ of erosion in the upper Sacobia River basin during those years. Sedimentation data analysis using a mass balance method suggests that about 22 million m³ of material flowed down the Abacan River system.

Mudflow and hyperconcentrated flow events delivered sediment to the upper and lower alluvial-fan complex during the 1991 rainy season. The Clark and Lake areas (see Figure B-17) were mainly impacted by thick mudflow events. Five to 10 m of channel aggradation occurred in those two reaches. Hyperconcentrated flow deposits covered a large area of the northern floodplain from Concepcion on downstream (see Figure B-17). The Concepcion area was flooded for several months as a result of levee breaches and sediment deposition in the channel. The volume of deposition in 1991 was calculated at 68 million m³. Most of the sediment came from main channel erosion in the pyroclastic flow deposits. Headward erosion and bank line failures were the dominant processes. Phreatic explosions were a secondary process.

The 1992 rainy season produced further massive mudflows and hyperconcentrated flows, but geomorphic processes changed. Main channel erosion became secondary to large secondary pyroclastic flow events. During this period, four large secondary flow events occurred in the middle basin (see Figure B-18) which yielded high volumes of sediment to the alluvial-fan complex. Not all of the sediment generated by these events exited the deposit area. Sediment filled long reaches of the channel, priming the system for rapid erosion during storm events. During subsequent storms, especially on August 29-30 and September 3-4, 1992, sediment cascaded out of the middle basin and deposited in the Clark and Lake reach channels and Lake overbank area. Portions of Mabalacat and Bamban were heavily damaged in August and September 1992. Mudflows and hyperconcentrated flows were the transport mechanism in the middle basin, while muddy water flows dominated on the alluvial-fan complex. Only minor sediment and flood impacts occurred in areas downstream of the San Francisco reach (see Figure B-17) in 1992. The Concepcion area experienced some local flooding due to 1991 sediment deposition blocking drainage channels.

The 1992 channel deposits in the Lake reach caused the Sacobia River to be diverted onto the southern floodplain at Mabalacat during all of 1993. Even though sediment yields were much less than the previous years, the diverted flow caused frequent flooding and significant sediment deposition on the floodplain between Mabalacat and the Magalang-San Francisco highway in 1993. The levee along the north bank near Bamban was breached in August 1993, causing prolonged flooding, but little sediment deposition on the northern floodplain.

5.2   Sediment Forecast

5.2.1 Sediment Production Events. Main channel erosion is expected to dominate future sediment yields. Sediment loading from secondary pyroclastic flows and bank line phreatic explosions will continue to disturb channel development. Field observations indicates that secondary pyroclastic flow locations are less susceptible to fluvial erosion and additional movement. These areas appear more stable and are hence likely to show a reduction in sediment yield and/or erosion rates.

Channel development on the pyroclastic deposit is a complex process. Channel geometry and plain form are impacted by secondary pyroclastic flows and bank line phreatic explosions. Pre-eruption basin geology hard points may influence these processes, with links to sediment yield. Trapezoidal and V-shaped channel geometry dominates (Figures B-14, B-15, and B-16). Data indicate that sedimentation processes and yields will continue to fluctuate, with links to the geomorphic processes impacting the upper and middle basin.

Hyperconcentrated flows and mudflows can be expected to occur regularly until channel geometry and alignment are stabilized. The channel bottom will reach a stable width of about 300 meters in a few years. The impact of secondary flow events and phreatic explosions will be reduced over time. Sediment production or erosion will shift down-basin; in about six years, the Clark reach will become a sediment supply zone.

5.2.2 10-Year Forecast. The Sacobia-Bamban River pyroclastic-flow deposit sediment yields (see Figure B-19) are expected to continue the rapid decline observed during the past three years. The sediment yields are forecast to decline from 19 million m³/year the first year to about 3 million m³/year in five years. By the year 2001, sediment yields may decline to pre-eruption levels. The development of the "stable" channel condition on the pyroclastic-flow deposits is the controlling factor. Basin analysis shows that under current short-term conditions, large secondary pyroclastic flows are not likely to have a direct impact on sediment yields. Allowing for 10 meters of additional incision along with channel bed widening of up to 300 m, the main channel erosion is expected to be 72 million m³ in the next 10 years.

The forecast distribution of sediment deposition over the next 10 years is shown on Table B-2. The hazard zones are outlined on Figure B-17. Nearly half of the deposition forecast for the Sacobia-Bamban River is expected to occur in the 12-km channel reach below the initial 1991 deposit. Mudflow deposition will dominate the Clark and Lake reaches, whereas hyperconcentrated flows and muddy water flows will dominate the lower reaches. The first five years will be dominated by mudflow events.

TABLE B-2 *Annual Sacobia-Bamban River sediment deposition in million m³*

YEAR & REACH IDENTIFICATION	FLOODING AND DEPOSITION ZONES				
	LEFT OVERBANK			RIGHT OVERBANK	
	OUTER	INNER	CHANNEL	INNER	OUTER
1993					
Clark	n/a	n/a	3	0	n/a
Lakes	n/a	n/a	8	4	0
San Francisco	n/a	n/a	0	3	0
Concepcion	n/a	n/a	0	1	0
1994					
Clark	n/a	n/a	3	0	n/a
Lakes	n/a	n/a	2	4	0
San Francisco	n/a	n/a	0	4	1
Concepcion	n/a	n/a	0	1	0
1995					
Clark	n/a	n/a	3	0	n/a
Lakes	n/a	n/a	1	2	0
San Francisco	n/a	n/a	0	3	1
Concepcion	n/a	n/a	0	1	0
1996					
Clark	n/a	n/a	1	0	n/a
Lakes	n/a	n/a	0	2	0
San Francisco	n/a	n/a	0	3	1
Concepcion	n/a	n/a	0	1	0
199?					
Clark	n/a	n/a	0	0	n/a
Lakes	n/a	n/a	0	1	0
San Francisco	n/a	n/a	0	3	0
Concepcion	n/a	n/a	0	1	0
1998-2002					
Clark	n/a	n/a	-1	0	n/a
Lakes	n/a	n/a	0	1	0
San Francisco	n/a	n/a	0	2	0
Concepcion	n/a	n/a	0	1	0

Overbank flooding and sedimentation will be nearly continuous along the south side of the channel because of the 1992 diversion of the Sacobia River at Mabalacat. Overbank sedimentation and flooding are expected to occur mainly in the southern Lake and San Francisco areas, with flood waters depositing some sediment in the Concepcion reach. Flooding will be frequent and flood waters will meander across a large geographical area. Sediment deposition will be a continuous process with a steady, gradual accumulation of material in the overbanks. The depth of deposition will vary from several meters near Mabalacat to a few centimeters in the Concepcion zone.

The sediment yield curve shown on Figure B-19 represents a forecast of average annual conditions. Variations in sediment yields can be expected due to above- or below-average rainfall, the occurrence or lack of secondary pyroclastic flows, or major changes in channel alignments. Therefore, sediment yields in any one year may be higher or lower than the forecast yields, but annual yields are expected to follow the forecast trend.

5.2.3 Long-term Yield Forecast. Erosion over the next 50 years could total 112 million m^3. The 10-year yield forecast is based on no new major volcanic action. Erosion rates are expected to decline (see Figure B-19) as the upper basin channel bed widens; the wider the channel bed, the more the active channel can meander without eroding high banks of pyroclastic deposits. Less frequent contact between channel and bank line reduces sediment loading and sediment yields. Sediment concentrations will drop, and hyperconcentrated flow and mudflow concentration occurrences diminish. Sediment yield to the lower alluvial-fan complex will also diminish. Channel degradation in the 14-km reach below the pyroclastic flow deposit will increase sedimentation and flooding in the lower Sacobia-Bamban system. This long-term sediment hazard has been estimated to be in the 1 to 3 million m^3/year range and will probably continue for years.

Analysis of pre-eruption aerial photographs (1974) shows the Clark and Lake channel reaches to have been highly braided and laden with sediment, indicating that the system was unstable and subject to high sediment yield events before 1991. Future sediment transport in the Sacobia-Bamban River is expected to be similar to those pre-eruption conditions. The type of flooding and sedimentation problems will be different due to the channel infill that has already occurred. Overbank flooding will be a frequent occurrence for the foreseeable future. The southern overbank will be the most frequently flooded because of the 1992 diversion at Mabalacat. However, the unstable channel conditions increase the risk of levee failures and flooding along the north bank. Floods should deposit only small amounts of sediment to the northern floodplain.

6. O'DONNELL RIVER BASIN ANALYSIS

The O'Donnell River basin includes two major rivers, the O'Donnell and the Bulsa. The O'Donnell system drains the northern slopes of Mount Pinatubo, with steep and narrow highly incised parallel channels in the headwaters. The drainage area of the pyroclastic deposit is only 11 km². Upstream of the Bulsa confluence O'Donnell River's drainage area is 266 km². The Bulsa River drains about 510 km² from its headwaters on the upper northeastern slopes of the Zambales Range. The entire basin system covers about 817 km² (see Figure B-1).

6.1 Sedimentation History

6.1.1 Pyroclastic Deposits. The 1991 eruption of Mount Pinatubo deposited 241 million m³ of pyroclastic flow material in the upper O'Donnell River basin. The material was deposited in a deep canyon between 2 and 9 km from the volcano's crater. The toe of the deposit is within an area of pyroclastic plateaus remaining from an ancient eruption. The pyroclastic material is predominantly sand, with lithic gravel and cobble found mainly within 6 km of the crater.

The deposits have maximum depths of 120 to 140 meters. The surface elevation of the deposit appears to have been controlled by the crest of the pre-eruption ridge dividing the O'Donnell and Bucao River basins. For much of the 1991 rainy season, the headwaters of the O'Donnell River within about 6 km from the crater were diverted into the Bucao River basin.

The initial pyroclastic surface was smooth and sloped down toward the east. This surface dip influenced the development of the drainage pattern, causing the main channel to move east, abandoning its pre-eruption alignment about 6.5 km from the crater. The new channel has incised into the pre-eruption ground in this area, just as it has incised into the 1991 material.

Aerial photographs show some phreatic explosion activity in 1991, but this does not seem to have been an important factor in drainage pattern development. Nor have secondary pyroclastic flows had much impact on the system. Only one secondary pyroclastic flow, near the base of the pyroclastic deposit, has been identified in the O'Donnell deposits (see Figure B-20).

6.1.2 1991-1993 Erosion and Deposition. Analysis of channel cross sections taken from aerial photographs show main channel erosion from June 1991 to November 1992 totaling 20 million m³, while tributary channels and smaller drainages accounted for 6 and 9 million m³ respectively. A review of the lahar deposits indicates that deposition and therefore erosion did not decline from 1991 to 1992, but were about equal in both years. Increased runoff may have offset the increasing stability of the established channel, resulting

in the nearly equal erosion. Two separate factors may have caused this increased runoff: 1) the recapture of the headwaters sometime around the end of August 1991, and 2) heavy rainfall. Analysis shows that much of the erosion in the upper 3 km of the pyroclastic channel occurred after August 10, 1992, a period corresponding with four weeks of steady rainfall recorded at Iba, Zambales (PAGASA, written communication, 1993).

Deposition in 1991 and 1992 was largely confined to the active channel area in the O'Donnell valley, upstream from the Bangat River (Swiss Disaster Relief, 1993). Downstream from the Bangat River, there may have been some deposition early in 1991, but PHIVOLCS river surveys showed the reach through Tarlac to have scoured in 1992. By the end of 1992, low-lying areas adjacent to the channel upstream of the Bangat River had been covered with less than 1 meter of sediment. Most of the 1992 lahar deposition occurred after August 10. As the channel between Santa Juliana and the Bangat River filled with sediment, flooding became a problem along the south side of the O'Donnell River in that reach.

Like the pre-eruption channel, the new main channel is very straight, with only one large meander. By November 1992, the main channel had incised 20 to 40 meters into both the 1991 pyroclastic material and the pre-eruption ground (see Figures B-21 and B-22). In the upper 4 km of the pyroclastic deposit, the 1992 channel was nearly 100 meters wide, with cobbles covering nearly half the channel. In the lower 4 km of the pyroclastic deposit, the river flows in a V-shaped channel with a narrow, sandy bed.

A review of photographs taken on August 31, 1993 shows that up to that time, 1993 erosion had been much less than the previous two years. In the upper reaches, within about 5 km of the crater rim, erosion was confined to a narrow, nearly straight channel that wandered within the broader 1992 active channel. The 1993 channel in that reach was estimated to be 20 to 30 meters wide and up to 5 meters deep. Farther downstream, the river continued to incise the bottom of the V-shaped channel to a maximum depth of around 5 meters.

The 1993 deposition followed the pattern of the previous two years, occurring mostly in the channels. Mudflow deposits appeared to be located upstream of Santa Juliana, within 10 km of the base of the pyroclastic deposit. Lahars continued to flow across southern overbank areas near the towns of O'Donnell and Santa Lucia. Signs of minor channel degradation were observed in the Bangat River at Santa Lucia in August 1993. In October 1993, flood waters eroded the southern abutment to the Bangat River Bridge at Santa Lucia. Downstream of the Bangat River, sedimentation continued to be minor and no significant flooding was observed.

6.2   Sediment Forecast

6.2.1   <u>Sediment Producing Events</u>. Main channel erosion is expected to dominate future sediment yields. Erosion may be especially high through the lower 4 km of the pyroclastic deposit channel. In this reach the V-shaped channel still has a narrow bed and high steep sides. Other pyroclastic deposit channels do not have sufficient drainage areas to be significant sediment sources.

Hyperconcentrated flows and mudflows can be expected to occur regularly until the deep V-shaped channel achieves a bottom width of over 100 meters. After that occurs, the frequency of these events should be reduced to about one or two per year.

Secondary pyroclastic flows are not expected to contribute significantly to sediment yields. The geometry of the pre-eruption watershed appears to limit the potential for secondary pyroclastic flows to the middle and west channels at the base of the pyroclastic deposit (see Figure B-20). The likelihood of secondary pyroclastic flows at these locations was not well defined, but was considered low. Should such a flow occur, it would have serious local impacts and could increase sediment yields for a short time afterward.

6.2.2   <u>10-Year Forecast</u>. The O'Donnell River pyroclastic deposit sediment yields (see Figure B-23) are forecast to decline from 13 million m³/year to about 2 million m³/year over a five year period. After that, sediment yields may continue to decline until yields approach the pre-eruption range. The projected sediment yields are controlled by the limited runoff from the pyroclastic deposit, as well geologic controls that tend to reduce erosion potential. The "stable" channel width ranges from 500 meters to as little as 125 meters. The wider reach lies just upstream of the current V-shaped channel, in an area where the main channel has been migrating to the east. The narrow widths are in a reach where the channel is incised into pre-eruption ground. Allowing for 10 meters of additional incision, main channel erosion is expected to be 27 million m³ in the next 10 years.

The sediment yields shown in Figure B-23 represent a forecast of average annual conditions. Variations in sediment yields can be expected due to above- or below-average rainfall, the occurrence of unexpected secondary pyroclastic flows, or major changes in channel alignment. Therefore, sediment yields in any one year may be above or below the forecast yields, but on the average, annual yields should follow the forecast trend and total volumes.

The forecast distribution of sediment deposition over the next 10 years is shown in Table B-3. The hazard zones are outlined in Figure B-24. Nearly half of the deposition forecast in the O'Donnell River basin in the next 10 years is expected to occur in the 10-km reach just downstream of the pyroclastic deposit. Most of that deposition will be due to mudflows in the first five years. Overbank areas likely to receive flooding and sediment deposition are all upstream of the Bangat River. Overbank flooding is expected to be frequent but shallow, as floodwaters spread out across the floodplain in the O'Donnell-Santa Lucia area. Sediment deposition from most floods will be less than 0.5 meters, but accumulations could reach 1 to 2 meters in some locations.

Overbank areas in the Maniknik and Tarlac reaches (Figure B-24) may be subject to flooding, but sediment deposition should not significantly exceed pre-eruption rates. Flooding may be more severe or more frequent due to levee failures caused by channel aggradation and/or meandering.

6.2.3 Long-Term Yield Forecast. Erosion over the next 50 years could total 67 million m³. Except for the first 10 years, the forecast erosion appears to be in the same range as the erosion that might have occurred even if the volcano had not erupted. Pre-eruption aerial photographs (1974) show a very active braided channel in the O'Donnell valley, suggesting high sediment yields from the upper basin. Unstable river conditions are likely to continue indefinitely. Flooding in the O'Donnell area could also remain a frequent problem because the channel infill will allow the river to meander across the overbanks.

How long the threat will exist of secondary pyroclastic flows at the base of the pyroclastic deposit is not currently known. Given the extreme local danger from such events and the limited knowledge about them, they should be considered a long-term hazard.

TABLE B-3 *Annual O'Donnell River sediment deposition in million m³*

YEAR & REACH IDENTIFICATION	FLOODING AND DEPOSITION ZONES				
	LEFT OVERBANK			RIGHT OVERBANK	
	OUTER	INNER	CHANNEL	INNER	OUTER
1993					
Bombing Range	n/a	1	5	1	n/a
O'Donnell	n/a	0	4	1	0
Maniknik	n/a	0	1	n/a	0
Tarlac	0	0	0	0	0
1994					
Bombing Range	n/a	1	3	1	n/a
O'Donnell	n/a	0	2	1	0
Maniknik	n/a	0	1	n/a	0
Tarlac	0	0	0	0	0
1995					
Bombing Range	n/a	0	2	0	n/a
O'Donnell	n/a	0	2	0	0
Maniknik	n/a	0	1	n/a	0
Tarlac	0	0	0	0	0
1996					
Bombing Range	n/a	0	1	0	n/a
O'Donnell	n/a	0	2	0	0
Maniknik	n/a	0	0	n/a	0
Tarlac	0	0	0	0	0
199- 2002					
Bombing Range	n/a	0	1	0	n/a
O'Donnell	n/a	0	1	0	0
Maniknik	n/a	0	0	n/a	0
Tarlac	0	0	0	0	0

7. BUCAO RIVER BASIN ANALYSIS

The Bucao Basin incorporates the Bucao River and its two major tributaries, the Balin-Buquero River and the Balintawak River. The Balin-Buquero system includes four major tributaries, of which only the Marouot River, is officially named. The watershed follows a generally northwesterly direction from the volcano to the South China Sea.

The upper basins of the Bucao and Balin-Buquero rivers are a large fan complex of relatively flat and low-lying terrain, separated from the coastal alluvial-fan complex by the north-south trending westernmost mountains of the Zambales Mountain Range. This fan complex was heavily impacted by pyroclastic flows during the 1991 and earlier eruptions.

The Balintawak River system, which received no pyroclastic-flow deposits but was only blanketed by airfall ash during the 1991 eruption. The Balintawak River system was not considered a significant sediment source and was not analyzed.

7.1 Sedimentation History

7.1.1 Pyroclastic Flows. At termination of the eruptive phase on June 15, 1991, a total of 3,000 million m³ of pyroclastic flow material had been deposited in the upper Bucao and Balin-Buquero basins. The bulk of the deposition occurred between 3 km and 10 km down-slope from the new crater. The pre-eruption drainage channels were filled, forming a broad and gentle western slope landscape. The upper basin was also covered with a blanket of airfall ash.

The headwaters of the Bucao River originate on the northwest slopes of Mount Pinatubo (see Figure B-25), at an elevation of about 900 meters. This region was covered with pyroclastic flow deposits ranging from only a few meters on the plateaus, to a maximum thickness of about 150 meters in the river valleys. The upper 6 km of the initial pyroclastic deposit was further modified by a 1992 secondary pyroclastic flow that originated along the divide with the O'Donnell River.

The Balin-Buquero drains the western upper flanks of Mount Pinatubo to the south of the Bucao River (Figure B-25). The Balin-Buquero basin and its tributaries were also covered with pyroclastic flow deposits ranging from only a few meters on the plateaus, to a maximum thickness of 150 meters in the river valleys. Deposition completely filled the Marouot River channel and diverted the river to the south, about 6 km northwest of the crater.

7.1.2 <u>1991-1993 Erosion and Deposition</u>. Eight major and numerous smaller tributaries transport sediment from the pyroclastic deposit to the main stems of the Bucao and Balin-Buquero rivers. A combination of rill and gully erosion, phreatic explosions, and secondary pyroclastic flows aided in the redevelopment of the drainage networks in the tributaries. Secondary pyroclastic flows have been a more important sediment producing process in the Bucao River basin than in the other basins. Cross-section analysis for the period of June 1991 to November 1992 shows that 600 million m³ of material was eroded from the initial pyroclastic deposit. No estimate is available for the amount eroded during 1993. Fluvial erosion of airfall ash from surrounding mountain slopes appears to have been a main sediment source only during the 1991 rainy season.

A large secondary pyroclastic flow occurred on the Maronut River during the 1991 rainy season. Headscarp movement was initiated about 6 km northwest of the new crater, but the flow crossed the Maronut drainage divide and continued down one of the minor Bucao tributaries and into the Bucao River. A number of phreatic explosions also occurred during the 1991 rainy season.

Secondary pyroclastic flow and phreatic explosion processes continued during the 1992 rainy season. Three major secondary pyroclastic flows appear to have provided the bulk of the 1992 sediment yield. A massive secondary pyroclastic flow occurred along the Bucao/O'Donnell divide. The flow averaged 1,000 meters wide and flowed 6 to 7 km down the channel. A total volume of 50 to 100 million m³ of sediment was delivered to the main stem of the Bucao River. A second major secondary pyroclastic flow occurred on a tributary of the Balin-Buquero River. Approximately 50 million m³ of pyroclastic material from the base of the deposit (near mid-basin), cascaded about 6 km into the lower valley. Since the lower slope is nearly flat, most of this flow was deposited in the tributary valley, but some sediments did flow into the main stem of the Balin-Buquero River. The downstream distribution of sediment from this event is not known, but it is likely that some of the sediment reached the Bucao River. The third and smallest major event that occurred during the 1992 rainy season impacted the upper reach of the "new" Maronut River. The failure surface is about 1,000 meters wide by 2,000 meters long. Sediment from this event remained in the upper channel area and thus produced no sedimentation impacts on the coastal alluvial-fan complex.

Field observations during the 1993 rainy season disclosed no additional major modifications on the upper alluvial-fan complex (upper basin area). Fluvial channel erosion appeared to progress the same as in other basins.

Mudflows seem to be limited to the upper reaches of the Bucao and Balin-Buquero rivers. In the middle reaches of the Bucao and Balin-Buquero Rivers, transport processes consisted mainly of hyperconcentrated flow events. The sediment transport concentrations in the lower Bucao River are highly variable, depending on the relative flow contributions from the sediment laden Bucao and Balin-Buquero rivers, and the cleaner Balintawak River.

Deposition has been very heavy in the upper reaches of the Bucao and Balin-Buquero rivers. Deposition has buried the town of Poonbato, located at the confluence of the Bucao and Balintawak rivers. Channel deposition ranges from around 20 m at Poonbato to about 5 m at the confluence of the Bucao and Balin-Buquero rivers at Malumboy. Deposition continues between this confluence and the South China Sea, with the active channel area or flood plain widening varying markedly from about 200 meters to 1,000 meters. Deposition thicknesses in the channel through the lower coastal fan complex are locally 2 to 3 meters. Distal thickness is less than 1 meter. Streamflow measurement data (Bureau of Research and Standards, unpublished) indicated about 1 m of deposition occurred at the Highway 7 bridge in 1991, with no additional accumulation in 1992. Field observations indicate that the transport mechanisms were muddy water to hyperconcentrated flow events. Flooding has not been a problem in the lower river.

7.2   Sediment Forecast

7.2.1   Sediment Producing Events. Rainfall/runoff is expected to continue to be the primary process delivering sediment to the lower reaches of the Bucao River. However, secondary pyroclastic flows are likely to be an important factor in sediment yields. There is a high risk of secondary pyroclastic flows or landslides in the zone extending from 6 to 12 km downstream from the crater area along the western flanks of the mountain. There is a low probability that the direct runout of these mass movements will reach the main stem of the Bucao River, but they will deposit additional sediment in the main channels that can then be eroded.

Normal geomorphic processes will continue to erode and transport material out of the upper basin. High sediment yields will continue for the next few years. Over time, channel processes and additional drainage development will reduce sediment yield from the upper basin. The V-shaped tributary channels are expected to widen to around 100 meters in the upper reaches and 200 meters near the base of the pyroclastic deposit. Frequent hyperconcentrated flows and mudflows are expected to continue to be generated in the pyroclastic deposit channels for the next 5 to 10 years. After that, unusually heavy rainfall may still generate these flows. Most mudflows will deposit upstream of the confluence of the Bucao and Balin-Buquero rivers.

Clean water entering the Bucao River from the Balintawak River increases transport capability in the lower 20 km, reducing the risk of mudflow hazards in the lower river reach. However, a gradual accumulation of sediment may occur in this reach.

7.2.2 10-Year Forecast. Sediment yields are forecast to decline at a rapid rate (see Figure B-31). Over the next 10 years a total of 101 million m³ is forecast to be eroded from the pyroclastic deposit, compared to over 600 million m³ in the first two years following the eruption.

The sediment yield curve shown in Figure B-31 represents a forecast of average annual conditions. Variations in sediment yields can be expected due to above- or below-average rainfall, the occurrence or lack of secondary pyroclastic flows, or major changes in channel alignments. Therefore, sediment yields in any one year may be higher or lower than the forecast yields, but annual yields are expected to follow the forecast trend.

The forecast distribution of sediment deposition over the next 10 years is shown on Table B-4. The hazard zones are outlined in Figure B-32. Nearly half of the deposition is forecast to occur in the headwaters reaches of the Bucao and Balin-Buquero rivers. Most of that deposition will be caused by mudflows during the first three years of the forecast.

An estimated 3 to 4 million m³/year will continuously be transported into the lower 10 km of the river. Most of this material will be transported to the South China Sea, but about 1 m³/year is expected to deposit in the San Juan reach. This gradual accumulation of sediment could over time, raise the river bed enough for floods to overtop the levee along the north side of the river. The rate and timing of this deposition is uncertain and should be monitored to improve the estimate.

7.2.3 Long Term Forecast. Erosion over the next 50 years could total 261 million m³. After the first 10 years, the forecast erosion appears to be similar to what might have occurred even if the volcano had not erupted. The accumulation of sediment in the San Juan reach could continue for many years. However, the river's behavior in this reach is not well understood and additional data should be collected and analyzed to improve this estimate.

How long the threat of secondary pyroclastic flows at the base of the pyroclastic deposit will exist is not currently known. Each occurrence seems to increase the stability of the pyroclastic deposit. However, this process is not well enough understood to justify concluding that if secondary pyroclastic flows do occur, there would be no subsequent risk. Given the extreme local danger from such events, they should be considered a long-term hazard.

TABLE B-4 *Annual Bucao River sediment deposition in million m³*

YEAR & REACH IDENTIFICATION	FLOODING AND DEPOSITION ZONES				
	LEFT OVERBANK			RIGHT OVERBANK	
	OUTER	INNER	CHANNEL	INNER	OUTER
1993					
Headwaters	-	-	25	-	-
Malumboy	-	-	10	-	-
San Juan	-	0	2	-	-
Botolan	-	-	0	0	0
1994					
Headwaters	-	-	10	-	-
Malumboy	-	-	5	-	-
San Juan	-	0	2	-	-
Botolan	-	-	0	0	0
1995					
Headwaters	-	-	5	-	-
Malumboy	-	-	2	-	-
San Juan	-	0	1	-	-
Botolan	-	-	0	0	0
1996					
Headwaters	-	-	0	-	-
Malumboy	-	-	1	-	-
San Juan	-	0	1	-	-
Botolan	-	-	0	0	0
1997-2002					
Headwaters	-	-	0	-	-
Malumboy	-	-	1	-	-
San Juan	-	0	0	-	-
Botolan	-	-	0	0	0

NOTE: Three million m³/year is expected to be discharged to the South China Sea.

8. SANTO TOMAS RIVER BASIN ANALYSIS

The Santo Tomas River basin watershed covers an area of about 262 km², draining the southwestern section of the mountain to the South China Sea (see Figure B-33). The Santo Tomas River system incorporates the Marella and Mapanuepe rivers, which join to become the Santo Tomas River. The reach length from the caldera to the confluence of the Marella and Mapanuepe Rivers is about 28 km. The Santo Tomas River begins at this confluence and flows about 23 km to the sea.

8.1 Sedimentation History

8.1.1 Pyroclastic Deposits. The June 1991 eruption left a total of 1,400 million m³ of pyroclastic material in the Santo Tomas-Marella River basin in two separate deposits. One fills a broad valley between 2 and 7 km south-southwest of the crater. The second deposit lies about 1 to 2 km farther west (see Figure B-33). The two deposits converge about 8 km from the crater rim.

The eastern valley varies in width from about 500 to 2,000 meters and has a slope of nearly 10 percent. The deposits range from 10 to 20 meters deep on the flatter upper terraces of the valley, to over 100 meters deep in the old stream channels (see Figures B-34 and B-35). About 7 km² of the upper watershed was diverted into a pre-eruption channel that flows along the southern boundary of the eastern pyroclastic deposit. A moderate-sized secondary pyroclastic flow occurred at the diversion point in 1991 (see Figure B-33). Because of the flow diversion, there are no large stream channels crossing the eastern pyroclastic deposit.

The western deposit ranges from 400 to 800 meters wide and up to 120 meters deep, with a main channel that drains the upper west side of the watershed. Near the base of the pyroclastic deposit the channel has been diverted to the east, around the pre-eruption hill shown on Figure B-33. A large secondary pyroclastic flow occurred in the abandoned river valley in early August 1992, depositing material in the main channels for several kilometers downstream.

8.1.2 1991-1993 Erosion and Deposition. Sediment deposition during 1991 totaled approximately 210 million m³. Sediment produced by rill, gully, and channel erosion on the pyroclastic surface was aggravated by the secondary pyroclastic flow in the eastern deposit, and by erosion of ash deposits on the steep mountains adjacent to the Marella River.

Most of the deposition occurred in the Marella River, with depths of approximately 30 meters near the base of the pyroclastic deposit and 20 meters at the confluence with the Mapanuepe River. Deposit depths continued to decline downstream in the Santo Tomas River to about 5 meters near the barangay of San Rafael and 1 meter at the Highway 7 Bridge.

A large lake formed on the Mapanuepe River because of the blockage at its confluence with the Marella River. The lake flooded over 4 km^2 and several communities in the Mapanuepe valley. The Mapanuepe River periodically overtopped the blockage, only to be dammed again by deposits from the Marella River. ZLSMG staff (Rodolfo and Umbal, personal communication, 1993) reported frequent discharges in the hyperconcentrated and mudflow range from both the pyroclastic deposit and Mapanuepe River. Overbank flooding occurred in the lower 7 km of the Santo Tomas River, impacting the towns of San Narciso and San Felipe.

Sediment yields in 1992 again totaled near 200 million m^3. Sediment yields on the Marella River, like those on the O'Donnell, did not follow the declining yield pattern described by Pierson et al. (1992) for other volcanoes. The higher than expected yields were most likely the result of the combination of a secondary pyroclastic flow and heavy rainfall. The drainage channels continued to evolve in a pattern similar to other channels around Mount Pinatubo, with the western channel forming a V-shaped valley incised about 40 meters into the pyroclastic deposit. However, a large secondary pyroclastic flow near the base of the deposit clogged both the east and west channels shortly before the onset of heavy rains in August 1992. Rainfall records from the Dizon Mines (written communication, 1993), which are located 6 km southeast of the Marella/Mapanuepe confluence, show that August 1992 had the third highest monthly rainfall in the last 10 years. It appears that the heavy rains rapidly eroded the secondary pyroclastic flow deposits from the main channels and contributed significantly to the unusually high sediment yield.

An additional 5 to 10 meters of aggradation occurred in the Marella River in 1992. The pre-eruption ridge at the Marella/Mapanuepe confluence was breached on the west side near the base of Mount Bagang. By November 1992, mudflows had traveled as far downstream as San Rafael where they deposited an additional 3 to 5 meters in the channel. However, no significant deposition occurred in the lower 10 km of the Santo Tomas River. The flooding of Dizon Mines by Mapanuepe Lake led to the construction of a new lake outlet on the southern side of the Santo Tomas River. Levees built by the Department of Public Works and Highways before the 1992 rainy season contained river flows and prevented flooding along the lower 20 km of the Santo Tomas River.

The pyroclastic deposit eroded much less in 1993 than in the previous two years. A rough estimate based on photographs places the total 1993 erosion at less than 60 million m^3. Sediment contributions from various source areas on the pyroclastic deposit could not be defined because weather conditions limited access to the area. However, it was clear that re-erosion of earlier deposits in the Marella River and contributed 5 to 10 million m^3 of sediment to the pyroclastic yield.

Sediment erosion and deposition in 1993 were dominated by two large typhoons, Rubing in August and Kadiang in October. Prior to August, deposition had been minor in the Marella River, but it had nearly filled the Santo Tomas River channel in the vicinity of San Rafael. Runoff from typhoon Rubing caused a large mudflow that traveled as far as San Rafael,

intersecting and overtopping a recently completed 3-meter-high levee just south of the barangay. The mudflow deposit reached depths of around 4 meters near the levee. Discharges from Mapanuepe Lake, flowing along the south side of the Santo Tomas River channel, were diverted over the levee by the mudflow deposit. The Mapanuepe discharges quickly eroded the levee and overflowed toward San Marcelino and San Antonio. Flooding continued for nearly a week, until the levees were repaired. Most overbank damages were the result of flooding, with sediment deposition generally limited to within 1 km of the levee.

During the late stages of typhoon Rubing, a new channel 2 to 5 meters deep and 100 to 150 meters wide was eroded into the deposits of the Santo Tomas and Marella Rivers from San Rafael upstream to the pyroclastic deposit. The channel was aligned along the west side of the Marella River and to the center and north side of the Santo Tomas. This channel was much larger than any other channel observed in this basin since the eruption.

Typhoon Kadiang produced 326 mm of rain at Dizon Mines on October 5, 1993 (Dizon Mines, written communication, 1993). This was 133 mm more than the next highest daily rainfall since the 1991 eruption, and the second highest daily total in 17 years at Dizon Mines. Sediment yields from the pyroclastic deposit were large during Kadiang, but perhaps not as large as might have been expected from a storm of this magnitude. Channel erosion continued in the Marella River channel downstream of the pyroclastic deposit, with an estimated 5 meters of additional bed erosion. Mudflows, possibly mixed with hyperconcentrated flows, followed the active channel of the Santo Tomas River for about 2 km before crossing the north overbank to Santa Fe, burying the town in 1 to 2 meters of sediment. Deposition in the river bottom near Santa Fe reached depths of up to 8 meters. Along the south side of the Santo Tomas channel, mudflows from the Marella River combined with Mapanuepe Lake discharges to breach the levee at the upstream end, again near San Rafael, and toward the downstream end near San Marcelino (ZLSMG, 1993). Flooding again lasted several days before emergency repairs closed the levee breaches.

8.2 Sediment Forecast

8.2.1 Sediment Producing Events. Rainfall/runoff is expected to continue to be the primary process delivering sediment to the Santo Tomas River. However, secondary pyroclastic flows are likely to be an important sediment source. The currently V-shaped western channel is expected to widen to approximately 100 meters in the upper reaches and 300 meters near the base of the pyroclastic deposit. The eastern branch cuts across the toe of the pyroclastic deposit at the site of the 1992 secondary pyroclastic flows. It is in this vicinity that additional secondary pyroclastic flows are most probable.

Frequent hyperconcentrated flows and mudflows are expected to continue to be generated in the pyroclastic deposit channels for the next 5 to 10 years. After that, unusually heavy rainfall may still generate these flows. As long as the large channel remains on the Marella River, mudflows will tend to be transported to the Santo Tomas River without as much

dispersion or attenuation as before August 1993. Lower concentration flows will likely erode through the Marella River.

8.2.2 <u>10-Year Forecast</u>. Sediment yields are forecast to decline at a rapid rate (see Figure B-36), continuing the trend started in 1993. Over the next 10 years a total of 130 million m' is forecast to be eroded from the pyroclastic deposit, compared to 212, 200, and 60 million m' in 1991, 1992, and 1993 respectively. Because of the high probability of secondary pyroclastic flows, an additional 15 million m' of sediment has been included in each of the first three years of the forecast. Once the sediment yields from the pyroclastic deposit have declined sufficiently, the Marella River channel is expected to begin to erode.

The sediment yield curve shown in Figure B-36 represents a forecast of average annual conditions. Variations in sediment yields can be expected due to above- or below-average rainfall, the occurrence or lack of secondary pyroclastic flows, or major changes in channel alignments. Therefore, sediment yields in any one year may be higher or lower than the forecast yields, but annual yields are expected to follow the forecast trend.

The forecast distribution of sediment deposition over the next 10 years is shown on Table B-5. The hazard zones are outlined in Figure B-37. Nearly half of the deposition is forecast to occur in the Santo Tomas River channel between the Mapanuepe River and a point about 2 km downstream of San Rafael. Most of that deposition will be caused by mudflows during the first three years of the forecast. The southern floodplain will receive most of the non-channel deposition, because the orientation of the Marella River will tend to build a fan toward the southwest. Sediment deposition is most likely near the Santo Tomas River and upstream of San Marcelino, but flooding may spread over most of the southern floodplain. Flooding could become more frequent as sediment deposition causes the river to meander across the broad channel and onto the overbanks.
Some sediment, in quantities smaller than can be analyzed in this study, will continuously be transported into the lower 10 km of the river. Much of this material will be transported to the South China Sea, but an unknown amount will deposit. Monitoring of conditions at the Highway 7 bridge would provide a better understanding of sedimentation in this lower reach.

TABLE B-5 *Annual Santo Tomas River sediment deposition in million m³*

YEAR & REACH IDENTIFICATION	FLOODING AND DEPOSITION ZONES				
	LEFT OVERBANK		CHANNEL	RIGHT OVERBANK	
	OUTER	INNER		INNER	OUTER
1993					
Upper Mapanuepe	n/a	5	10	n/a	n/a
Mapanuepe	4	n/a	20	n/a	n/a
San Marcelino	1	3	1	n/a	n/a
San Falipe	0	0	1	0	0
1994					
Upper Mapanuepe	n/a	1	5	n/a	n/a
Mapanuepe	4	n/a	15	n/a	n/a
San Marcelino	1	3	1	n/a	n/a
San Falipe	0	0	0	0	0
1995					
Upper Mapanuepe	n/a	1	5	n/a	n/a
Mapanuepe	4	n/a	10	n/a	n/a
San Marcelino	1	3	1	n/a	n/a
San Falipe	0	0	0	0	0
1996					
Upper Mapanuepe	n/a	0	0	n/a	n/a
Mapanuepe	0	n/a	4	n/a	n/a
San Marcelino	0	1	1	n/a	n/a
San Falipe	0	0	0	0	0
1997					
Upper Mapanuepe	n/a	0	0	n/a	n/a
Mapanuepe	0	n/a	2	n/a	n/a
San Marcelino	0	1	1	n/a	n/a
San Falipe	0	0	0	0	0
1998					
Upper Mapanuepe	n/a	0	-2	n/a	n/a
Mapanuepe	1	n/a	2	n/a	n/a
San Marcelino	0	1	1	n/a	n/a
San Falipe	0	0	0	0	0

TABLE B-8 (Continued) *Annual Santo Tomas River sediment deposition in million m³*

1999

Upper Mapanuepe	n/a	0	-2	n/a	n/a
Mapanuepe	1	n/a	2	n/a	n/a
San Marcelino	0	1	1	n/a	n/a
San Falipe	0	0	0	0	0

2000

Upper Mapanuepe	n/a	0	-2	n/a	n/a
Mapanuepe	1	n/a	2	n/a	n/a
San Marcelino	0	1	1	n/a	n/a
San Falipe	0	0	0	0	0

2001

Upper Mapanuepe	n/a	0	-3	n/a	n/a
Mapanuepe	1	n/a	2	n/a	n/a
San Marcelino	0	1	1	n/a	n/a
San Falipe	0	0	0	0	0

2002

Upper Mapanuepe	n/a	0	-3	n/a	n/a
Mapanuepe	1	n/a	2	n/a	n/a
San Marcelino	0	1	1	n/a	n/a
San Falipe	0	0	0	0	0

NOTE: An unknown amount of sediment will be discharged to the South China Sea each year.

8.2.3 <u>Long Term Forecast</u>. Erosion over the next 50 years could total 160 million m³. After the first 10 years, the forecast erosion appears to be similar to what might have occurred even if the volcano had not erupted. Ten years ago, sediment yields from the Marella basin were high enough to annually fill the irrigation reservoir near the Mapanuepe River (Alejandrino et al., personal communication, 1993). Unstable river conditions are likely to continue indefinitely. Flooding and overbank sedimentation is likely to be more severe that prior to the eruption because the river channels have been filled by sediment. In the future, the river will be able to meander outside of the former channel boundaries and routinely cause flooding unless actions are taken to contain the river.

How long the threat of secondary pyroclastic flows at the base of the pyroclastic deposit will exist is not currently known. Each occurrence seems to increase the stability of the pyroclastic deposit. However, this process is not well enough understood to justify concluding that if the forecast three secondary pyroclastic flows do occur, there would be no subsequent risk. Given the extreme local danger from such events, they should be considered a long-term hazard.

9. COMPARISON OF SEDIMENT YIELD FORECASTS

PHIVOLCS and the USGS have collaborated on analyses of the Mount Pinatubo eruption and subsequent lahar problems. As part of that analyses they have calculated the pyroclastic deposit volumes and made total sediment yield forecasts for each basin (Pierson et al., 1992; PHIVOLCS, 1993). Table B-6 presents the pyroclastic deposit and forecast volumes prepared by PHIVOLCS/USGS and those presented in this report.

The PHIVOLCS/USGS sediment forecast is based on fixed percentages of material eroding from each of the pyroclastic deposits. A value of 40 percent was used for the Pasig-Potrero, Sacobia-Bamban, and O'Donnell rivers, and 50 percent was used for the Bucao and Santo Tomas rivers. The higher value was used for the west side rivers to account for the higher annual rainfall on that side of Mount Pinatubo. An additional 10 percent was used in all basins to account for erosion of pre-eruption material. The range of sediment yields resulted from applying the percentages to the range of pyroclastic deposits calculated by PHIVOLCS/USGS.

In this report, a total of 1.9 billion m', out of the 5.6 billion m' of total pyroclastic flow material deposited on the flanks of Mount Pinatubo during the June 1991 eruption, was forecast to be eroded within 50 years after the eruption (Table B-6). This erosion volume represents 34 percent of the total initial pyroclastic flow deposit volume and includes the erosion amounts which occurred during the period from June 1991 to November 1992. In the individual basins, the forecast erosion to initial deposit ratios are; Pasig-Potrero, 33 percent; Sacobia-Bamban, 41 percent; O'Donnell, 42 percent; Bucao, 29 percent; and Santo Tomas, 41 percent. The variations in yield ratios are due to variations in the complexity of the geomorphic processes occurring within each basin, as described earlier in this report.

TABLE B-6 *USACE and PHIVOLCS/USGS sediment volumes in million m³*
(Note: This includes 1991-1992 erosion volumes)

	PYROCLASTIC DEPOSIT	TOTAL YIELD
PASIG-POTRERO RIVER		
USACE	302	100
PHIVOLCS/USGS		
Low	300	120
High	500	200
SACOBIA-BAMBAN RIVER		
USACE	602	250
PHIVOLCS/USGS		
Low	700	280
High	1,100	440
O'DONNELL RIVER		
USACE	241	102
PHIVOLCS/USGS		
Low	300	180
High	600	360
BUCAO RIVER		
USACE	3,000	863
PHIVOLCS/USGS		
Low	2,500	1,250
High	3,100	1,550
SANTO TOMAS RIVER		
USACE	1,400	572
PHIVOLCS/USGS		
Low	1,000	500
High	1,300	650
TOTAL OF ALL BASINS		
USACE	5,900	1,887
PHIVOLCS/USGS		
Low	4,800	2,330
High	6,600	3,200

10. CONCLUSIONS

Sediment yields have declined dramatically at Mount Pinatubo, but will remain a dangerous threat for several more years. Mudflows can be expected to occur several times a year on all five rivers for the next 5 to 10 years. After that time, annual sediment yields to the fan areas will drop to near pre-eruption levels. However, mudflows may still be occur on an infrequent bases. The Pasig-Potrero, Sacobia-Bamban, O'Donnell, and Santo Tomas channels on the alluvial fans are already filled with sediment and future lahars can spill onto the populated floodplains.

Sediment yields may be highly variable over both short and long time periods. Secondary pyroclastic flows or other basin disturbances could cause immediate, large surges of sediment. The occurrence or lack of unusually large storms will also cause variations in sediment yields. Monitoring of the pyroclastic deposits and the river channels needs to continue in order to evaluate changing conditions.

In October 1993, heavy rainfall and rapid erosion caused about 21 km^2 of the Sacobia River basin to be diverted into the Pasig River basin. This large increase in Pasig River drainage area is very likely to cause a tremendous increase in sediment yield in 1994 and beyond. The full impact of this basin change has not been evaluated for this report, but it is judged to present an extreme hazard to communities along the Pasig-Potrero River and also to endanger surrounding areas. Sediment yields and lahars in the Pasig River in 1994, are expected to be similar to those experienced in the Sacobia River in 1991 or 1992. Pasig-Potrero River sediment deposition of 50 to 100 million m^3 is considered possible in 1994. A complete analysis of this situation is needed before the 1994 rainy season.

REFERENCES

Alejandrino, Angel, Rhoel Villa, and Leonardo Liongson, Philippine National Hydraulic Research Center, August 1993, personnel communications

Bureau of Research and Standards, Philippine Department of Public Works and Highways, Sediment Load Analysis, unpublished

Crandell, Dwight, R., 1980. Recent eruption history of Mt Hood, Oregon, and potential hazards from future eruptions: U.S. Geological Survey Bulletin, number 1492, pp.81.

Carey, Steve, N., 1991. Transport and deposition of tephra by pyroclastic-flows and surges. In Edt. by R.V. Fisher and G.A. Smith, Sedimentation in Volcanic Settings, SEPM Special Pub., No., 45. p. 39-57.

Daag, A., Philippine Institute of Volcanology and Seismology, September 1991, written communications

Daag, Arturo and Norman Tungol, Philippine Institute of Volcanology and Seismology, November 1992, personnel communications

Delfin, F.G. Jr., 1984, Geology and Geothermal Potential of Mt. Pinatubo Geothermal Prospect, unpublished report, Philippine National Oil Company, pp 36.

Dizon Mine, written communications, 1993

Dolan, Mike, Michigan Technological University, August 1993, personnel communications

Elliott, J. W., 1979. Evolution of large arroyos, the Rio Puerco of New Mexico: Unpublished Master of Science thesis. Colorado State University, Fort Collins, Colorado, p.106.

Eriksen, Karl W., 1989, Limitations of Modeling High Concentration Streams, Proceedings of the International Symposium on Sediment Transport Modeling, ASCE, New Orleans

Fairchild, L. H., 1987. The importance of lahar initiation processes. Reviews in Engineering Geology, Geol. Soc. of America, v. VII, pp.51-61.

Francis, P.W. and M.C. Baker, 1977, Mobility of Pyroclastic Flows, Nature, Vol. 270, pp. 164-165

Hey, R. D., 1978. Determinate hydraulic geometry of river channels. ASCE, Journal Hydraulic Division., v. 104, pp.869-885.

Henderson, F. M., 1961. Stability of alluvial channels: Jour. Hyd. Div. ASCE, v.87, pp.109-138

Janda, R. J., et al, December 1991, Lahars Accompanying the Mid-June 1991 Eruptions of Mount Pinatubo, Tarlac and Pampanga Provinces, The Philippines, abstract in American Geophysical Union Bulletin, San Francisco.

Japan International Cooperation Agency, September 1978, Planning Report on the Pasig-Potrero River Flood Control and Sabo Project, Tokyo, Japan

Julian, Pierre Y. and Yongqiang Lan, 1989, Laboratory Analysis of Hyperconcentrations, Colorado State University

Keller, E. A., 1972. Development of alluvial stream channels: A five-stage model: Geol. Soc. America Bull., v. 83, pp.1531-1536.

Lane, E. W., 1937. Stable channels in erodible material: Am. Soc. Civil Trans., v. 102, pp. 123-142.

Love, D. W., 1979. Quaternary fluvial geomorphic adjustments in Chaco Canyon, New Mexico: In Adjustment of the Fluvial System. (Editors, Rhodes, D., and Williams, G. P.) Kendall-Hunt, Dubuque, Iowa, pp. 277-280.

Meyer, D.F. and J.E. Dodge, 1988, Post-Eruption Changes in Channel Geometry of Streams in the Toutle River Drainage Basin, 1983-85, Mount St. Helens, Washington, USGS Open File Report 87-549.

Northwest Hydraulic Consultants Inc., 1993, Mount Pinatubo Regional Analysis of Hydrometeorologic Data, prepared for Portland District, U S Army Corps of Engineers

Park, C.C., 1976. The relationship of slope and stream channel form in the River Dart, Devon. Journal of Hydrology, v. 29, pp.139-147.

Parker, R.S., 1977. Experimental study of basin evolution and its hydrologic implications, unpublished PhD. Dissertation, Colorado State Univ., Fort Collins, CO., 331 pp.

Pearson, M.L., 1986. Sediment yields from the debris avalanche for water years 1980-1983: in Keller, S.A.C., ed., Mount St. Helens: Five Years Later: Eastern Washington University Press, Cheney, p.87-107.

Pearson, M.L. and K.W. Eriksen, 1994 (in preparation), Post-Eruption Evaluation of the Upper Sacobia River Basin, The Philippines, U.S. Army Waterways Experiment Station Misc. Report, Vicksburg, Mississippi

Penning-Rowsell, E. and Townshend, J. R. G., 1978: The influence of scale on the factors affecting stream channel slope: Trans. Institute British Geographers, v. 3, pp.395-415.

Philippine Atmospheric, Geophysical, and Astronomical Services Administration (PAGASA), Climatology Branch, Rainfall Intensity Duration frequency Data of the Philippines, 1981.

Philippine Atmospheric, Geophysical, and Astronomical Services Administration, 1993, unpublished rainfall data

Philippine Department of Public Works and Highways, September 1992, contour maps of Potrero River, Acre Surveying and Development, Quezon City

Philippine Institute of Volcanology and Seismology (PHIVOLCS), 1993, Pinatubo Volcano: Past Events and Future Outlook

Philippines Star newspaper, September 1991, Bacolor villages to be converted into lahar catch basins

Pierson, T.C., Janda, R.J., Umbal, J.V., and Daag, A.S., 1992. Immediate and long-term hazards from lahars and excess sedimentation in rivers draining Mt. Pinatubo, Philippines. USGS, Water-Resources Inv. Rep. 92-4039, p. 35.

Pierson, Thomas, U.S. Geological Survey, August 1992, personnel communications

Pierson, Thomas and Willie Scott, U.S. Geological Survey, July 1992, personnel communications .

Punongbayan, R. S., et al, December 1991, Initial Stream Channel Responses to Large 1991 Volumes of Pyroclastic-Flow and Tephra-Fall Deposits at Mount Pinatubo, Philippines, abstract in American Geophysical Union Bulletin, San Francisco.

Rodolfo, Kelvin S. and A. Tevfik Arguden, 1991, Rain Lahar Generation and Sediment Delivery Systems at Mayon Volcano, Philippines, Sedimentation in Volcanic Settings, ed. R.V. Fisher and G.A. Smith, SEPM Special Publication No. 45

Rodolfo, Kelvin and Jesse Umbal, Zambales Lahar Scientific Monitoring Group, April 1993, personnel communications

Rodolfo, Kelvin and Jesse Umbal, Zambales Lahar Scientific Monitoring Group, June 1993, written communications

Sasitharan,S., Robertson, P.K., Sego, D.C., and Morgenstren, N.R., 1992. Collapse Behavior of Sand: Submitted to Canadian Journal, November 09,1992.

Schumm, S. A., 1961. The shape of alluvial channels in relation to sediment type: U.S. Geol. Survey Prof. Paper 352-B, pp.1-30.

Schumm, S. A., 1961. The effects of sediment characteristics on erosional and deposition in ephemeral channels: U.S. Geol. Survey Prof. Paper 352-C, pp.31-70.

Schumm, S.A., Mosley, M. P., and Weaver, W.E., 1987. Experimental Fluvial Geomorphology: John Wiley and Sons, New York, NY.

Schumm, S.A., Harvey, M.D., and Watson, C.C., 1984. Incised Channels Morphology, Dynamics and Control. Water Resource Publications, Littleton, Colorado.

Scott, K., U.S. Geological Survey, October 1992, personnel communications

Scott, W., U.S. Geological Survey, July 1992, personnel communications

Swiss Disaster Relief, 1993. Lahars in the O'Donnell River System, Mt. Pinatubo, Philippines; Hazard assessment and engineering measures: Government of Switzerland, Swiss Disaster Relief, pp.1-68.

Umbal, Jesse, et al, December 1991, Lahars Remobilized by a Breaching of a Lahar-dammed Non-volcanic Tributary, Mount Pinatubo, Philippines, abstract in American Geophysical Union Bulletin, San Francisco.

U.S. Army Corps of Engineers, Portland District, 1984, Mount St. Helens, Cowlitz and Toutle Rivers Sedimentation Study/1984, Portland, Oregon

U.S. Army Corps of Engineers, Portland District, 1985, Mount St. Helens Washington, Decision Document, Portland, Oregon

U.S. Army Corps of Engineers, Portland District, September 1992, (Preliminary) Report on Mount Pinatubo's Soil Investigation, RZA Agra Inc, Portland, Oregon

U.S. Army Corps of Engineers, 1993. Mount Pinatubo Interim Action Report, prepared for the United States Agency for International Development (USAID), Final June 1993.

U.S. Army Corps of Engineers, Portland District, 1993, Cowlitz River Basin Water Year 1992 Hydrologic Summary, Mount St. Helens, Washington, Portland, Oregon

Yang, Chih Ted, 1973, Incipient Motion and Sediment Transport, Journal of Hydraulics Division, ASCE, Vol. 99, No. HY 10

Zambales Lahar Scientific Monitoring Group, 11 October 1993, Lahar Update.

Zimmermann, Markus and D. Rickenmann
Swiss Disaster Relief,
Eigerstrass 71, 3003 Bern, Switzerland
phone : +41 (31) 61 31 24; Fax + 41 (31) 45 83 34
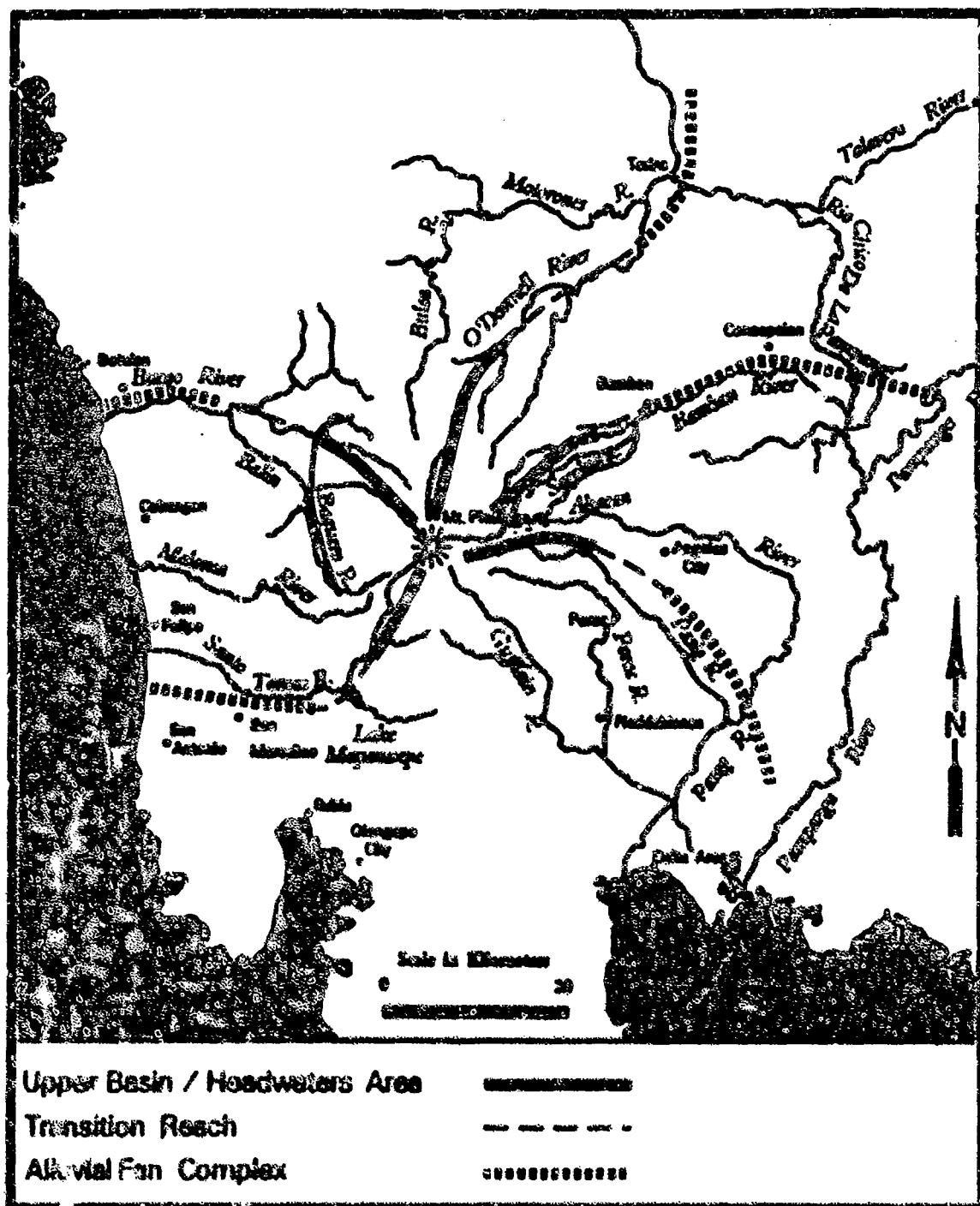
Figure B-1. General Location Map, Mount Pinatubo. Illustrating the Three Geomorphological Zone in Each of the Major Basins, Upper Basin/Headwaters, Transition Reach, and the Alluvial Fan Complex.

Figure B-2. Pyroclastic Flow Deposit Location Map, Mount Pinatubo. Illustrates Pyroclastic Flow Location in the upper Basin/Headwaters of the five basins.

Figure B-3. Secondary Pyroclastic Flow Deposit Location Map, Mount Pinatubo. Illustrates major Secondary Pyroclastic Flow Areas which developed between June 1991 and November 1993.
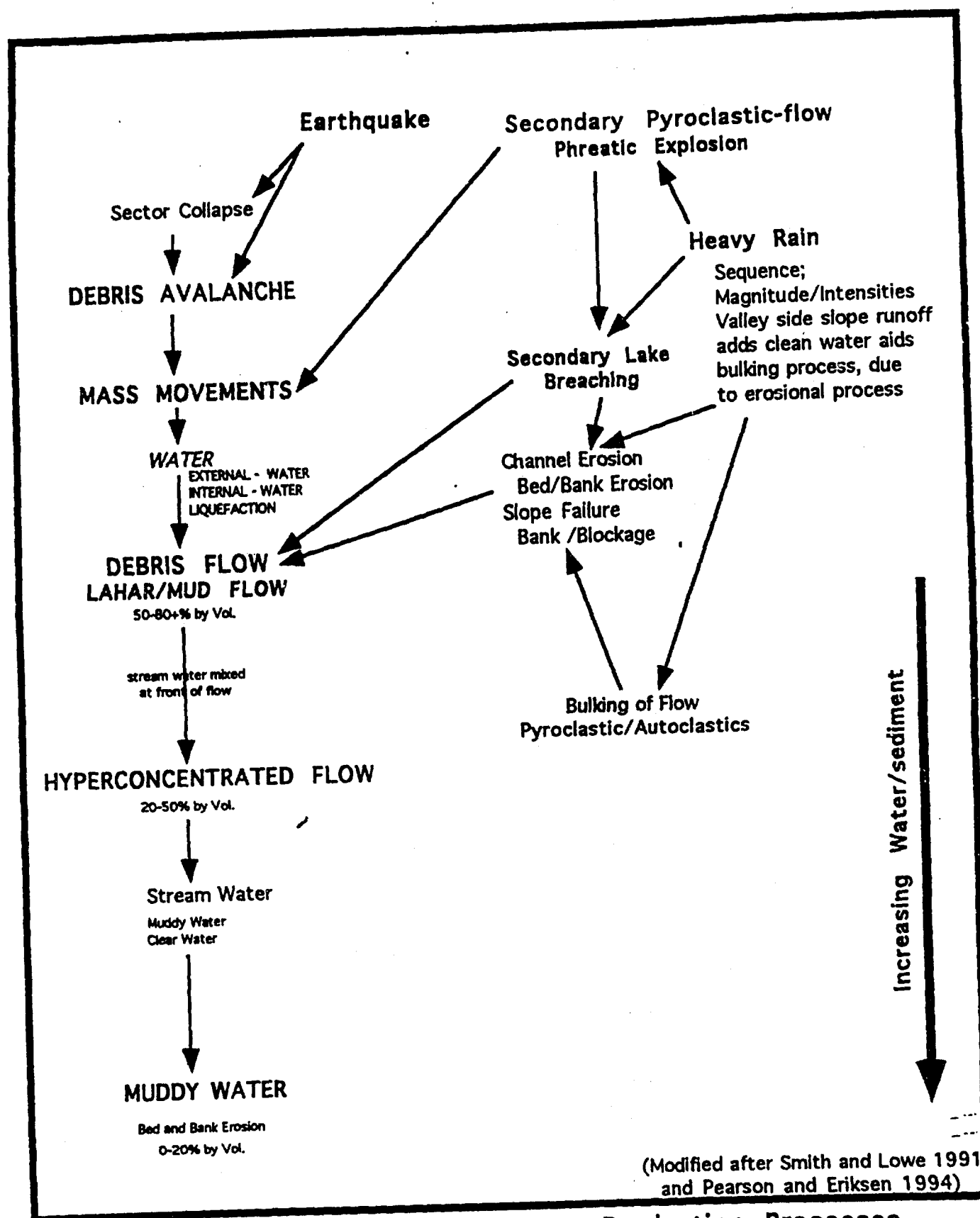
Figure B-4 Schematic of Sediment Production Proceeses.
Illustration of princilpe processes related to sediment transport and deposition of volcanic sediment. Type of flow phenomena and water to sediment relationships are also indicated.
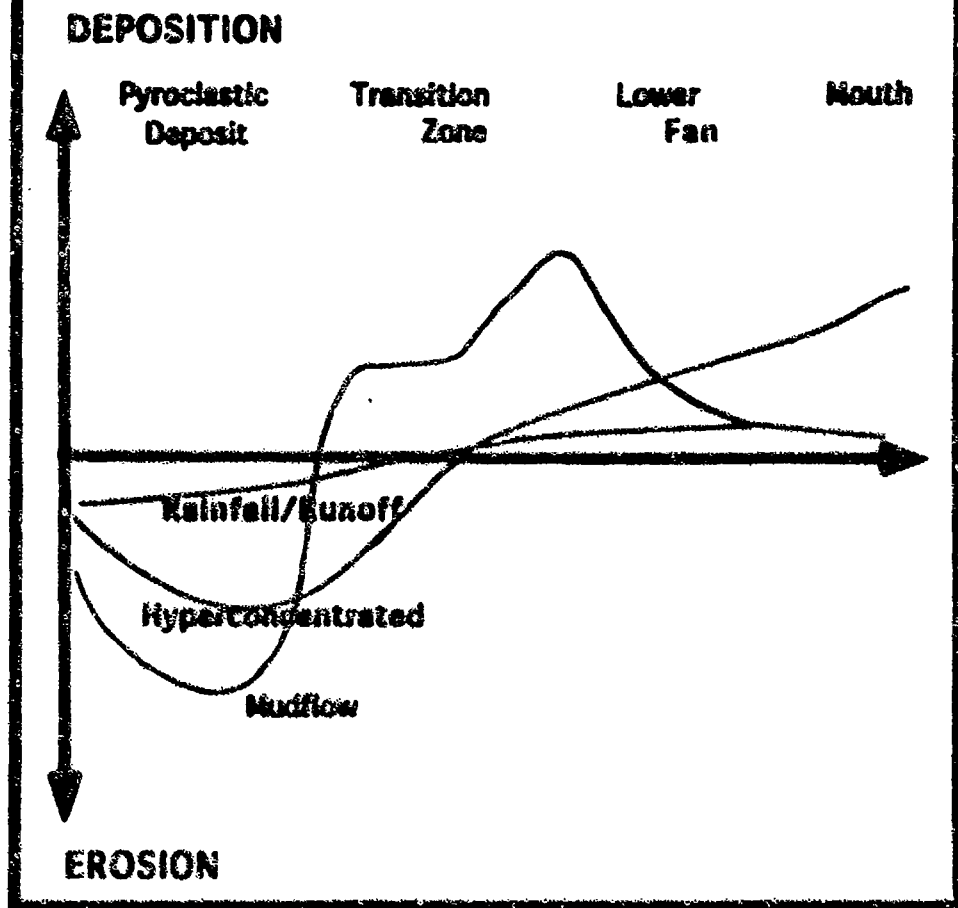
Figure B-5. Schematic Diagram of Relative
Magnitude of Erosion and Deposition Through
an Impacted Basin.
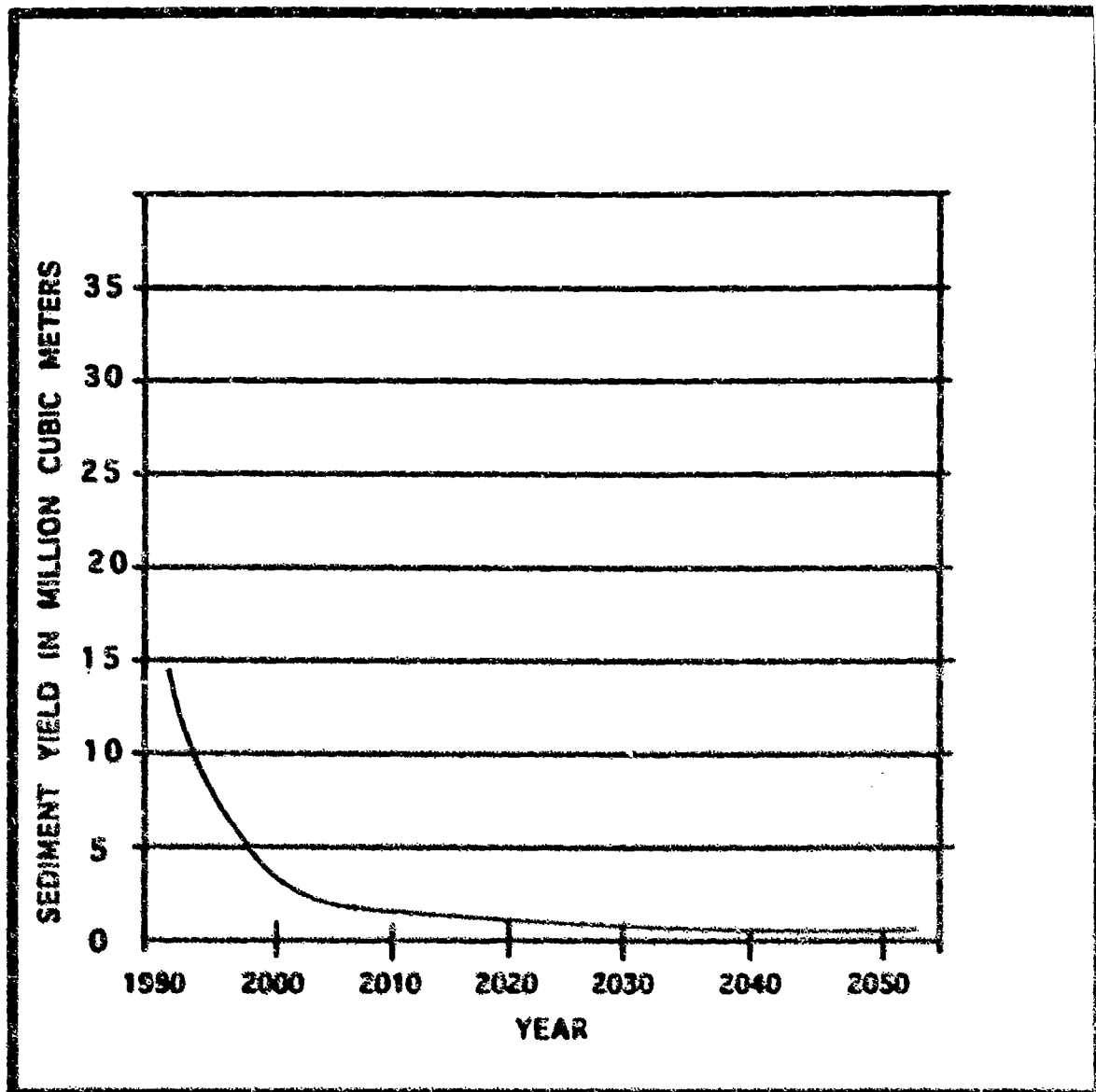
Figure B-6. Idealized Plot of Average Annual Sediment Yield, Mount Pinatubo, The Philippines.
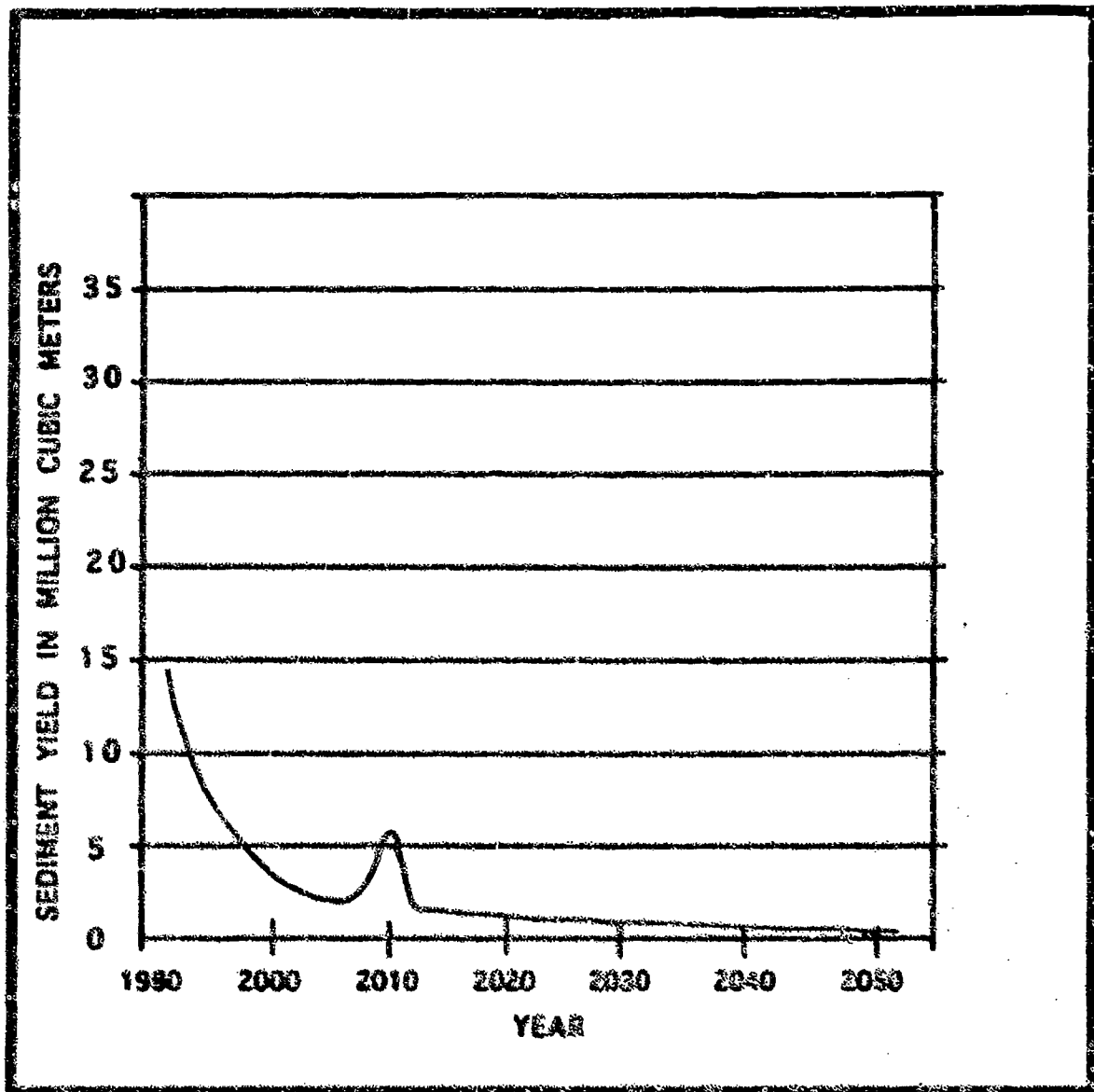
Figure B-7. Potential Impact of Large Strom Events on Averag Annual Sediment Yield, Mount Pinatubo, The Philippines.
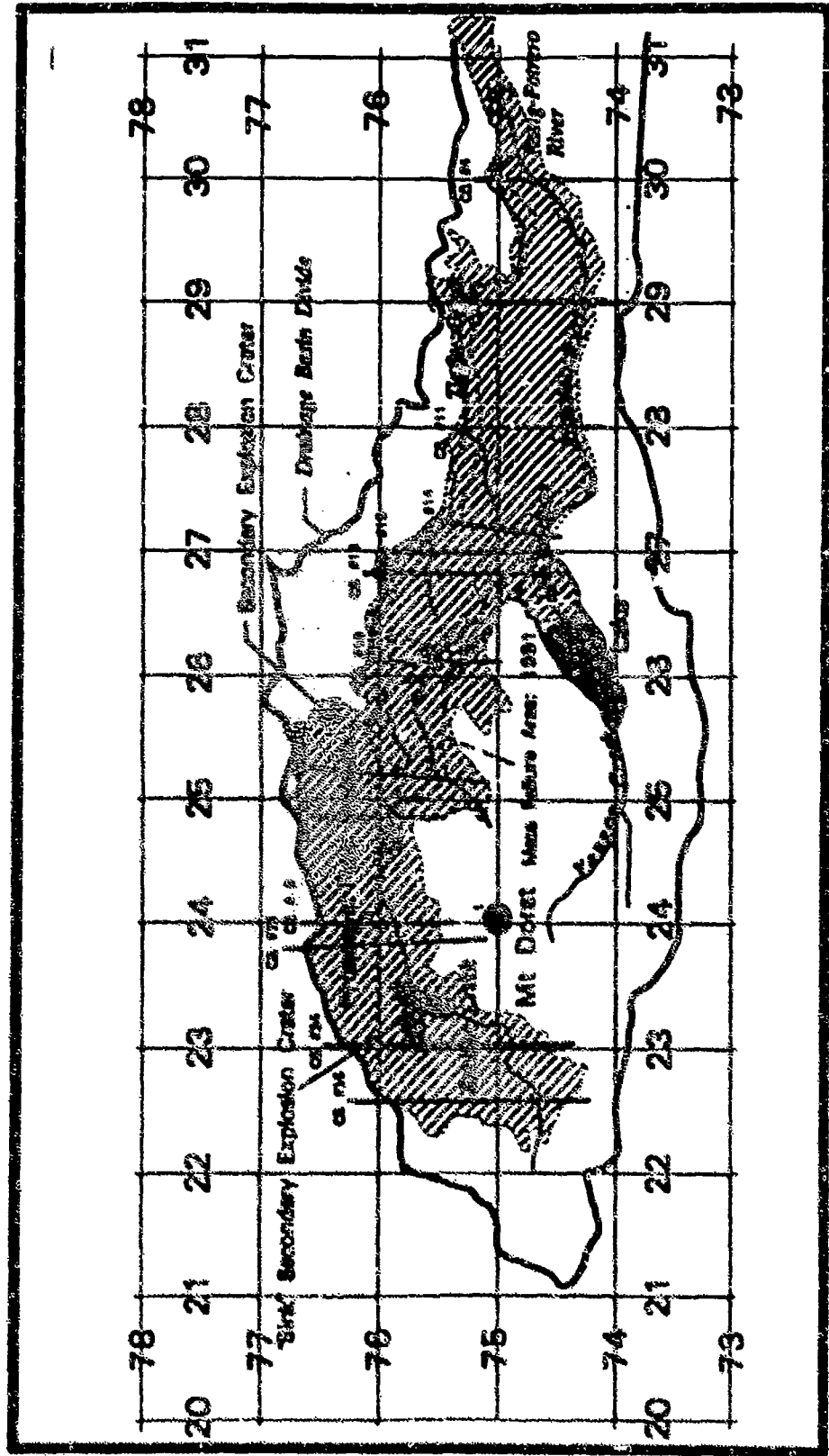
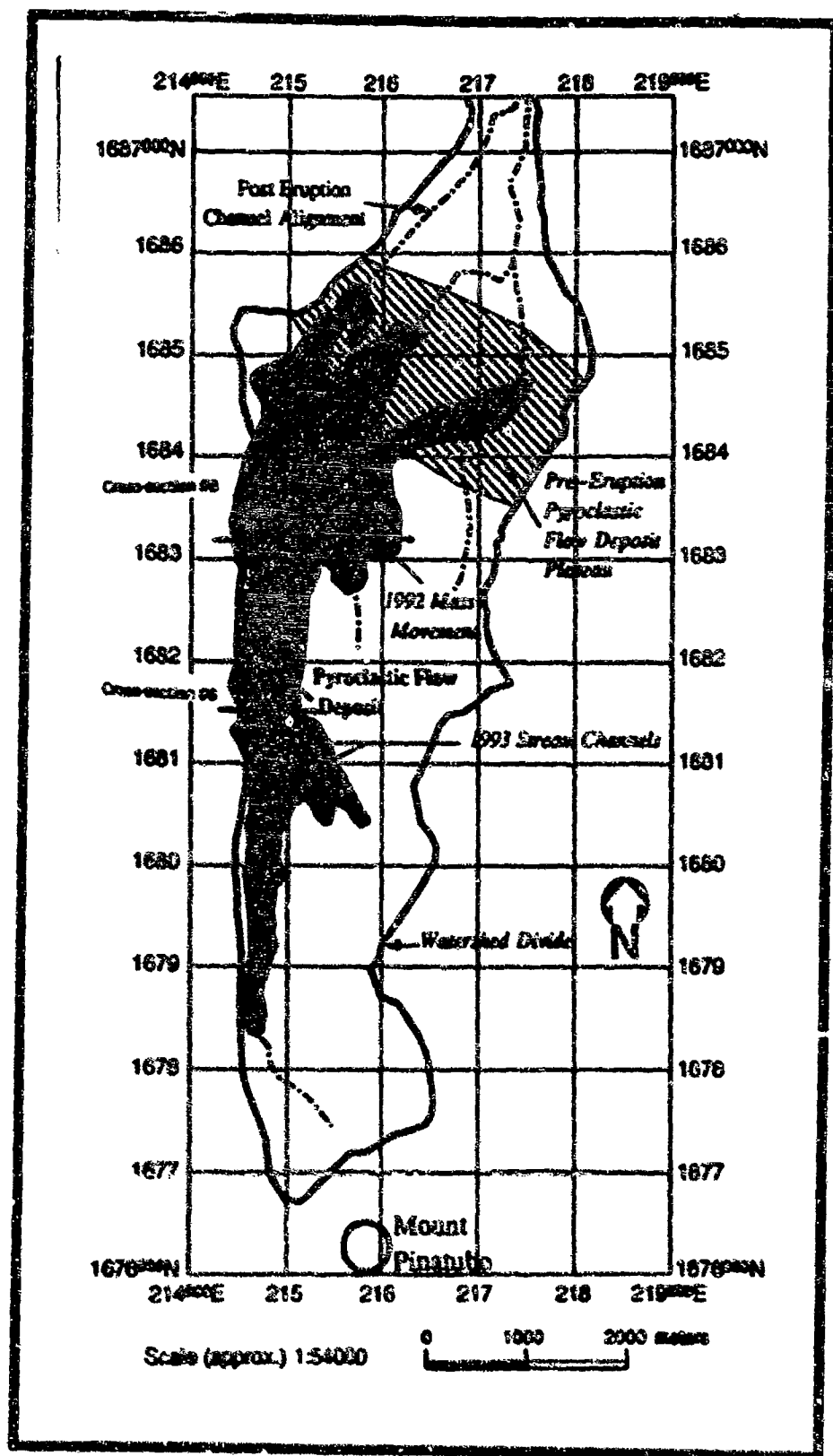Figure B-8. Upper Pasig/Potrero River Basin Map. Illustrating Pyroclastic flow deposit and major geomorphic features produced between June 1991 - June 1993.

HAZARD AREA
PASIG BASIN

Compiled by MLP / KWE – 83

Mudflow Impact
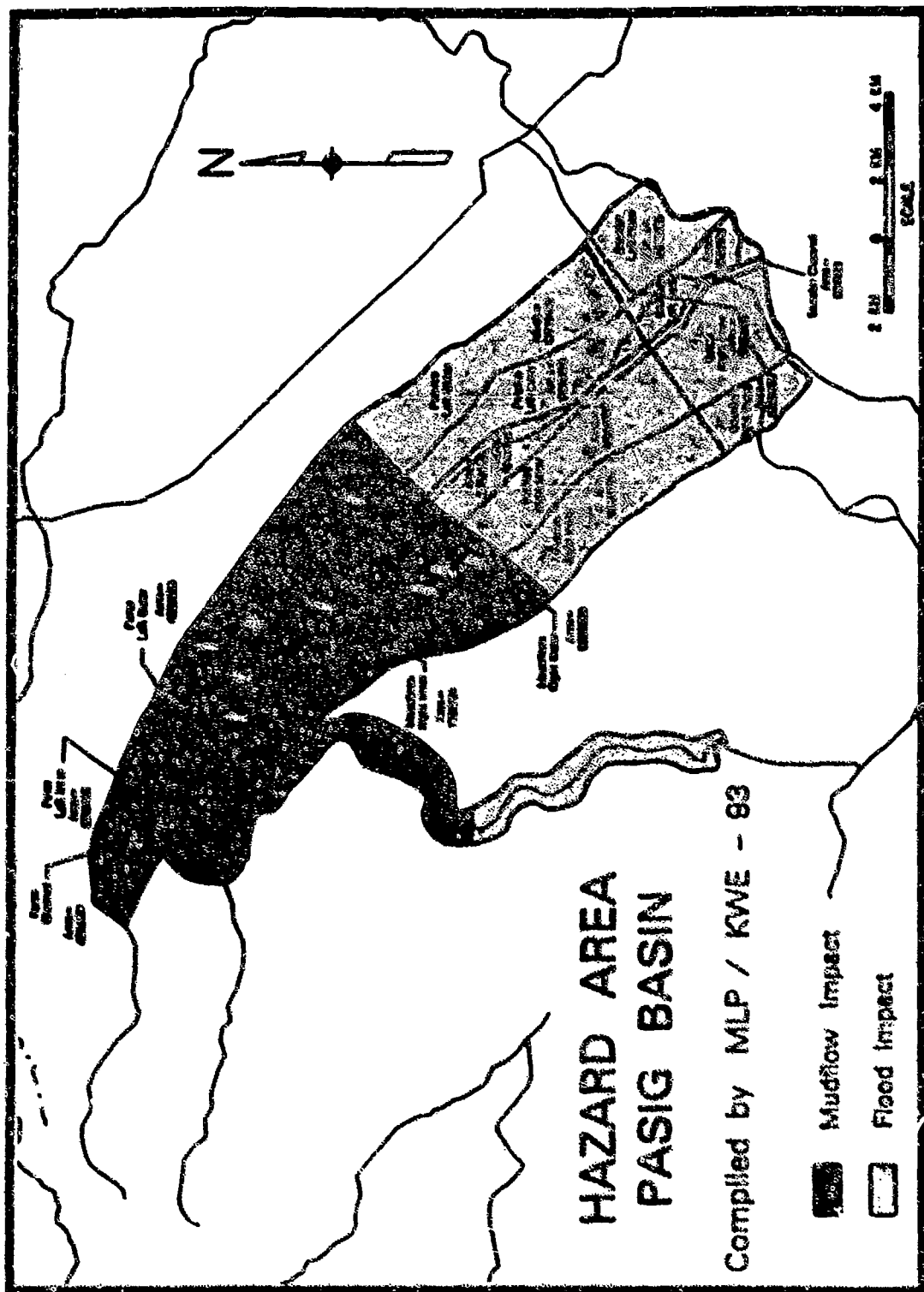
Flood Impact

Figure B-9. Lower Pasig/Potrero River Basin Hazard Area.
Diagraming Mudflow and Flood Impact Zones.
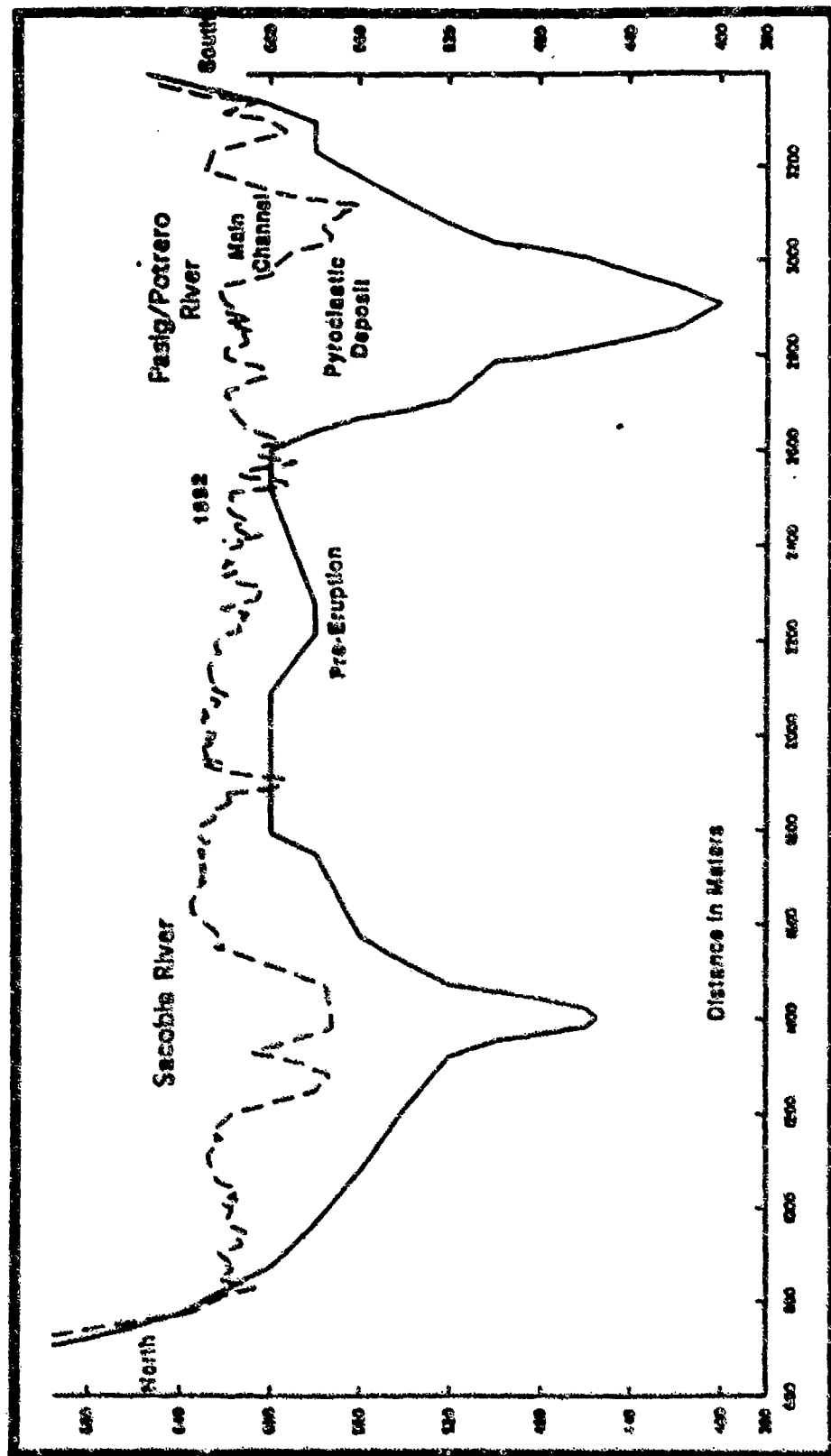
Figure B-10. Upper Pasig/Potrero River Channel Cross-Section #9.
Illustrating Pre- and Post- Eruption channel geometry. Both Sacobia and Pasig/Potrero Rivers are plotted. Data based on USA topographic map and 1992 aerial photography.
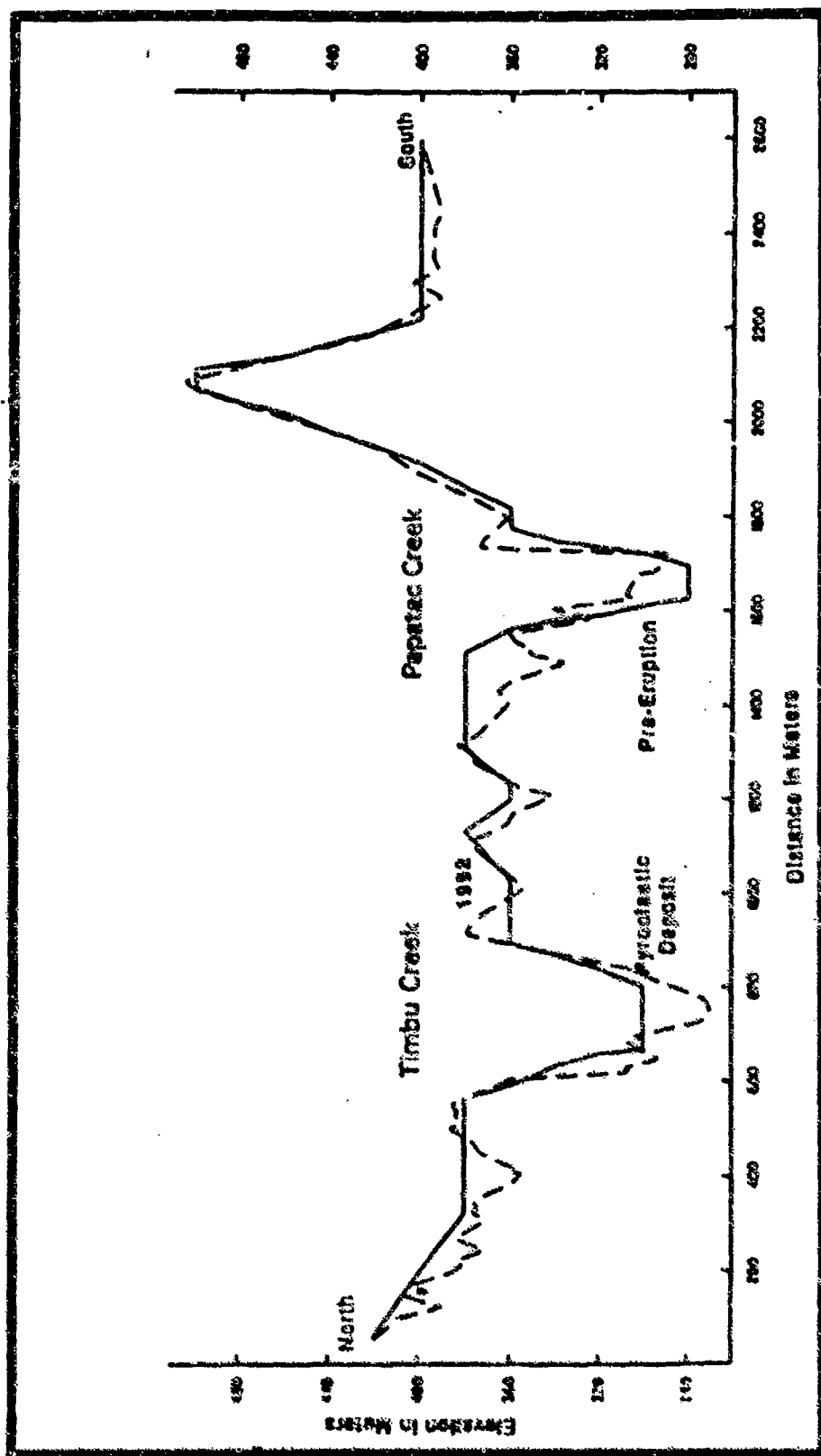
Figure B-11. Upper Pasig/Potrero River Channel Cross-Section #5.
Illustrating Pre- and Post- Eruption channel geometry of the Pasig/Potrero River. Cross-Section
illustrates both Timbu and Papatac Creeks which form the Pasig/Potrero River system.
Data based on DMA topographic map and 1992 aerial photography.
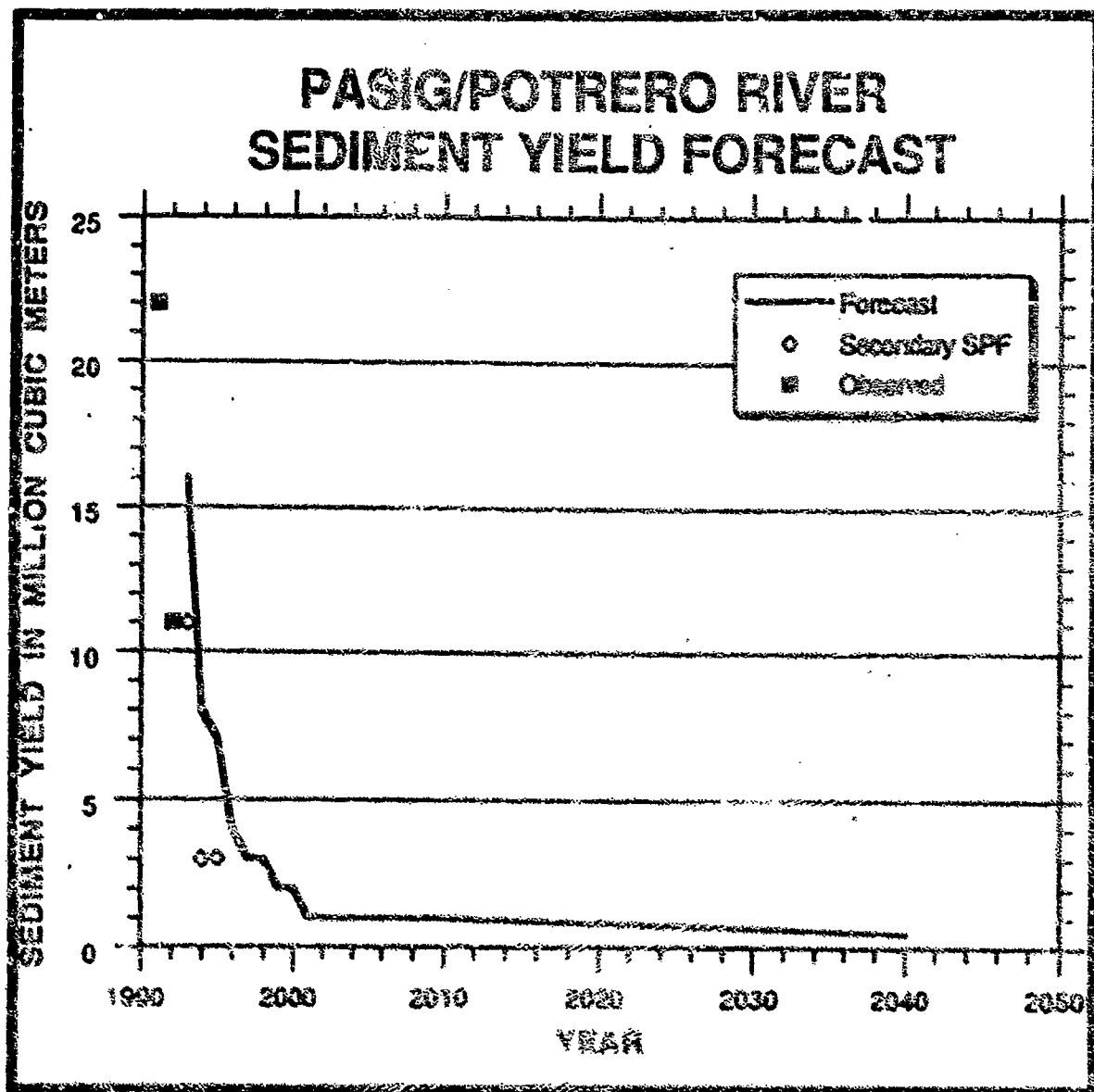
Figure B-12. Sediment Yield Forecast for the
Pasig-Potrero River Pyroclastic Deposit.
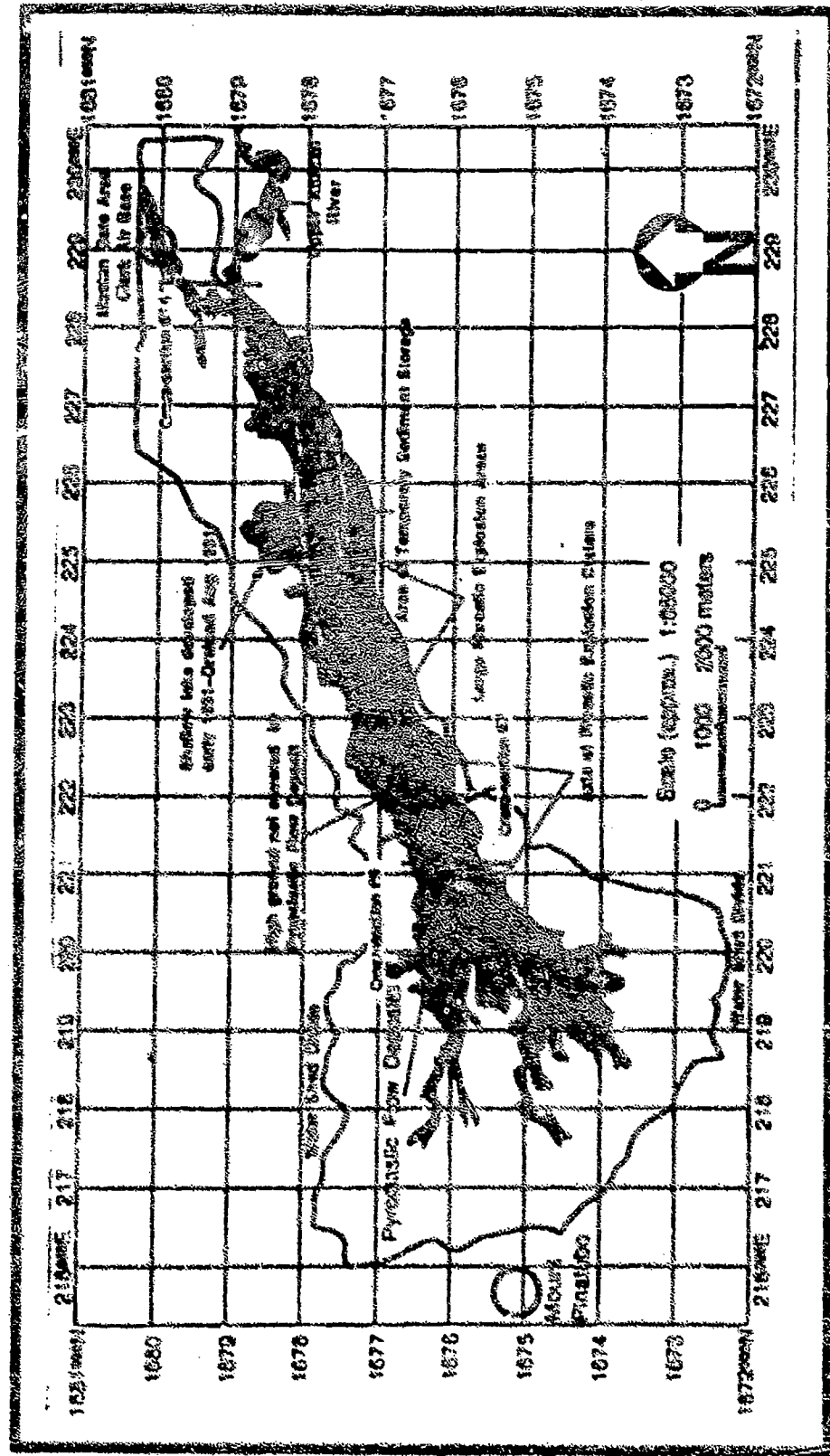
Figure B-13. Upper Sacobia River Basin Map. Illustrating Pyroclastic flow deposit and major geomorphic features produced during 1991.
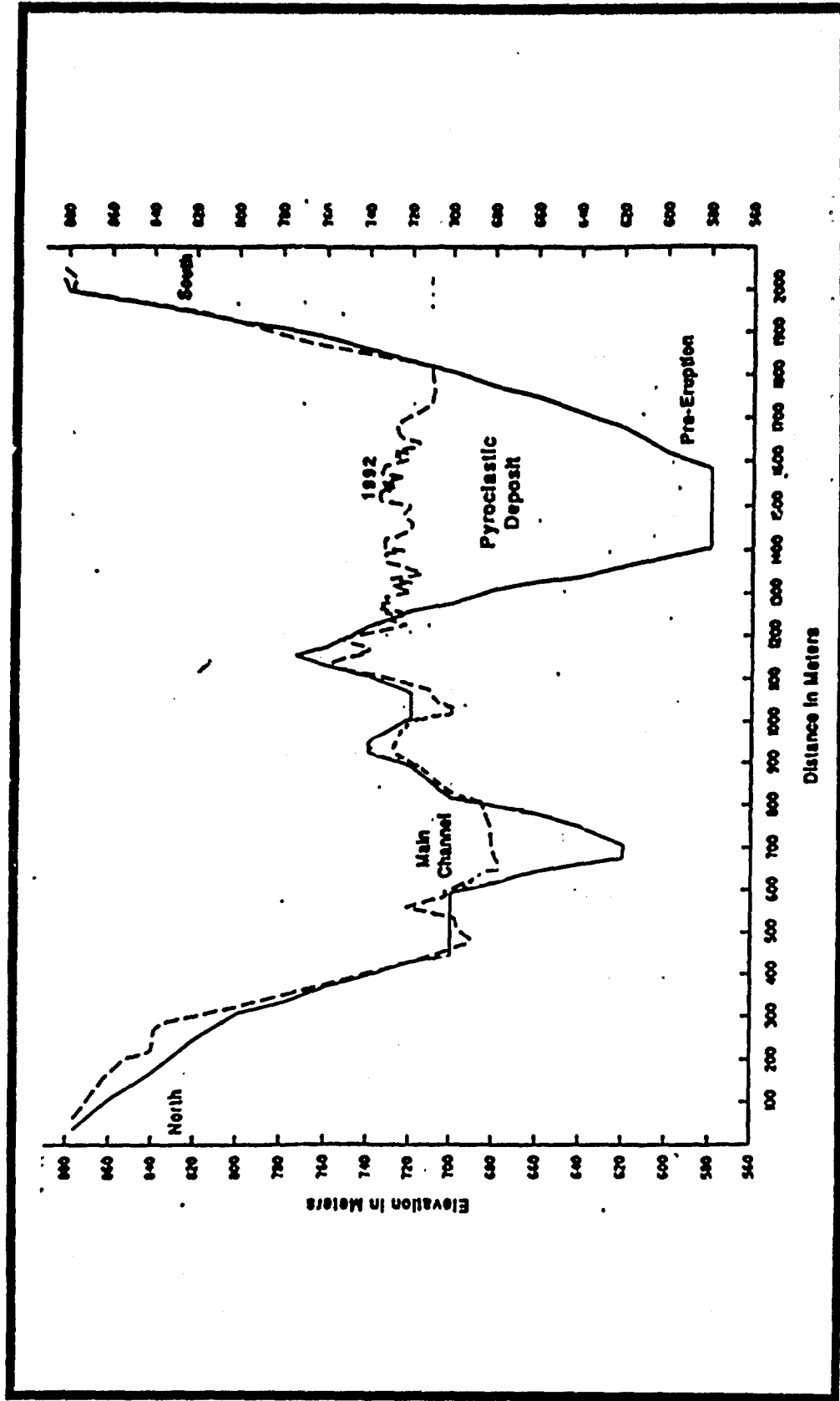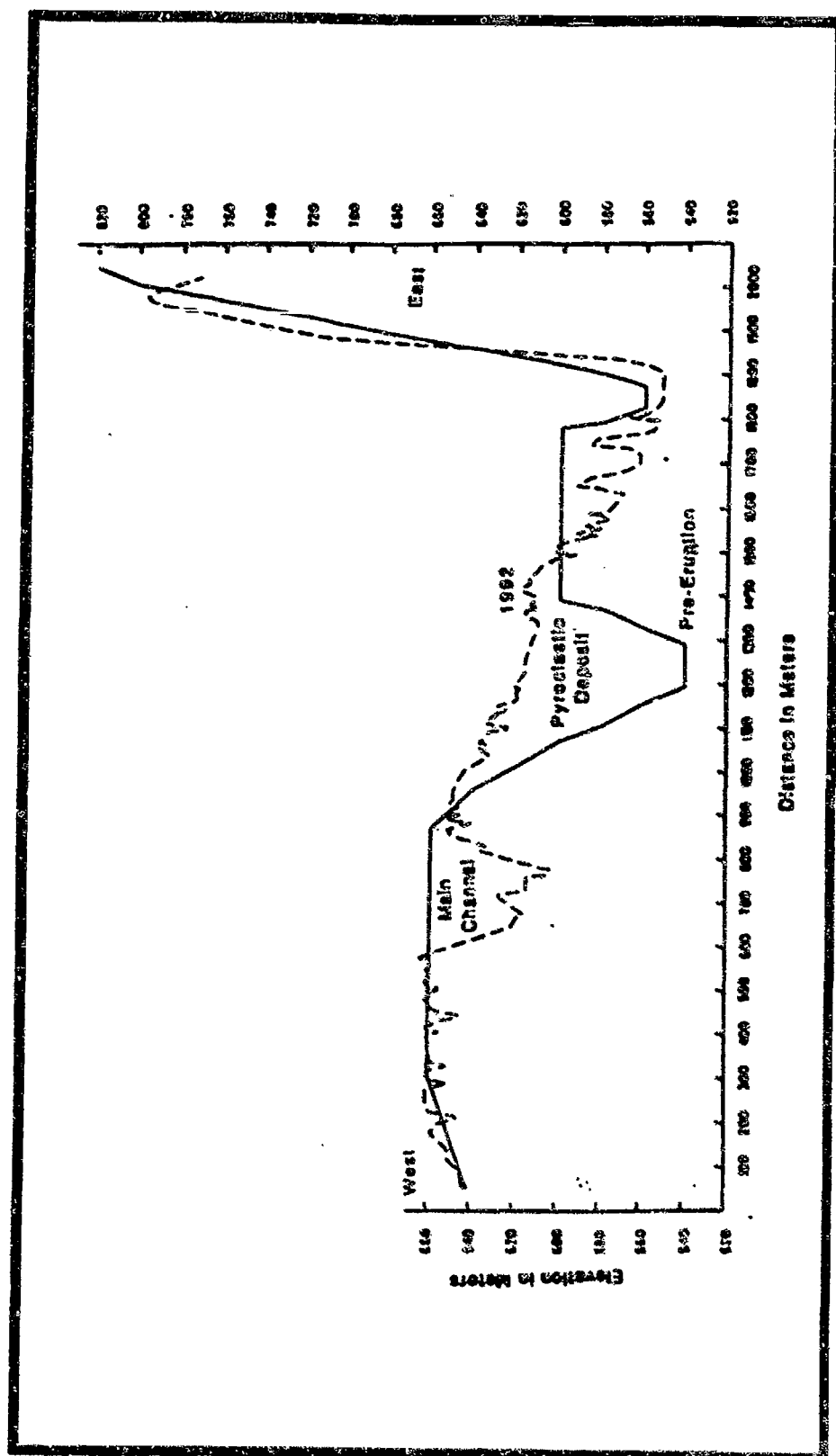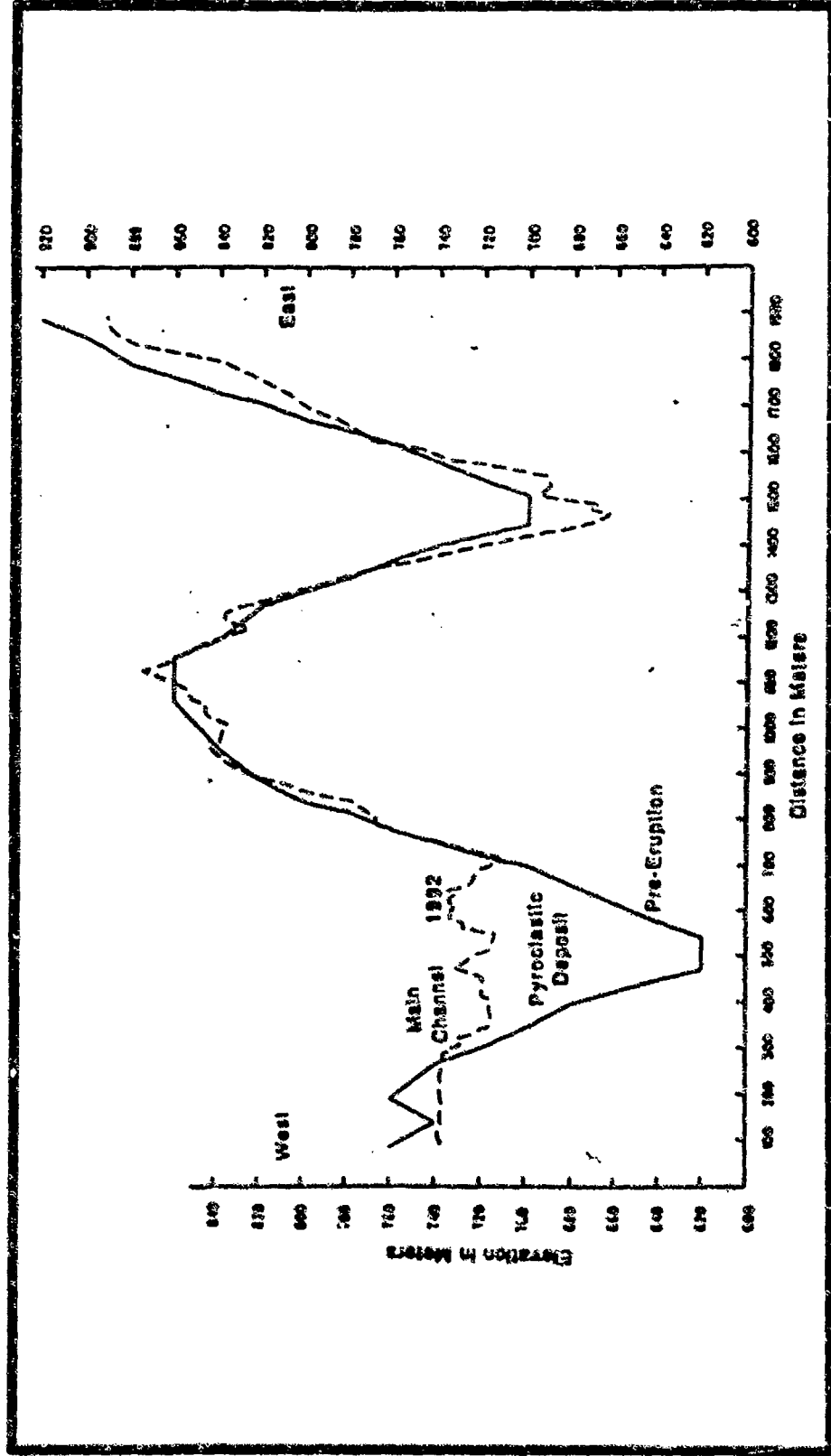
Figure B-14. Upper Sacobia River Channel Cross-Section #6.
Illustrating Pre- and Post- Eruption channel geometry of the Sacobia River. Cross-Section illustrates the upper two channels of the Sacobia River. Location shown on figure B-13. Data based on DMA topographic map and 1992 aerial photography.
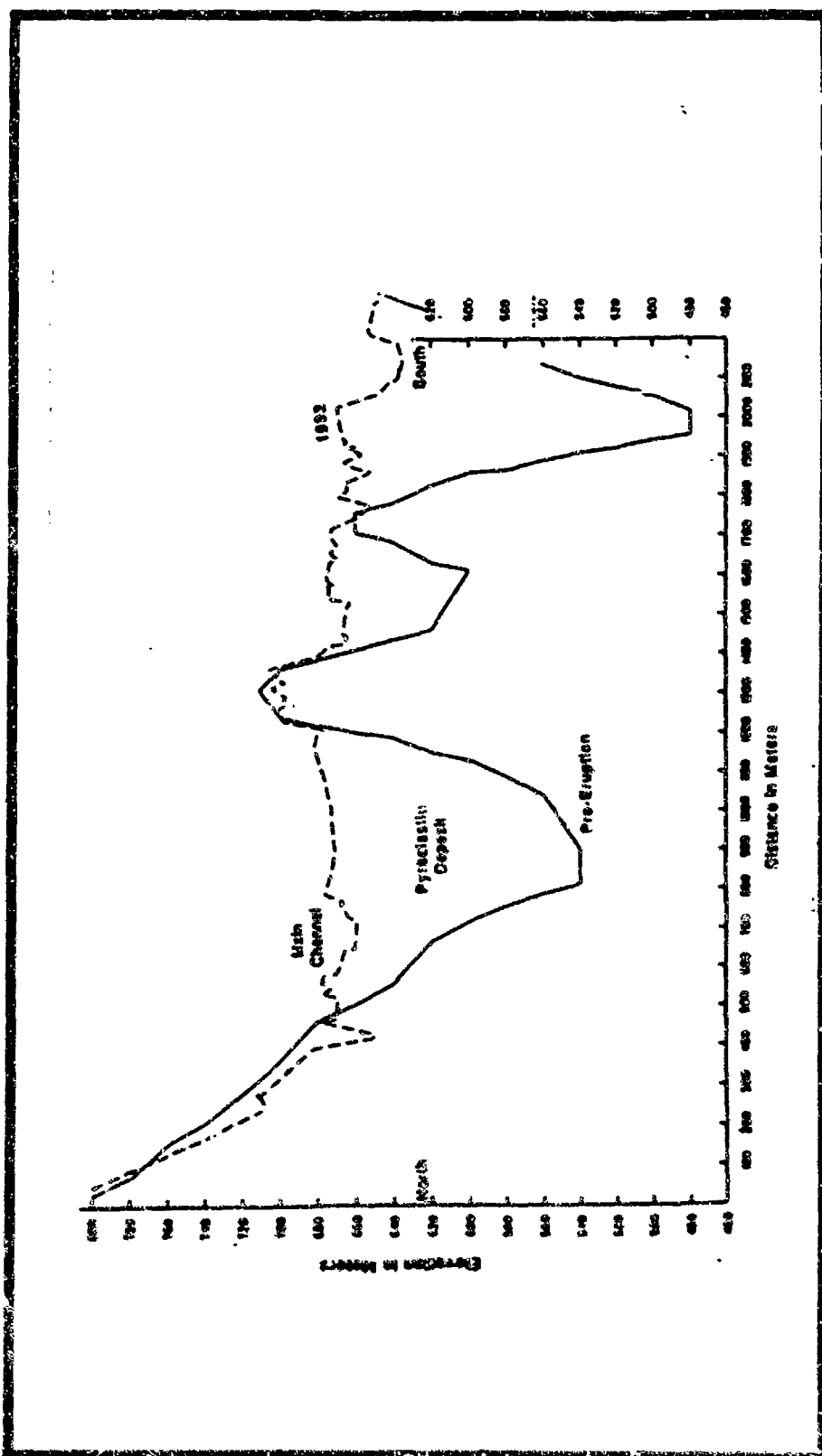
Figure B-15.   Upper Sacobia River Channel Cross-Section #7.
Illustrating Pre- and Post- Eruption channel geometry of the Sacobia River.   Cross-Section
illustrates the Sacobia River and a portion of the Pasig/Potrero River Basin.   Location shown
on figure B-13.   Data based on DMA topographic map and 1992 aerial photography.
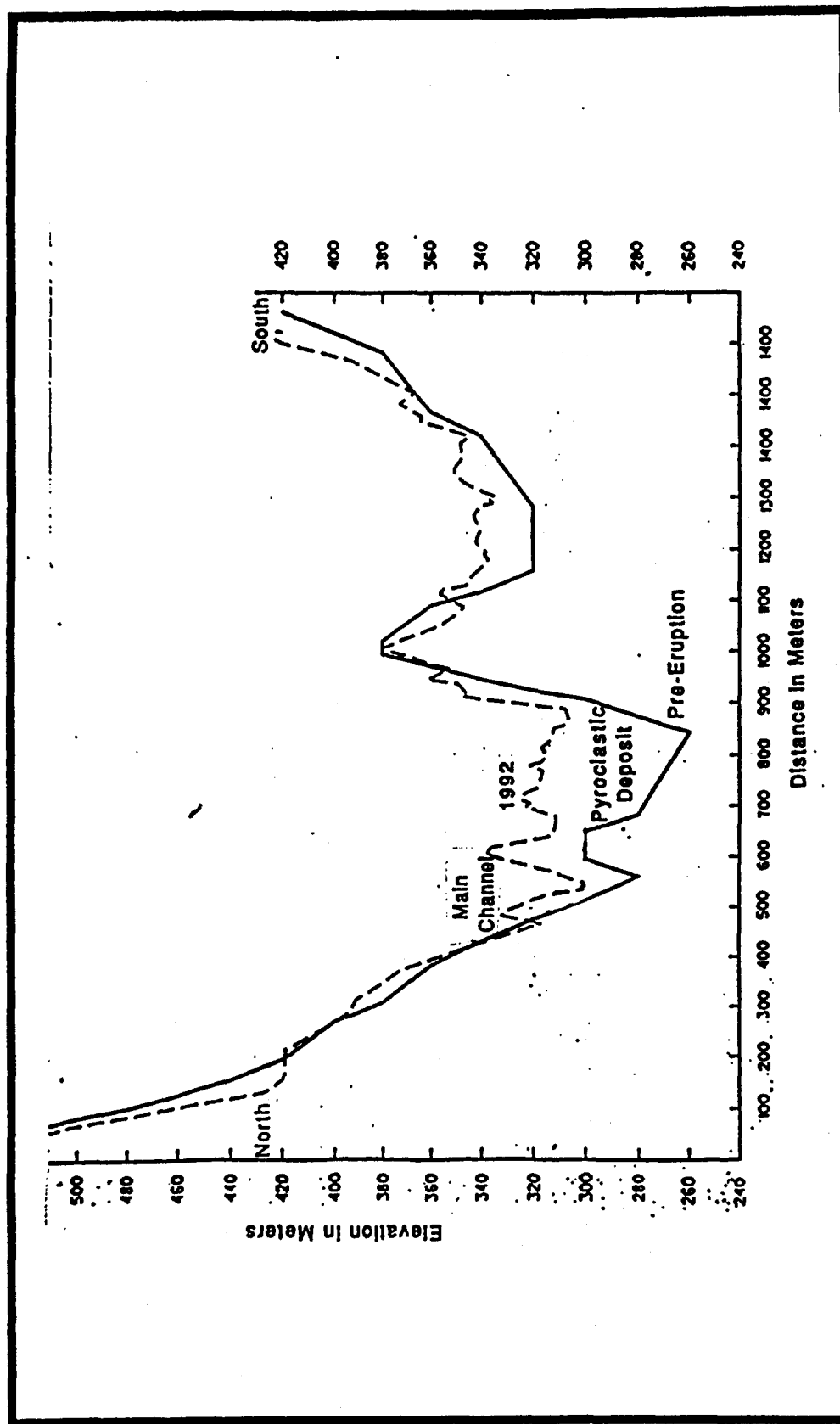
Figure B-16.   Upper Sacobia River Channel Cross-Section #14.
Illustrating Pre- and Post- Eruption channel geometry of the Sacobia River.   Cross-Section
illustrates the Sacobia River and the Abacan River downstream of the "Gates of the Abacan" area.
Location shown on figure B-13.   Data based on DMA topographic map and 1992 aerial photography.
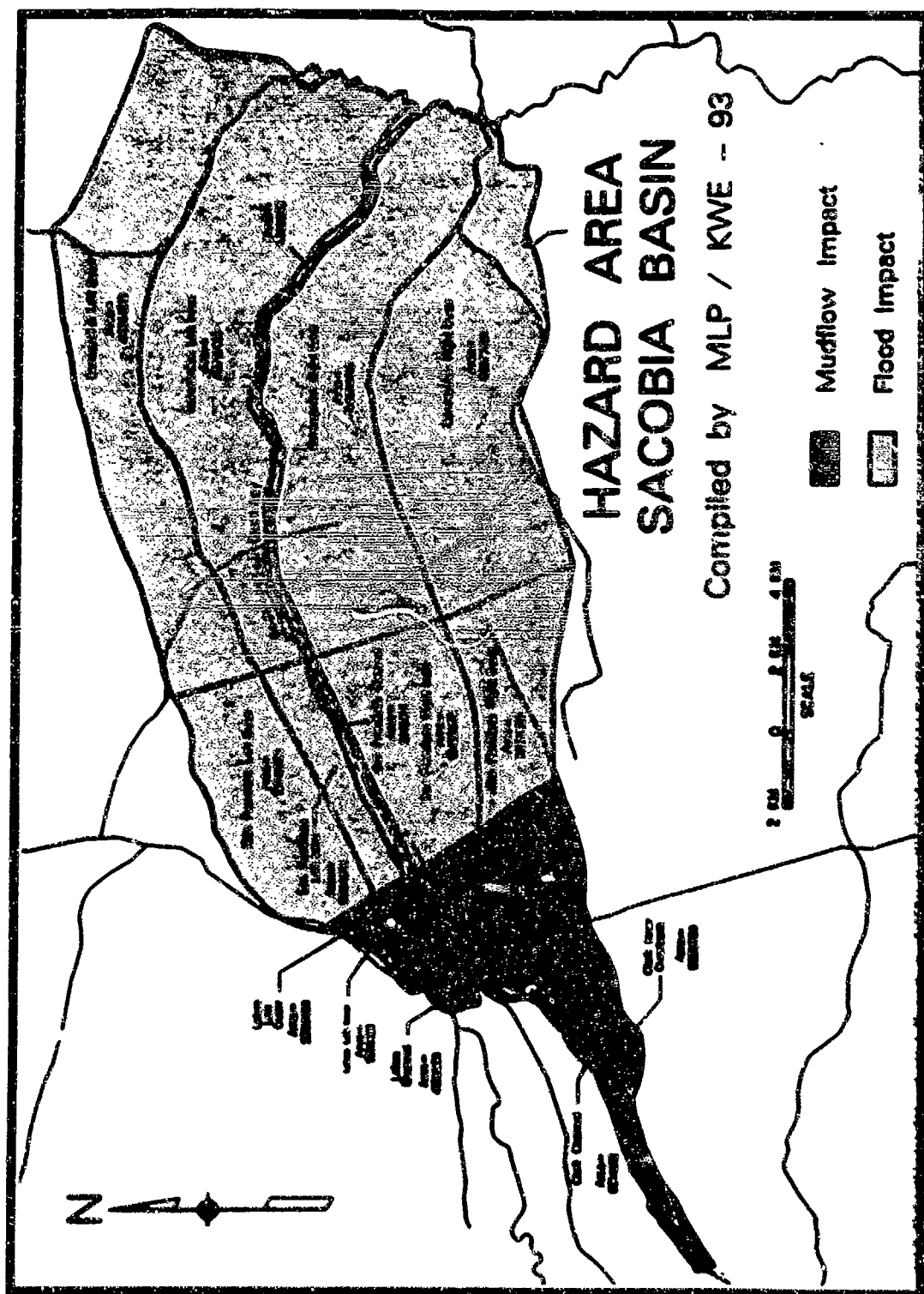
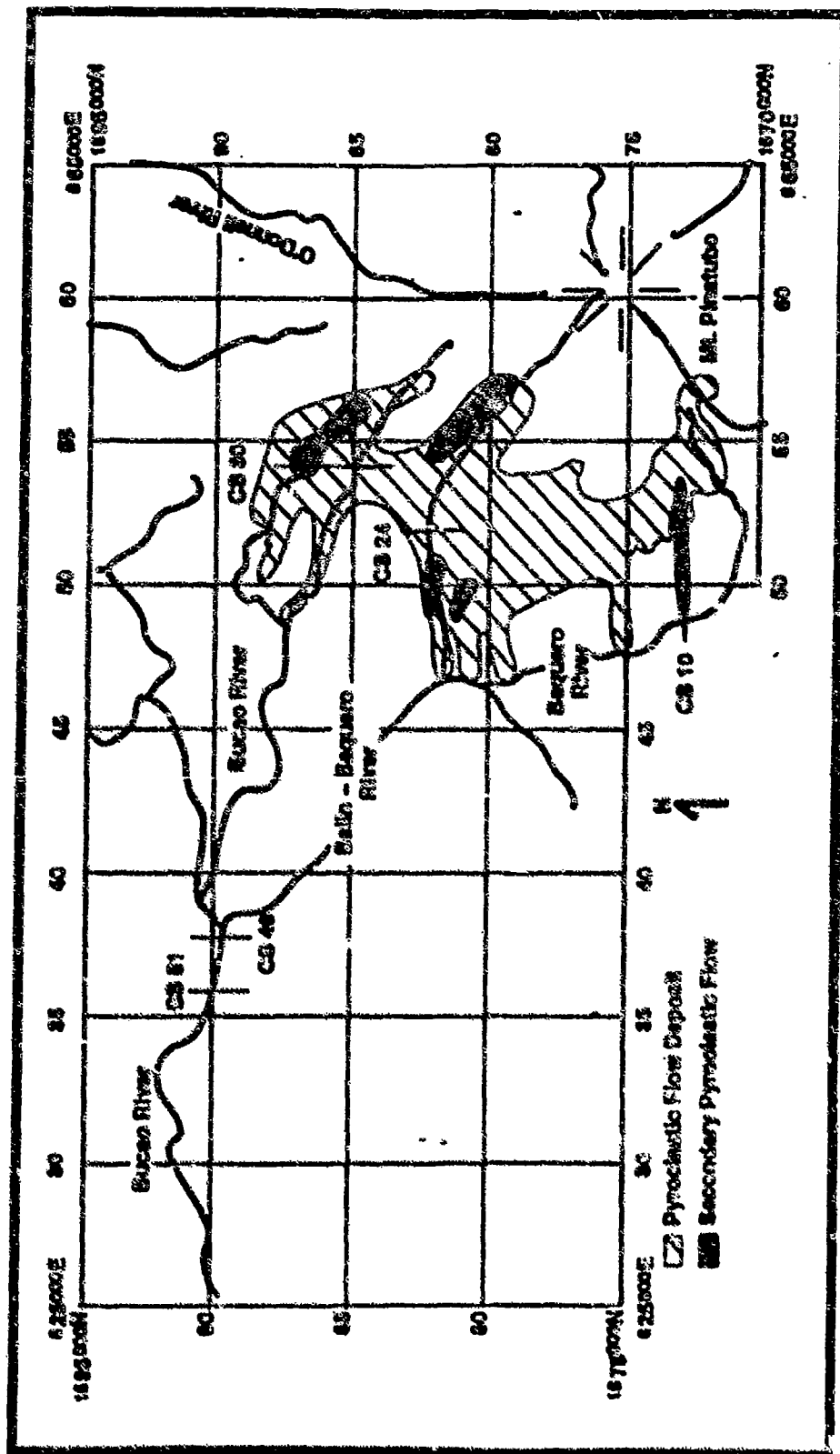**Figure B-17. Lower Sacobie River Basin Hazard Area.**
Diagraming Mudflow and Flood Impact Zones.
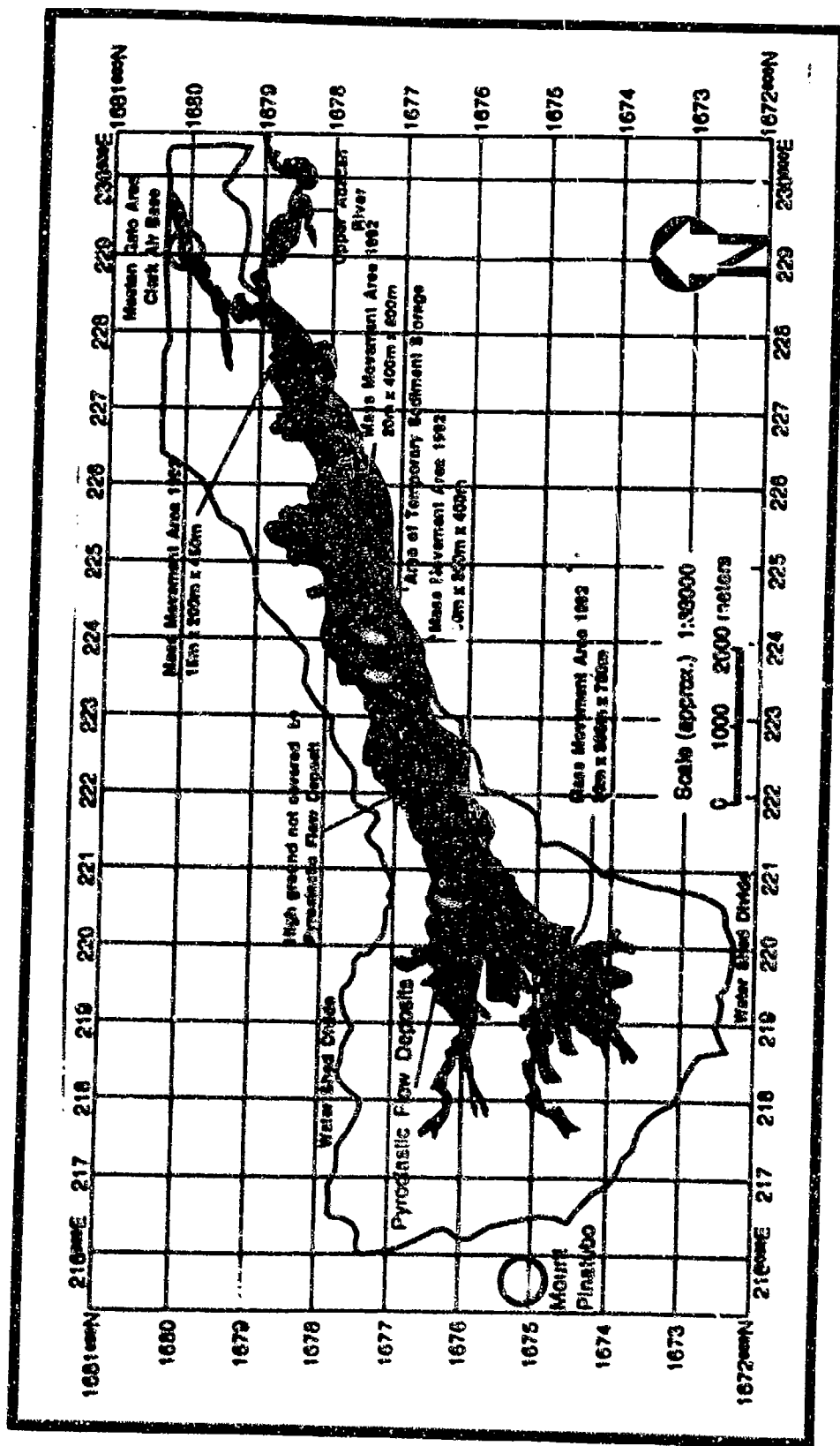
Figure B-18. Upper Sacobia River Basin Map. Illustrating Pyroclastic flow deposit and major geomorphic features produced during 1992.

SACOBIA/BAMBAN RIVER
SEDIMENT YIELD FORECAST
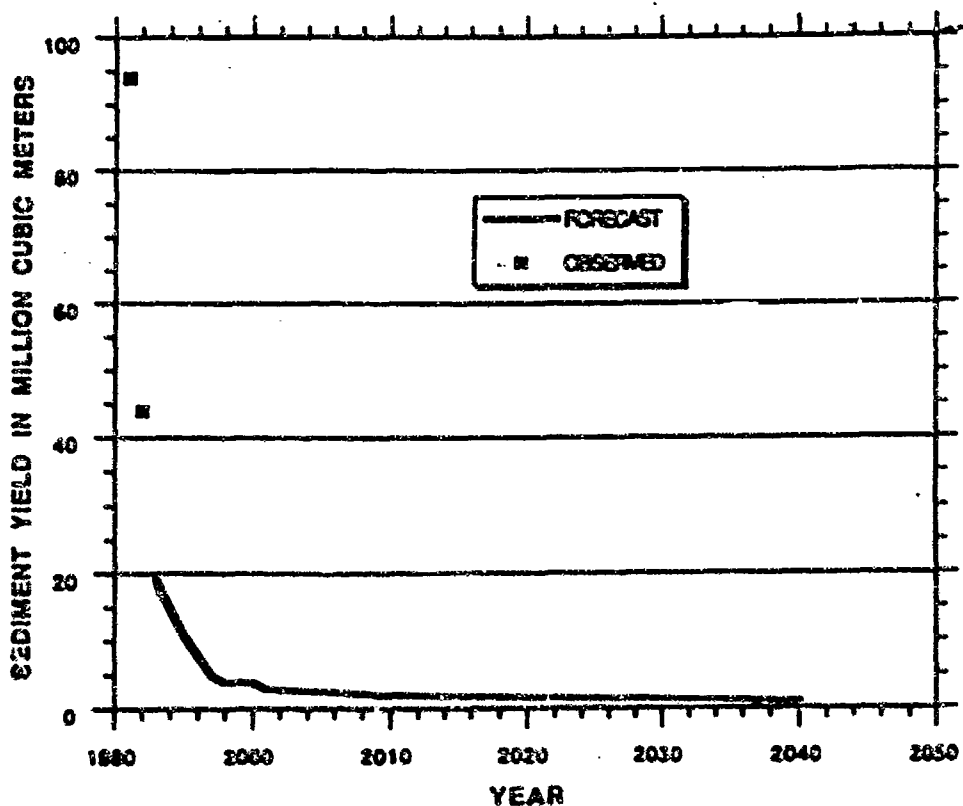
Figure B-19. Sediment Yield Forecast for the Sacobia/Bamban River Pyroclastic Deposit.

Figure B-20. Upper O,Donnell River Basin Map.
Illustrating Pyroclastic flow deposit and major geomorphic features
producted between June 1991 - August 1993.

Figure B-21. Upper O'Donnell River Channel Cross-Section #8.
Illustrating Pre- and Post- Eruption channel geometry of the O'Donnell River. Cross-Section Location shown on figure B-20. Data based on DMA topographic map and 1992 aerial photography.
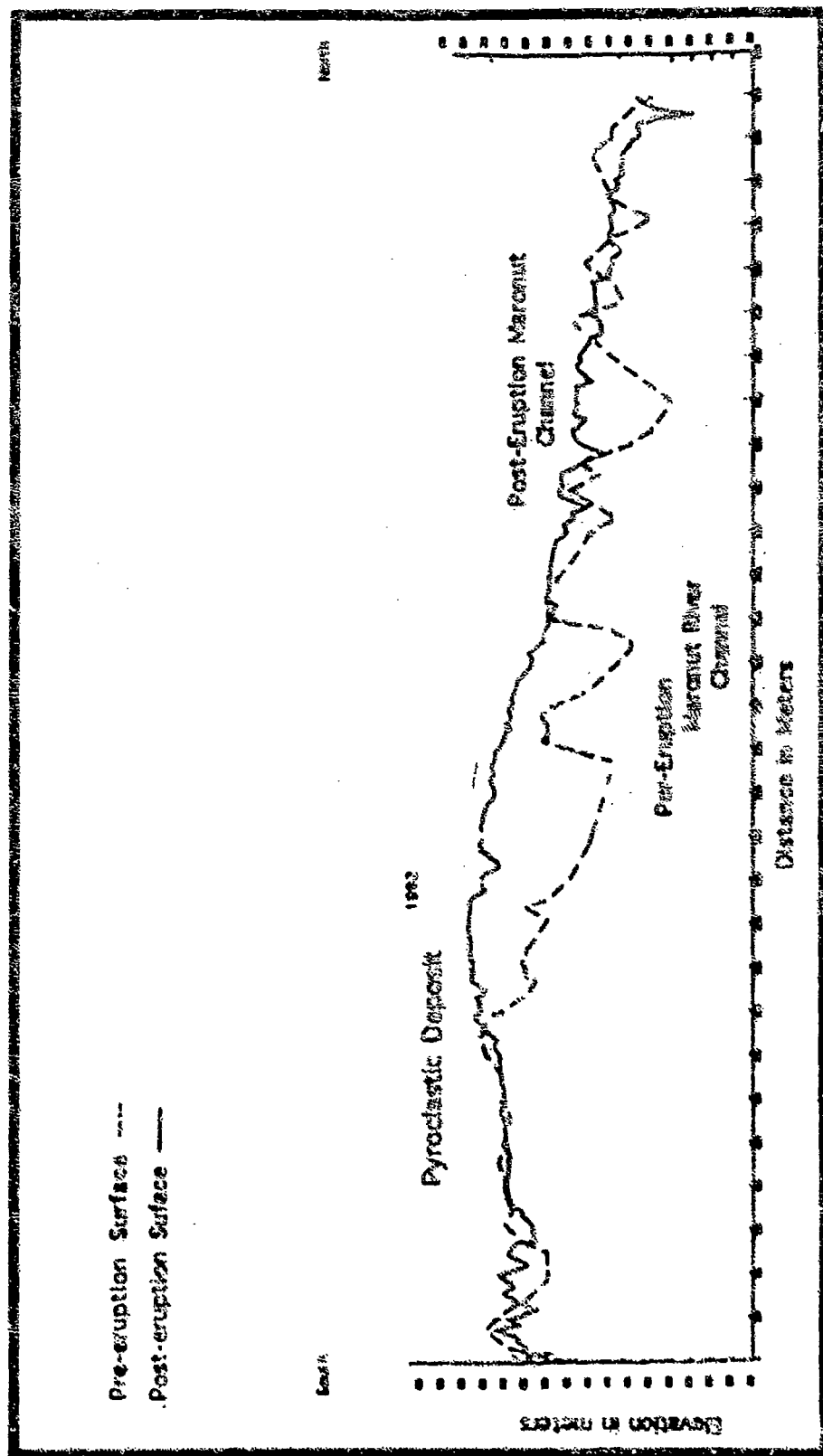
Figure B-22. Upper O'Donnell River Channel Cross-Section #6.
Illustrating Pre- and Post- Eruption channel geometry of the O'Donnell River. Cross-Section
Location shown on figure B-20. Data based on DMA topographic map and 1992 aerial photography.
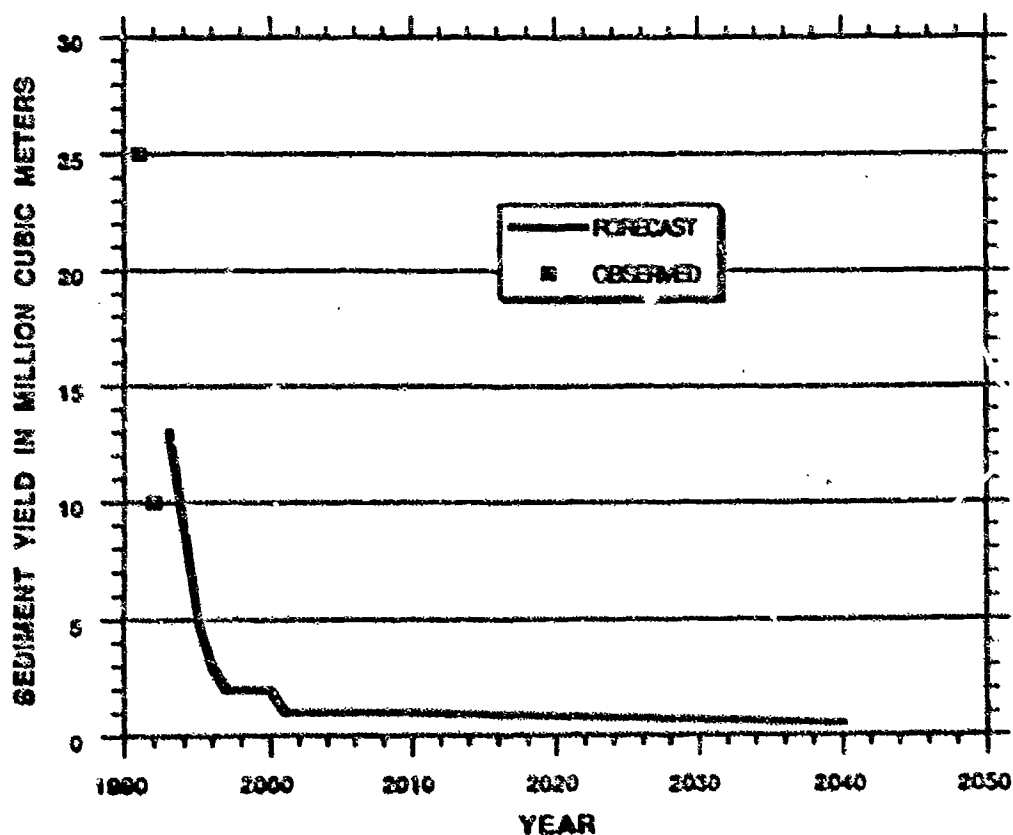
Figure B-23. Sediment Yield Forecast for the O'Donnell River Pyroclastic Deposit.

HAZARD AREA
O'DONNELL BASIN

Compiled by MLP / KWE - 93

Mudflow Impact

Flood Impact

Figure B-24   Lower O'Donnell River Basin Hazard Area.
Diagraming Mudflow and Flood Impact Zones.
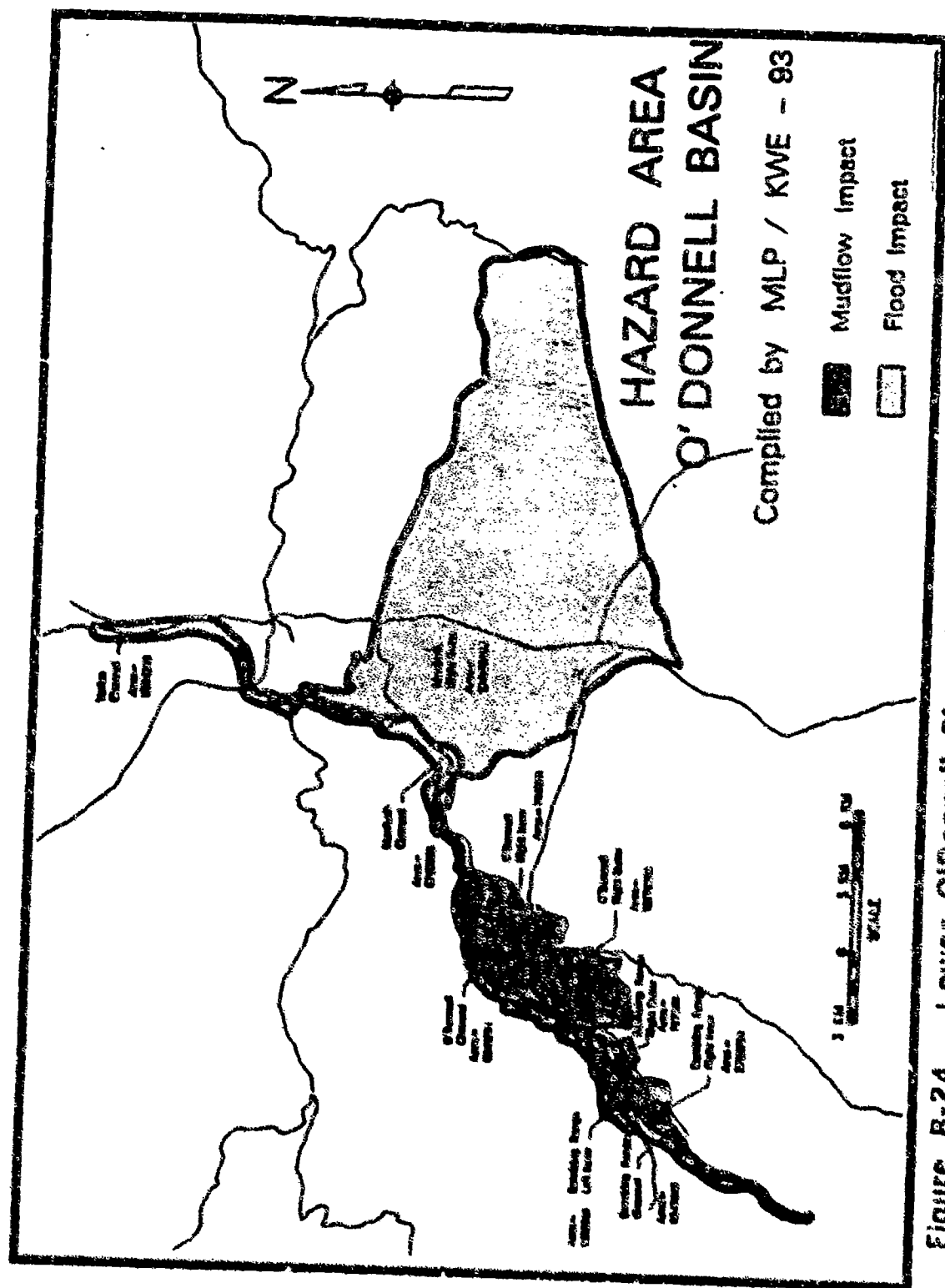
Figure B-25. Upper and Lower Bucao River Basin Map. Illustrating Pyroclastic flow deposit and major geomorphic features produced between June 1991 - June 1993.
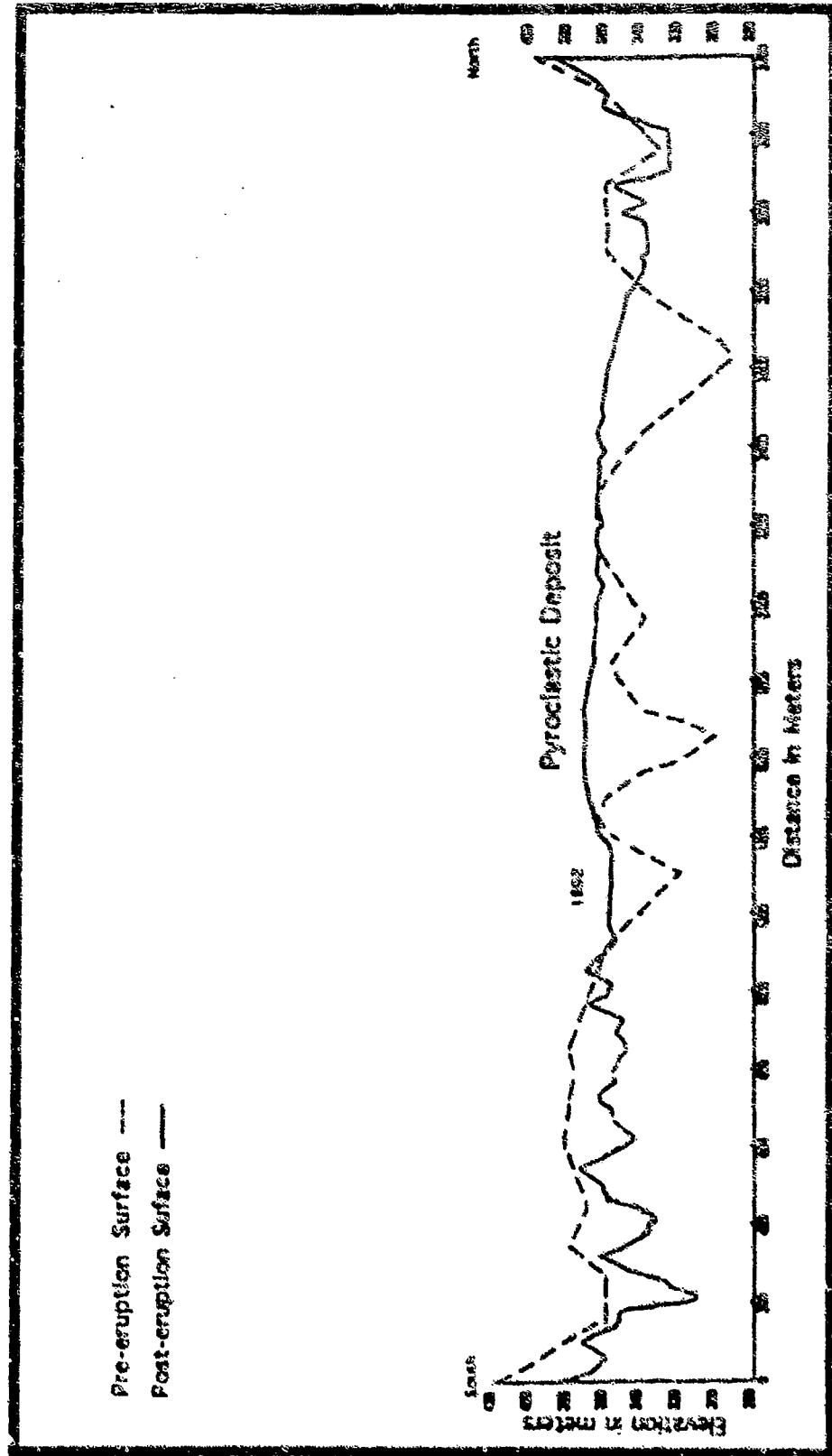
Figure B-26. Upper Bucao River Channel Cross-Section #30.
Illustrating Pre- and Post- Eruption channel geometry of the Bucao River. Cross-Section
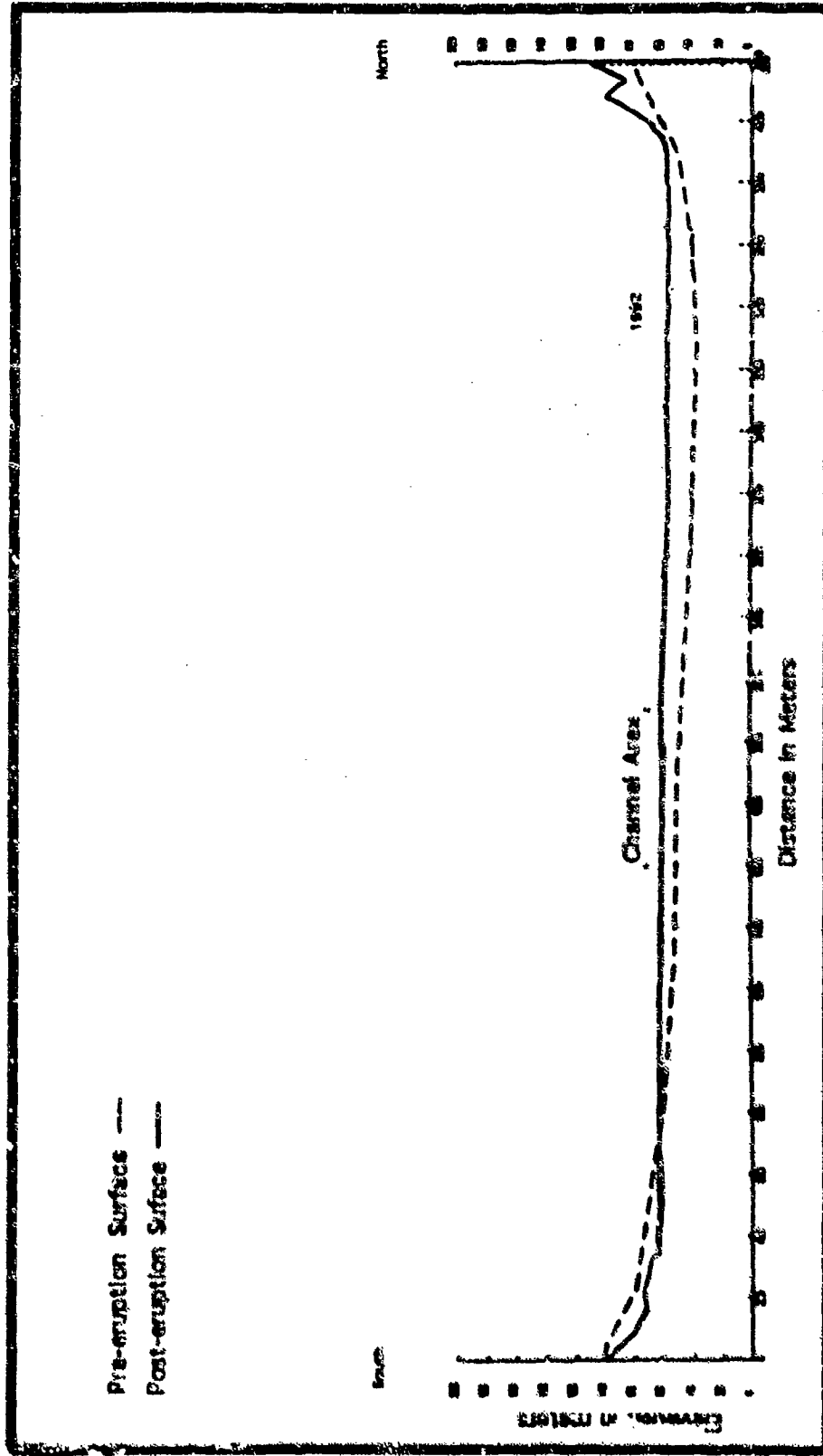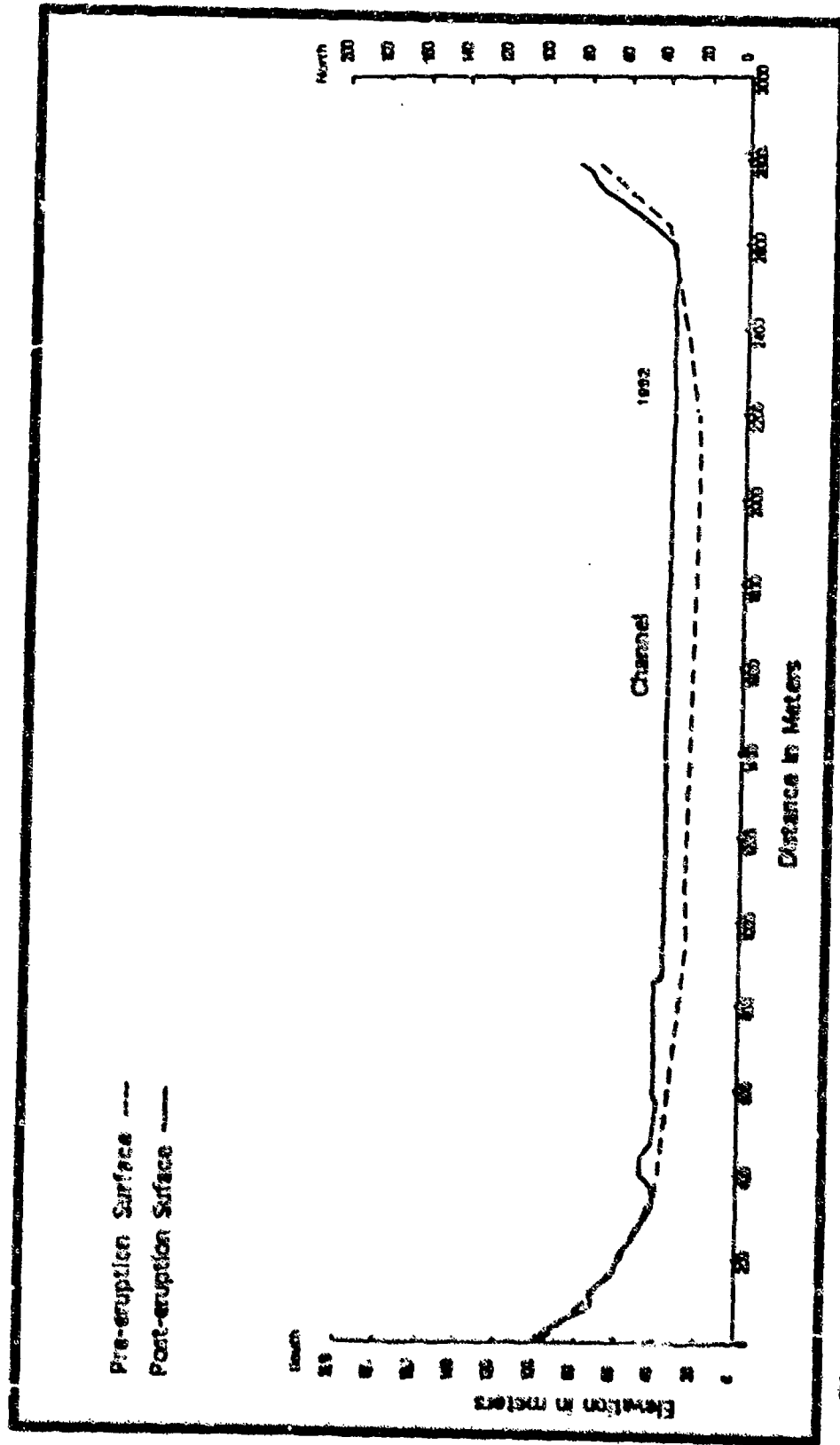Location shown on figure B-25. Data based on DMA topographic map and 1992 aerial photography.

Figure B-27. Upper Bucao River Basin Channel Cross-Section #24.
Illustrating Pre- and Post-Eruption channel geometry of the Marunut River, a tributary to the Balin-Buquero River. Cross-Section Location shown on figure B-25. Data based on DMA topographic map and 1992 aerial photography.
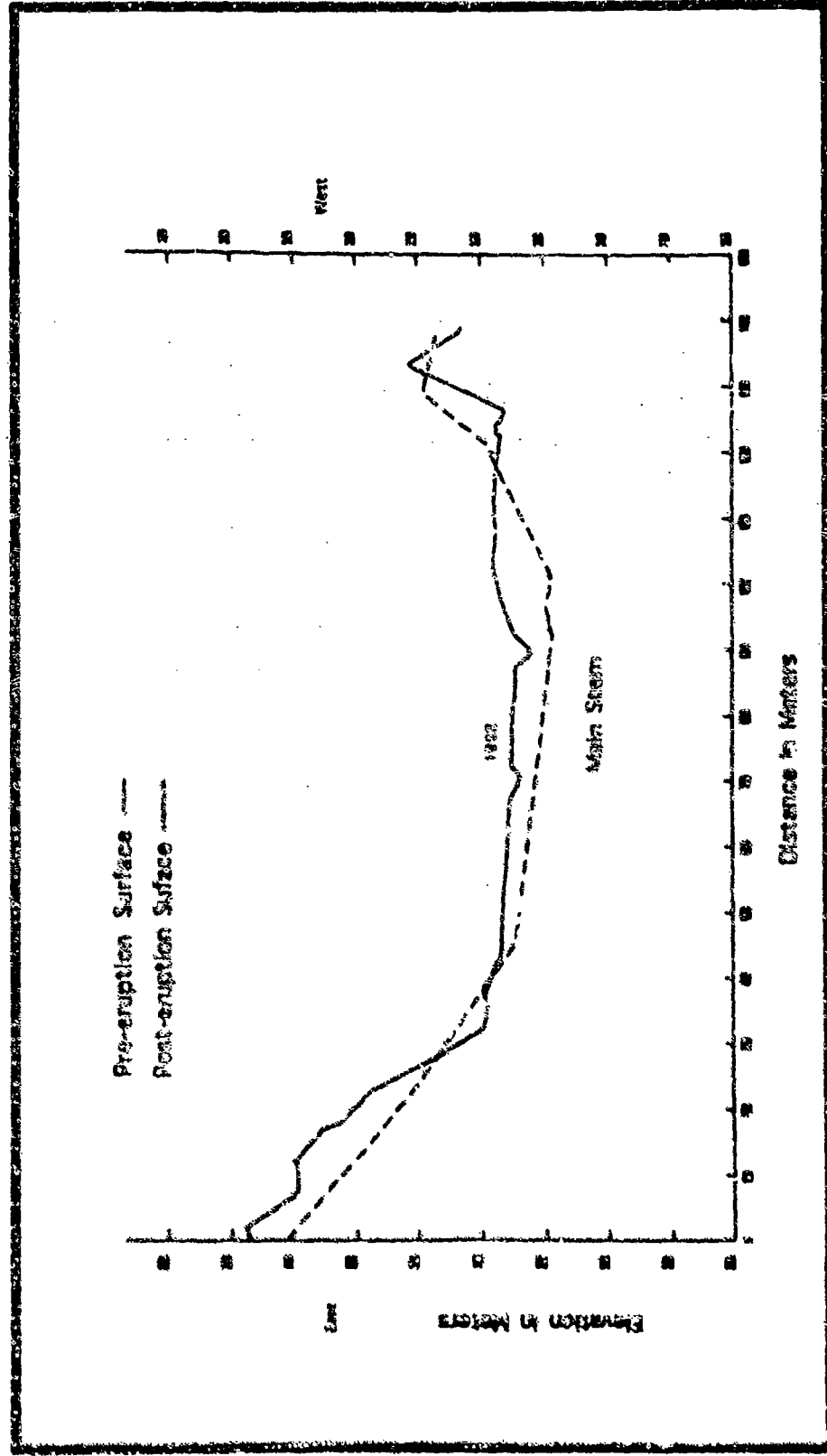
Figure B-28. Upper Bucao River Basin Channel Cross-Section #10. Illustrating Pre- and Post- Eruption channel geometry of the Balin-Baquero River, a major tributary to the Bucao River. Cross-Section Location shown on figure B-25. Data based on DMA topographic map and 1992 aerial photography.

Figure B-29. Bucao River Basin Channel Cross-Section #49.
Illustrating Pre- and Post- Eruption channel geometry of the Bucao River. Cross-Section Location shown on figure B-25.
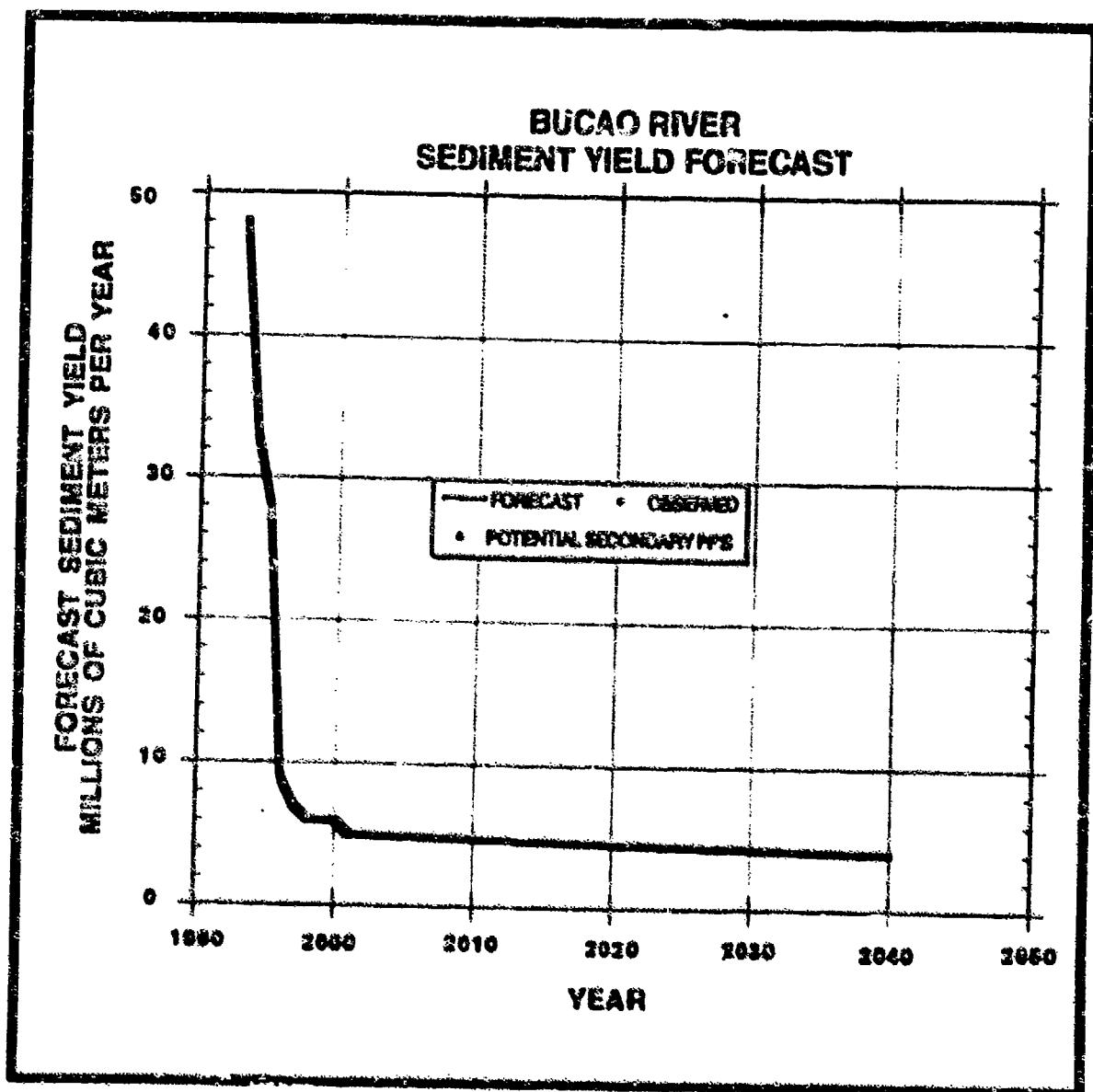Data based on DMA topographic map and 1992 aerial photography.

Pre-eruption Surface ----
Post-eruption Surface ——

Figure B-30. Bucao River Basin Channel Cross-Section #51.
Illustrating Pre- and Post- Eruption channel geometry of the Bucao River. Cross-Section Location shown on figure B-25. Data based on DMA topographic map and 1992 aerial photography.

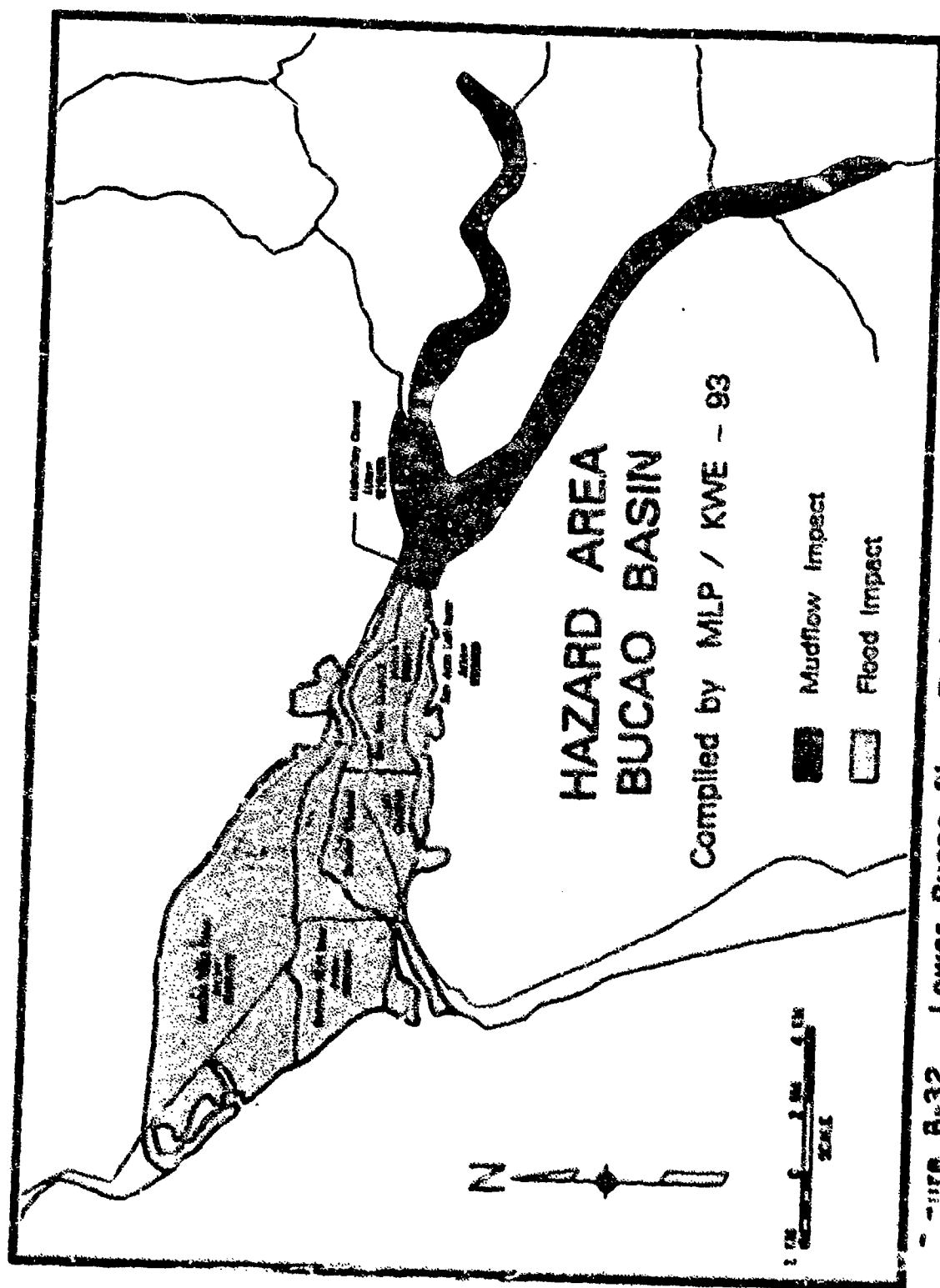Figure B-31. Sediment Yield Forecast for the Bucao River Pyroclastic Deposit.

HAZARD AREA
BUCAO BASIN

Compiled by MLP / KWE – 93

■■■ Mudflow Impact

☐ Flood Impact

N

SCALE

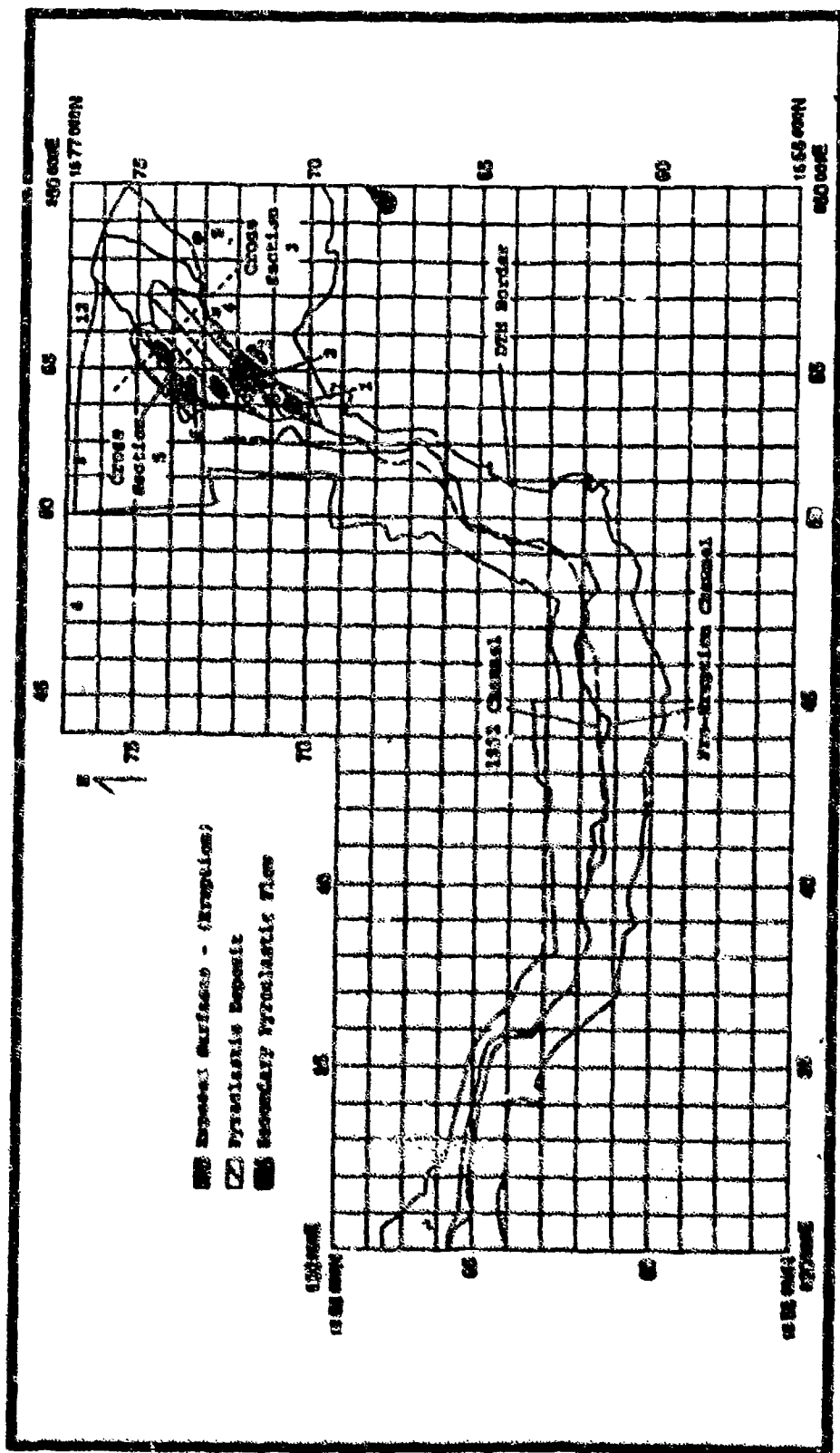Figure B-32. Lower Bucao River Basin Hazard Area.
Flood Impact Zones.

Figure B-33. Upper and Lower Santo Tomas River Basin Map. (Illustrating Pyroclastic flow deposit and major geomorphic features produced between June 1991 - June 1993.
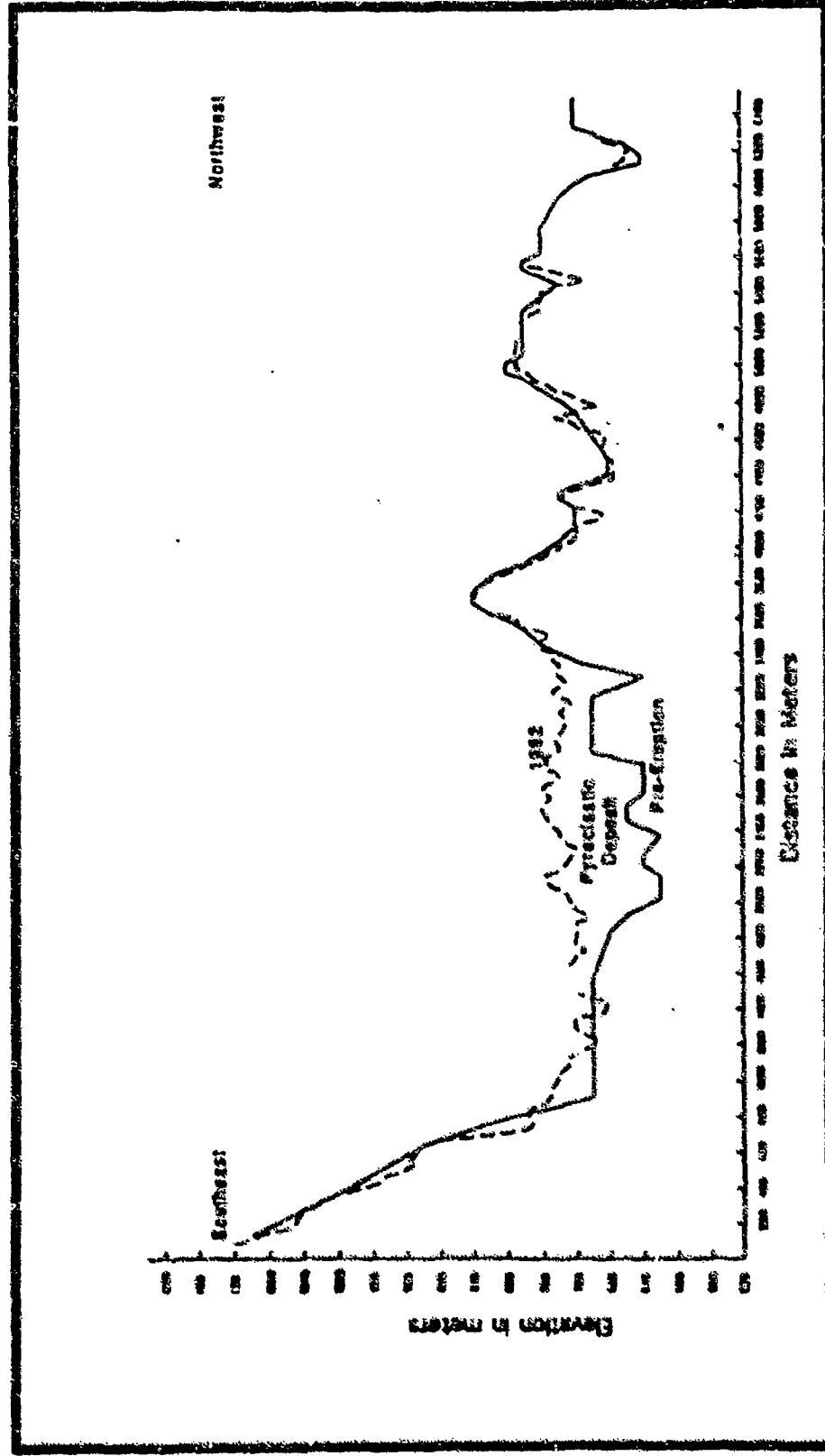
Figure B-34. Santo Tomas River Basin Channel Cross-Section #3.
Illustrating Pre- and Post- Eruption channel geometry of the Santo Tomas River.
Cross-Section Location shown on figure B-33. Data based on DMA topographic map and 1992 aerial photography.
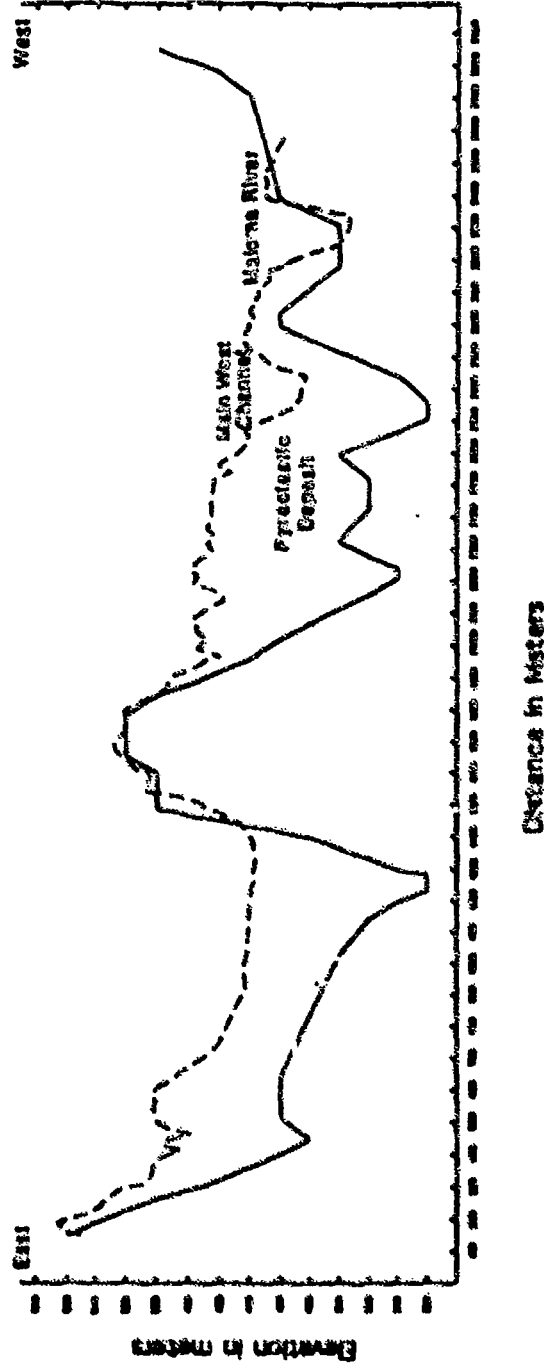
Figure B-35. Santo Tomas River Basin Channel Cross-Section #5.
Illustrating Pre- and Post- Eruption channel geometry of the Bucao River.
Cross-Section Location shown on figure B-33. Data based on DMA topographic map and 1992 aerial photography.
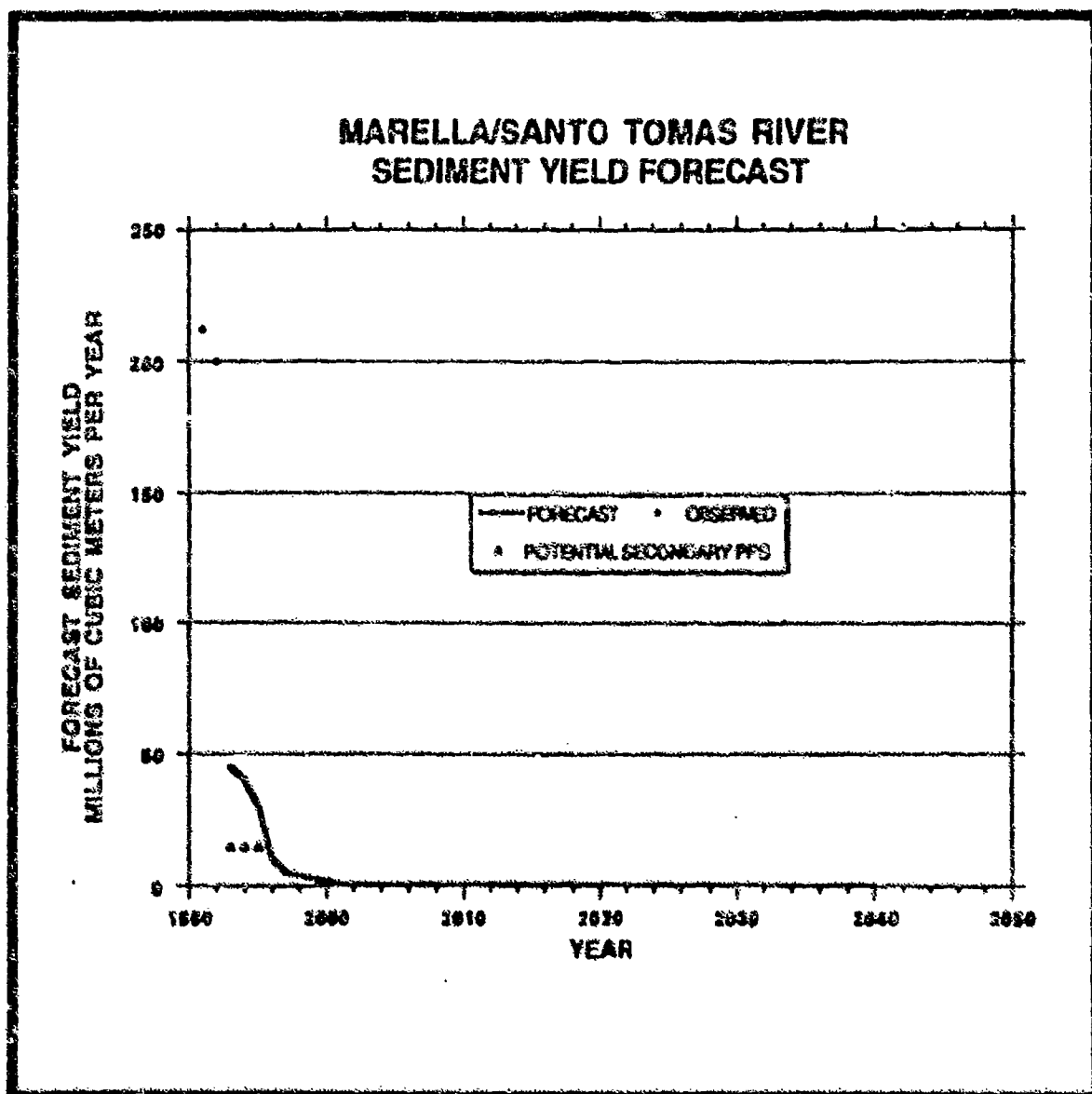
**MARELLA/SANTO TOMAS RIVER
SEDIMENT YIELD FORECAST**

Figure B-36. Sediment Yield Forecast for the
Marella/Santo Tomas Pyroclastic Deposit.

HAZARD AREA
SANTO TOMAS BASIN
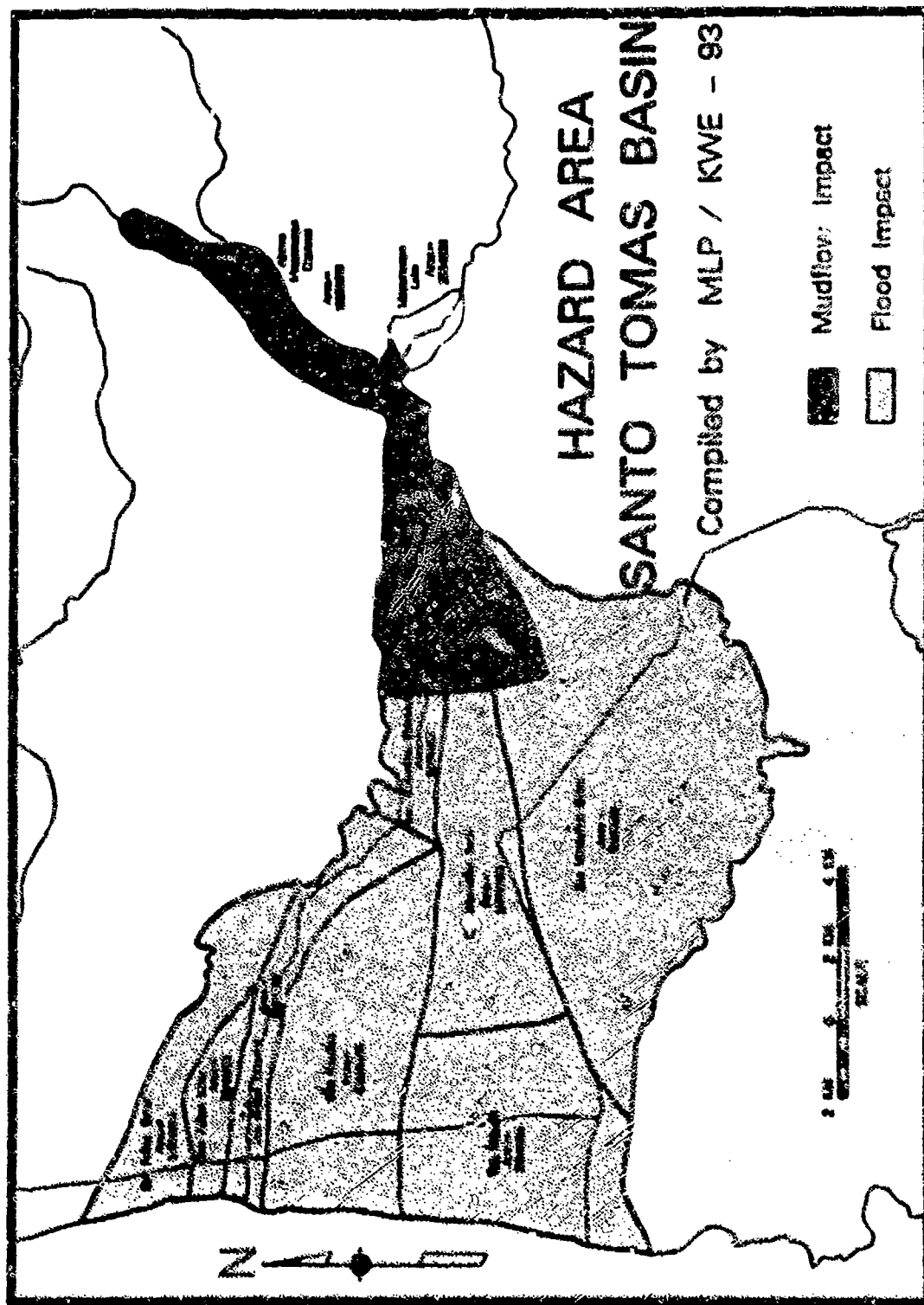
Compiled by MLP / KWE – 93

Mudflow Impact

Flood Impact

Figure B-37. Lower Santo Tomas River Basin Hazard Area.
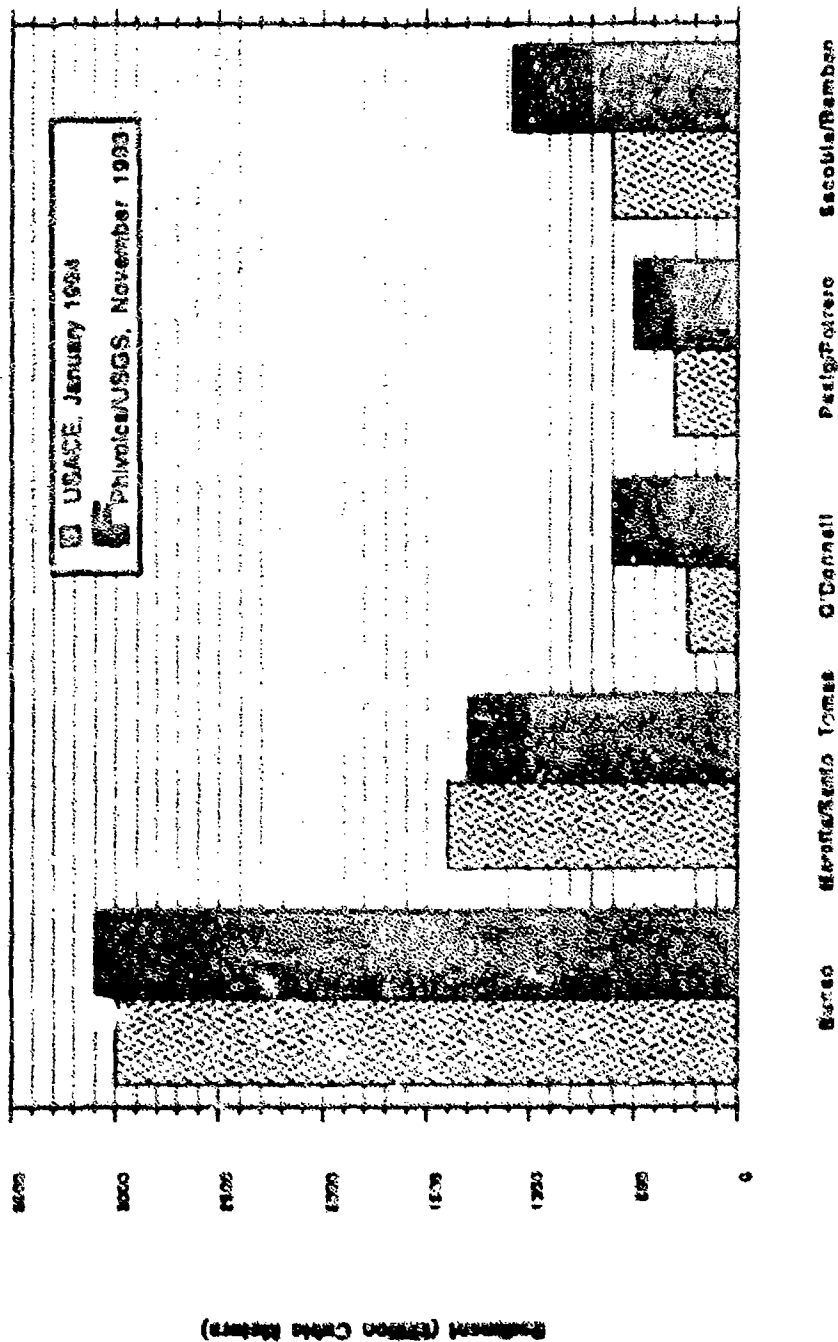Diagraming Mudflow and Flood Impact Zones.

Figure B-38. Pyroclastic Flow Deposit Volume Comparison.
Total volume comparison of Pyroclastic Flow Deposit for Mount Pinatubo
by USACE, January 1994 and Punviolcs/USGS, November 1993.

REPORT DOCUMENTATION PAGE

Public reporting burden for this collection of information is estimated to average 1 hour per response, including the time for reviewing instructions, searching existing data sources, gathering and maintaining the data needed, and completing and reviewing the collection of information. Send comments regarding this burden estimate or any other aspect of this collection of information, including suggestions for reducing this burden, to Washington Headquarters Services, Directorate for Information Operations and Reports, 1215 Jefferson Davis Highway, Suite 1204, Arlington, VA 22202, and to the Office of Management and Budget, Paperwork Reduction Project (0704-0188), Washington, DC 20503

1. AGENCY USE ONLY (Leave Blank)	2. REPORT DATE	3. REPORT TYPE AND DATES COVERED
	May 1994	Final report

4. TITLE AND SUBTITLE

Geomorphic and Sedimentation Investigation of the 15 June 1991
Eruption of Mount Pinatubo, The Philippines

5. FUNDING NUMBERS

6. AUTHOR(S)

Monte L. Pearson, Karl W. Eriksen

7. PERFORMING ORGANIZATION NAME(S) AND ADDRESS(ES)

U.S. Army Engineer Waterways Experiment Station
3909 Halls Ferry Road, Vicksburg, MS   39180-6199;
U.S. Army Engineer District, Portland
Hydraulics and Hydrology Branch, 333 S.W. First, Portland, OR   97204

8. PERFORMING ORGANIZATION REPORT NUMBER

Technical Report GL-94-14

9. SPONSORING/MONITORING AGENCY NAME(S) AND ADDRESS(ES)

U.S. Agency for International Development
U.S. Embassy, Manila, The Philippines

10. SPONSORING/MONITORING AGENCY REPORT NUMBER

11. SUPPLEMENTARY NOTES

Available from National Technical Information Service, 5285 Port Royal Road, Springfield, VA   22151

12a. DISTRIBUTION/AVAILABILITY STATEMENT

Approved for public release; distribution is unlimited.

12b. DISTRIBUTION CODE

13. ABSTRACT (Maximum 300 words)

This investigation provides a geomorphic framework and sedimentation analysis for five basins affected by the catastrophic eruption of Mount Pinatubo, The Philippines, on 15 June 1991. Medium- to fine-grained pyroclastic-flow material of approximately 5.6 billion cubic meters was deposited in the upper watershed areas around Mount Pinatubo. Rainfall-runoff has rapidly eroded eruption material, causing lahars that have flooded low-lying areas. Flooding and sedimentation from Mount Pinatubo lahars have displaced tens of thousands of people from their homes, destroyed bridges and crops, and decreased the amount of land available to agriculture in the lower basin. The purpose of this analysis is to assess the future sedimentation hazards due to continuing erosion of the 1991 pyroclastic deposits around Mount Pinatubo. A sediment yield forecast is presented for each basin containing large amounts of pyroclastic material. The areas most likely to experience sediment deposition were also identified. That information is used throughout this report to determine future damages, plan and design sediment control measures, and to assess the potential benefits (economic and physical) for those control measures.

14. SUBJECT TERMS

Geomorphology
Mud flows
Pyroclastic flows
Secondary pyroclastic flows
Sedimentation
Volcanic eruption

15. NUMBER OF PAGES

106

16. PRICE CODE

17. SECURITY CLASSIFICATION OF REPORT	18. SECURITY CLASSIFICATION OF THIS PAGE	19. SECURITY CLASSIFICATION OF ABSTRACT	20. LIMITATION OF ABSTRACT
UNCLASSIFIED	UNCLASSIFIED		